Universität Potsdam
Institut für Erd- und Umweltwissenschaften
und
Helmholtz-Zentrum Potsdam – Deutsches GeoForschungsZentrum GFZ
Sektion 5.2 – Klimadynamik und Landschaftsentwicklung

Extreme Events in Geoarchives: Deciphering Processes of Detrital Flood Layer Formation in Lake Sediments

Kumulative Dissertation

zur Erlangung des akademischen Grades
"doctor rerum naturalium" (Dr. rer. nat.)
in der Wissenschaftsdisziplin Geologie

eingereicht an der
Mathematisch-Naturwissenschaftlichen Fakultät
der Universität Potsdam

von
Lucas Kämpf

Potsdam, Januar 2015

Published online at the
Institutional Repository of the University of Potsdam:
URN urn:nbn:de:kobv:517-opus4-85961
http://nbn-resolving.de/urn:nbn:de:kobv:517-opus4-85961

Table of contents

List of figures

List of tables

Abstract

A main limitation in the field of flood hydrology is the short time period covered by instrumental flood time series, rarely exceeding more than 50 to 100 years. However, climate variability acts on short to millennial time scales and identifying causal linkages to extreme hydrological events requires longer datasets. To extend instrumental flood time series back in time, natural geoarchives are increasingly explored as flood recorders. Therefore, annually laminated (varved) lake sediments seem to be the most suitable archives since (i) lake basins act as natural sediment traps in the landscape continuously recording land surface processes including floods and (ii) individual flood events are preserved as detrital layers intercalated in the varved sediment sequence and can be dated with seasonal precision by varve counting.

The main goal of this thesis is to improve the understanding about hydrological and sedimentological processes leading to the formation of detrital flood layers and therewith to contribute to an improved interpretation of lake sediments as natural flood archives. This goal was achieved in two ways: first, by comparing detrital layers in sediments of two dissimilar peri-Alpine lakes, Lago Maggiore in Northern Italy and Mondsee in Upper Austria, with local instrumental flood data and, second, by tracking detrital layer formation during floods by a combined hydro-sedimentary monitoring network at Lake Mondsee spanning from the rain fall to the deposition of detrital sediment at the lake floor.

Successions of sub-millimetre to 17 mm thick detrital layers were detected in sub-recent lake sediments of the Pallanza Basin in the western part of Lago Maggiore (23 detrital layers) and Lake Mondsee (23 detrital layers) by combining microfacies and high-resolution micro X-ray fluorescence scanning techniques (µ-XRF). The detrital layer records were dated by detailed intra-basin correlation to a previously dated core sequence in Lago Maggiore and varve counting in Mondsee. The intra-basin correlation of detrital layers between five sediment cores in Lago Maggiore and 13 sediment cores in Mondsee allowed distinguishing river runoff events from local erosion. Moreover, characteristic spatial distribution patterns of detrital flood layers revealed different depositional processes in the two dissimilar lakes, underflows in Lago Maggiore as well as under- and interflows in Mondsee. Comparisons with runoff data of the main tributary streams, the Toce River at Lago Maggiore and the Griesler Ache at Mondsee, revealed empirical runoff thresholds above which the deposition of a detrital layer becomes likely. Whereas this threshold is the same for the whole Pallanza Basin in Lago Maggiore (600 m^3s^{-1} daily runoff), it varies within Lake Mondsee. At proximal locations close to the river inflow detrital layer deposition requires floods exceeding a daily runoff of 40 m^3s^{-1}, whereas at a location 2 km more distal an hourly runoff of 80 m^3s^{-1}

and at least 2 days with runoff above 40 m^3s^{-1} are necessary. A relation between the thickness of individual deposits and runoff amplitude of the triggering events is apparent for both lakes but is obviously further influenced by variable influx and lake internal distribution of detrital sediment.

To investigate processes of flood layer formation in lake sediments, hydro-sedimentary dynamics in Lake Mondsee and its main tributary stream, Griesler Ache, were monitored from January 2011 to December 2013. Precipitation, discharge and turbidity were recorded continuously at the rivers outlet to the lake and compared to sediment fluxes trapped close to the lake bottom on a basis of three to twelve days and on a monthly basis in three different water depths at two locations in the lake basin, in a distance of 0.9 (proximal) and 2.8 km (distal) to the Griesler Ache inflow. Within the three-year observation period, 26 river floods of different amplitude (10-110 m^3s^{-1}) were recorded resulting in variable sediment fluxes to the lake (4-760 g $m^{-2}d^{-1}$). Vertical and lateral variations in flood-related sedimentation during the largest floods indicate that interflows are the main processes of lake internal sediment transport in Lake Mondsee. The comparison of hydrological and sedimentological data revealed (i) a rapid sedimentation within three days after the peak runoff in the proximal and within six to ten days in the distal lake basin, (ii) empirical runoff thresholds for triggering sediment flux at the lake floor increasing from the proximal (20 m^3s^{-1}) to the distal lake basin (30 m^3s^{-1}) and (iii) factors controlling the amount of detrital sediment deposition at a certain location in the lake basin. The total influx of detrital sediment is mainly driven by runoff amplitude, catchment sediment availability and episodic sediment input by local sediment sources. A further role plays the lake internal sediment distribution which is not the same for each event but is favoured by flood duration and the existence of a thermocline and, therewith, the season in which a flood occurred.

In summary, the studies reveal a high sensitivity of lake sediments to flood events of different intensity. Certain runoff amplitudes are required to supply enough detrital material to form a visible detrital layer at the lake floor. Reasonable are positive feedback mechanisms between rainfall, runoff, erosion, fluvial sediment transport capacity and lake internal sediment distribution. Therefore, runoff thresholds for detrital layer formation are site-specific due to different lake-catchment characteristics. However, the studies also reveal that flood amplitude is not the only control for the amount of deposited sediment at a certain location in the lake basin even for the strongest flood events. The sediment deposition is rather influenced by a complex interaction of catchment and in-lake processes. This means that the coring location within a lake basin strongly determines the significance of a flood layer record. Moreover, the results show that while lake sediments provide ideal archives for reconstructing flood frequencies, the reconstruction of flood amplitudes is a more complex issue and requires detailed knowledge about relevant catchment and in-lake sediment transport and depositional processes.

Kurzfassung

Die Erforschung von Hochwasserereignissen, ihrer Wiederkehrhäufigkeiten und Entwicklung im Zuge des prognostizierten Klimawandels wird durch die kurzen instrumentellen Datenreihen stark begrenzt. Diese umfassen selten mehr als die letzten 50 bis 100 Jahre. Das Klima verändert sich jedoch auf kurzen bis hin zu sehr langen Zeitskalen, welche tausende Jahre umfassen können. Die Feststellung von kausalen Zusammenhängen zwischen Klimaänderungen und dem Auftreten hydrologischer Extremereignisse bedarf daher längerer Datenreihen. Aus diesem Grund sind in den letzten Jahren Geoarchive als Zeugen vergangener Hochwasserereignisse stärker in den Fokus der Forschung gerückt. Besonders geeignete Archive sind jährlich laminierte (warvierte) Seesedimente. Da Seebecken natürliche Stoffsenken in der Landschaft bilden, zeichnen die Sedimente kontinuierlich Erdoberflächenprozesse auf. Hochwasserereignisse führen zum erhöhten Eintrag von Material aus dem Einzugsgebiet und zur Bildung detritischer Lagen. Eingelagert innerhalb der warvierten Hintergrundsedimente können die einzelnen detritischen Lagen durch Warvenzählung mit saisonaler Präzision datiert werden.

Das Ziel der vorliegenden Arbeit ist es, das Verständnis über die hydrologischen und sedimentologischen Prozesse, die zur Bildung von detritischen Hochwasserlagen in Seesedimenten führen, zu erweitern und damit zu einer verbesserten Interpretation von Seesedimenten als natürliche Hochwasserarchive beizutragen. Dieses Ziel wurde auf zwei unterschiedlichen Wegen verfolgt: zum einen werden Zeitreihen von Hochwasserlagen in zwei unterschiedlichen perialpinen Seen, Lago Maggiore in Norditalien und Mondsee in Oberösterreich, mit Zeitreihen instrumenteller Hochwasserdaten verglichen und zum anderen werden Hochwasserereignisse durch ein umfassendes Messnetz am Mondsee vom Niederschlag bis zur Sedimentablagerung am Seegrund überwacht.

Die detritischen Lagen in subrezenten Sedimenten aus der Pallanzabucht im Westen des Lago Maggiore und aus dem Mondsee sind bis zu 17 mm und zum Teil weniger als einen Millimeter dick und wurden mittels Mikrofaziesanalysen und hochauflösenden Mikroröntgenfluoreszenz Scanverfahren (µ-XRF) detektiert. Das Alter jeder einzelnen der jeweils 23 detritischen Lagen wurde durch Warvenzählung im Mondsee und durch detaillierte Korrelation zu einer bereits datierten Kernsequenz im Lago Maggiore bestimmt. Die Korrelation detritischer Lagen zwischen fünf Sedimentkernen im Lago Maggiore und 13 Sedimentkernen im Mondsee ermöglichte es zum einen, solche Lagen, die durch Hochwasserereignisse gebildet wurden, von lokalen Erosionsereignissen zu unterscheiden. Zum anderen konnten anhand der unterschiedlichen räumlichen Verbreitungsmuster von Hochwasserlagen verschiedene Bildungsprozesse in den

beiden Seen abgeleitet werden. Während im Lago Maggiore grundberührende Underflows die wichtigsten Transportmechanismen für die Hochwasserlagenbildung sind, wird im Mondsee das detritische Material vor allem durch Interflows entlang der Thermokline über das Seebecken verteilt. Vergleiche der Zeitreihen detritischer Lagen und Abflussdaten der Hauptzuflüsse, dem Toce am Lago Maggiore und der Griesler Ache am Mondsee, zeigten für beide Standorte, dass die Ablagerung von detritischen Lagen ab einem bestimmten Abflusswert wahrscheinlich wird. Dieser empirische Grenzwert für die Hochwasserlagenbildung ist in der gesamten Pallanzabucht im Lago Maggiore gleich (Tagesabfluss: 600 m^3s^{-1}). Im Mondsee hingegen steigt der Grenzwert vom Delta (Tagesabfluss: 40 m^3s^{-1}) zur Seemitte hin an (stündlicher Abfluss: 80 m^3s^{-1}, 2 Tage über 40 m^3s^{-1} Tagesabfluss). Weiterhin wurde für beide Seen eine Beziehung zwischen der Stärke des Abflusses und der Dicke der Hochwasserlagen festgestellt, welche offensichtlich zusätzlich durch Variationen im Sedimenteintrag und in der Verbreitung innerhalb des Seebeckens beeinflusst wird.

Um die Prozesse der Hochwasserlagenbildung im Detail zu verstehen, wurden im Mondsee und seinem Hauptzufluss, der Griesler Ache, verschiedene hydro-meteorologische und sedimentologische Parameter von 2011 bis 2013 aufgezeichnet. Niederschlag, Abfluss und Trübung wurden kontinuierlich am Austritt der Griesler Ache in den Mondsee gemessen und mit dem Sedimentflux am Seeboden verglichen. Letzterer wurde mittels Sedimentfallen an zwei Lokationen im See, in 0.9 km (proximal) und in 2.8 km Entfernung zum Delta der Griesler Ache (distal), gesammelt. Nahe dem Seeboden wurde der Sedimentflux in einer zeitlichen Auflösung von drei bis zwölf Tagen und monatlich in drei unterschiedlichen Wassertiefen ermittelt. Innerhalb des dreijährigen Messzeitraums wurden 26 Hochwasserereignisse mit unterschiedlicher Magnitude (10-110 m^3s^{-1}) und Sedimentflux am Seeboden aufgezeichnet (4-760 g $m^{-2}d^{-1}$). Vertikale und horizontale Variationen in der Sedimentation während der stärksten Hochwasserereignisse zeigen, dass Interflows die bedeutendsten Transportmechanismen für die seeinterne Sedimentverteilung sind. Der Vergleich von hydrologischen und sedimentologischen Daten offenbarte (i) eine rasche Sedimentation innerhalb von drei Tagen nach dem Hochwasserscheitel im proximalen und innerhalb von sechs bis zehn Tagen im distalen Teil des Seebeckens, (ii) empirische Abflusswerte für erhöhten Sedimentflux am Seeboden im proximalen (20 m^3s^{-1}) und distalen Teil des Seebeckens (30 m^3s^{-1}) und (iii) verschiedene Faktoren, welche die abgelagerte Sedimentmenge nach einem Hochwasserereignis kontrollieren. Der Sedimenteintrag zum See ist hauptsächlich durch Abflussstärke, Sedimentverfügbarkeit im Einzugsgebiet und episodischen Sedimenteintrag von lokalen Quellen bestimmt. Eine weitere Rolle spielt die Verteilung des Sediments innerhalb des Seebeckens. Diese ist nicht für jedes Hochwasserereignis gleich, sondern ist durch die Dauer des Hochwasserereignisses und die Existenz der Thermokline in den Sommermonaten limitiert.

Insgesamt zeigen die Untersuchungen eine hohe Sensitivität von Seesedimenten für Hochwasserereignisse unterschiedlicher Intensität. Eine bestimmte Hochwasserstärke ist notwendig, dass genügend detritisches Material für eine sichtbare Hochwasserlage am Seeboden abgelagert wird. Verantwortlich sind positive Rückkopplungsmechanismen zwischen Hochwasserstärke, Erosion,

Sedimenttransport im Fluss und die Sedimentverteilung innerhalb des Seebeckens. Das Zusammenspiel dieser Faktoren wirkt unterschiedlich in verschiedenen Seen. Deshalb sind die hydrologischen Grenzwerte für die Hochwasserlagenbildung standortsspezifisch. Die Untersuchungen dieser Arbeit zeigen weiterhin, dass die Menge an abgelagertem Sediment am Seeboden nicht nur durch die Abflussstärke bestimmt wird. Die Sedimentation ist vielmehr durch die komplexe Wechselwirkung von Prozessen im Einzugsgebiet und innerhalb des Sees kontrolliert. Dies bedeutet, dass die Kernlokation innerhalb eines Seebeckens die Signifikanz eines Hochwasserarchivs maßgeblich beeinflusst. Weiterhin zeigen diese Ergebnisse, dass Seesedimente für die Rekonstruktion von Hochwasserhäufigkeiten ideale Archive darstellen. Die Ableitung von Hochwasserstärken aus der Dicke einzelner Hochwasserlagen ist allerdings komplexer und setzt eine detaillierte Kenntnis der relevanten Transport- und Ablagerungsprozesse im See und seinem Einzugsgebiet voraus.

Acknowledgements

First of all, I want to thank my supervisor Achim Brauer, head of Section 5.2 "Climate Dynamics and Landscape Evolution" at the Helmholtz Centre Potsdam German Research Centre for Geosciences (GFZ), for his constant encouragement during the last years. I greatly benefited from your ideas, our inspiring discussions as well as your guidance and constructive criticism! I also wish to thank the external examiners for their critical review of my thesis. Furthermore, I am grateful to the German Federal Ministry for Education and Research (BMBF) funding my PhD student position as a part of the PROGRESS joint project.

I am grateful to the members of the PROGRESS project part A.3, especially Philip Mueller, for his effort, loyalty and friendship during the last years but also Andreas Güntner and Bruno Merz for making available all the data that significantly contributed to the manuscripts presented in this thesis and the fruitful and stimulating discussions at any stage of my work. I am also grateful to the scientific partners not directly involved in PROGRESS. Thomas Weisse and Rainer Kurmayer from the Research Institute for Limnology Mondsee supported the monitoring set-up and provided own data on phytoplankton in Lake Mondsee. They are further acknowledged for fruitful discussions and their initiatives for future collaboration.

Piero Guilizzoni from the CNR-Istituto per lo Studio degli Ecosistemi in Verbania is acknowledged for giving me the possibility to work on sediments of Lago Maggiore and sharing his great expertise in paleolimnology and the lake site.

This thesis would not have been possible without the support of the technical and scientific staff at the GFZ Potsdam and the Research Institute for Limnology in Mondsee: Hannes Höllerer, Kurt Mayrhofer and Richard Niederreiter (UWITEC) assisted sediment coring and sediment trap recovering and produced new ideas to improve the monitoring whenever needed; Heiko Thoss maintained the river gauging stations and is especially acknowledged for his invaluable field work during the severe June 2013 flood; Michael Köhler (MK Factory), Gabriele Arnold, Dieter Berger and Brian Brademann prepared the thin sections, but also had a solution for any technical problem which arose during the past years; Jens Mingram gave the two sequential traps and helped with the microscopic analyses; Birgit Plessen and Petra Meier provided the carbon and stable isotope analyses; Peter Dulski and Brigitte Richert ran the µ-XRF measurements; Rudolf Naumann provided XRD measurements; Georg Schettler and Ursula Kegel helped with the preparation of the sediment trap samples; Helga Kemnitz and Juliane Herwig assisted during the SEM sessions; Sebastian Lorenz (University of Greifswald) as well as Christoff Andermann, Elisabeth and Michael Dietze provided grain size measurements – many thanks for your invaluable help with all the analyses and

your useful comments concerning the interpretation of the data! Last but not least, I want to thank the non-scientific backbone of Section 5.2 at the GFZ: Christine Gerschke managed all the administrative and bureaucratic stuff, Andreas Hendrich and Manuela Dziggel provided solutions for any graphical problem and Marcus Günzel and Matthias Köppl kept the computer running – your help made life much easier!

A special thank goes out to my roommates Isabel Dorado Liñán, Celia Martin Puertas, Florian Ott and Markus Czymzik for the right mixture of concentration, discussion and a lot of fun, to my further Phd fellows Anoop Ambili, Praveen Mishra, Ina Neugebauer, Stefan Lauterbach, Gordon Schlolaut, Tina Swierczynski, Nadine Dräger for open ears and open minds at each time as well as everyone at Section 5.2 of the GFZ Potsdam for their astonishing engagement, continuous support, and patience.

Last but not least, I would like to thank my friends, my whole family and especially Anke for their patience and encouragement during the last years- this work would not have been possible without you!

1 Introduction

1.1 Scientific context

River floods are the most common and widespread natural hazards and there is an ongoing debate about how such events will change under future climate scenarios (e.g. Milly *et al.*, 2001; Mudelsee *et al.*, 2003; Min *et al.*, 2011). However, until now evaluating linkages between flood occurrence and changing climate boundary conditions are limited by only short instrumental records as stated in the special IPCC report on extreme events from 2012: *"There is limited to medium evidence available to assess climate-driven observed changes in the magnitude and frequency of floods at regional scales because the available instrumental records of floods at gauge stations are limited in space and time"*. Therefore, for evaluating flood variability on all relevant time-scales it is necessary to extend instrumental flood records using historical and geological archives (Knox, 2000; Mudelsee *et al.*, 2003; Merz and Bloeschl, 2008; Merz *et al.*, 2014).

For this purpose, lake sediments are particularly suitable research objects (Gilli *et al.*, 2013) because lakes form traps in the landscape and continuously record land surface processes including extreme events (Brauer and Casanova, 2001). Detrital layers formed by river floods ideally contrasts to the background sedimentation and can be than detected using optical methods, e.g. microscopy (Mangili *et al.*, 2005, Brauer *et al.*, 2009) and spectroscopy (Debret *et al.*, 2010), physical methods, e.g. density and magnetic susceptibility (Thorndycraft *et al.*, 1998), and geochemical methods, e.g. micro-X-ray fluorescence (µ-XRF) (Brauer *et al.*, 2009, Czymzik *et al.*, 2010).

Detrital layers in lake sediments were first recognized as flood deposits in the 1970s (Gilbert, 1973; Lambert *et al.*, 1976; Sturm and Matter, 1978) but their potential for establishing long flood calendars was not explored until the early 1990s, when first flood records were established from sediments of Lake Uri in Switzerland (Siegenthaler and Sturm, 1991) and Lilloet Lake in Canada (Desloges and Gilbert, 1994). Since then a growing number of flood reconstructions has been established particularly in the Alpine realm of Central and Northern Europe and North America. Palaeoflood frequencies are based on the occurrence intervals of detrital layers (Czymzik *et al.*, 2010; Swierczynski *et al.*, 2012; Glur *et al.*, 2013,), whereas flood intensities have been inferred from the thickness (Brown *et al.*, 2000; Wilhelm *et al.*, 2012, Wirth *et al.*, 2013) and grain size distribution (Siegenthaler and Sturm, 1991; Kaufmann *et al.*, 2011; Lapointe *et al.*, 2012) of individual deposits. Varved sediment records provide most precise flood chronologies with seasonal resolution giving the unique possibility to compare and link sediment-based and instrumental flood time series (Leemann and Niessen,

1994; Lamoureux, 2000; Francus *et al.*, 2002; Chutko and Lamoureux, 2008; Menounos and Clague, 2008; Trachsel *et al.*, 2008; Czymzik *et al.*, 2010; Schiefer *et al.*, 2006; 2011).

Despite the great potential especially of varved lake sediments for reconstructing long flood time series, there are still some confinements with respect to interpretation of detrital layer records due to a lack of understanding the complex chain of processes leading to the formation of detrital layers spanning from an extreme rainfall event to the final deposition of a detrital layer at the lake floor. One important issue under discussion is the completeness of detrital layer flood time series. Detailed comparisons of flood layer chronologies with instrumental hydrological data have revealed that detrital layer records can be biased by (I) individual layers which are not triggered by floods but by local erosion events as debris flows (e.g. Irmler *et al.*, 2006; Swierczynski *et al.*, 2009 and 2012) and subaqueous slumps (Lamoureux, 1999; Girardclos *et al.*, 2007; Lauterbach *et al.*, 2012) and (II) 'missing flood layers', i.e. layers which are not detectable in the sediment record (Czymzik *et al.*, 2010) or floods which did not result in detrital layer deposition due to either reduced sediment flux from the catchment or variable sediment distribution within the lake basin (Lamoureux, 2000; Gilli *et al.*, 2003; Swierczynki *et al.*, 2009; Czymzik *et al.*, 2010; Schiefer *et al.*, 2011). A second critical issue under discussion is how the amount of deposited sediment is linked to flood amplitude and to which extend other factors in the catchment and the lake itself might play a role.

To gain more knowledge about detrital flood layer formation in lake sediments, several approaches have been initiated in the past including (I) in situ monitoring of water and sediment fluxes from rivers to lakes (Gilbert, 1973; Lambert *et al.*, 1976; Weirich, 1986; Lambert and Giovanoli, 1988; Best *et al.*, 2005; Dugan *et al.*, 2009), (II) sediment trapping (Blass *et al.*, 2007; Cockburn and Lamoureux, 2008; Crookshanks and Gilbert, 2008; Dugan *et al.*, 2009) and (III) detailed comparisons of single flood deposits with instrumental flood data (Desloges and Gilbert, 1994; Leemann and Niessen, 1994; Lamoureux, 1999; Gilbert *et al.*, 2006; Schiefer *et al.*, 2006 and 2011; Czymzik *et al.*, 2010; Kämpf *et al.*, 2012a).

1.2 Scientific objectives and tasks

The aim of this thesis is to improve the interpretation of detrital layers in lake sediments as archives for flood events by deciphering and understanding processes of detrital layer formation. This goal is achieved by (I) an event-based calibration of detrital layers with instrumental flood data applied in sub-recent sediments of two dissimilar basins, Lake Mondsee (Upper Austria) and Pallanza Basin in the western part of Lago Maggiore (Northern Italy), and (II) a combined hydro-sedimentary monitoring in Lake Mondsee and its catchment. Lake Mondsee was chosen for this in-depth monitoring since the sediments from the deepest part of the lake contain a varved detrital layer record covering the last 7100 years (Swierczynski *et al.*, 2013).

(I) The calibration of detrital layer records requires:

- Microscopic microfacies analyses on overlapping thin sections and X-ray fluorescence scanning at 200 µm step size on the upper 12-40 cm of 13 surface sediment cores in Lake Mondsee and the upper 18-75 cm of 5

surface sediment cores in Lago Maggiore.

- Establishing age-depth models for each sediment core by microscopic varve counting for Lake Mondsee and intra-basin correlation to a dated core sequence for Lago Maggiore.

- Intra-basin correlation of detrital layers by means of varve chronology and lithological markers.

- Comparing sediment and instrumental hydrological data (Mondsee: runoff, precipitation; Lago Maggiore: runoff, lake level) for the time when instrumental and sedimentological datasets are available (Mondsee: 1976-2005, Lago Maggiore: 1965-2006).

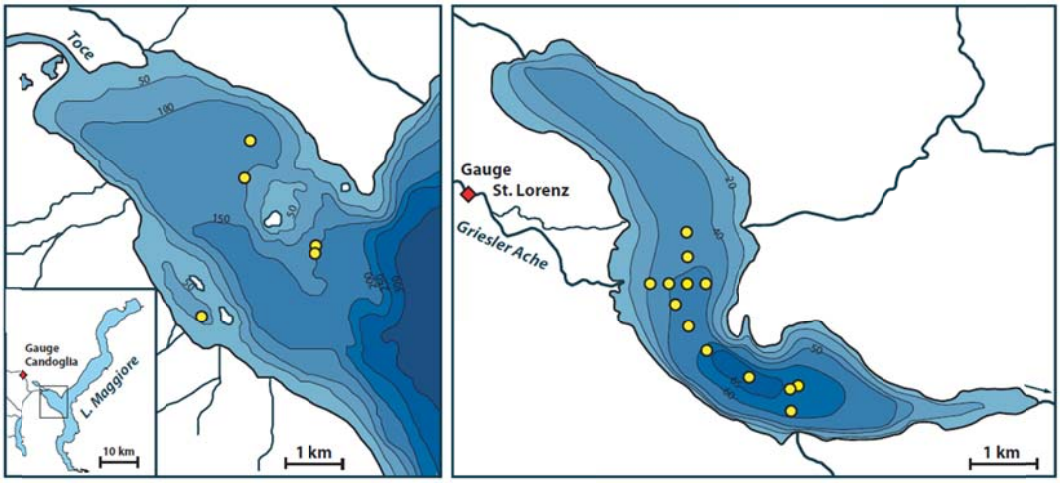

Figure 1.1. Bathymetric maps of the Pallanza basin at Lago Maggiore (left) and Mondsee (right) indicating the coring locations (yellow dots), the main tributary rivers and the location of the gauging stations providing daily discharge data used for flood layer calibration.

(II) To track hydro-sedimentary processes during floods from the initial rainfall to the deposition of detrital material at the lake floor, a comprehensive monitoring network has been set up in Lake Mondsee and its catchment including (Fig. 1.2):

- Five river gauging stations recording precipitation, runoff, electrical conductivity, water temperature and turbidity and equipped with a water sampler for autonomous event sampling. The gauges are arranged from the headwaters to the outlet into Lake Mondsee following a nested catchment approach.
- Four monitoring buoys in Lake Mondsee recording meteorological and limno-physical variables as temperature, electrical conductivity, turbidity and water current velocity and direction in different water depths
- Two chains of sediment traps collecting sediment on a 3-12 day basis (sequential traps) close to the lake bottom and on a monthly basis (integral traps) in three different water depths, respectively. The buoy and traps were arranged from the main tributary to the site where the long sediment record for flood reconstruction was retrieved.

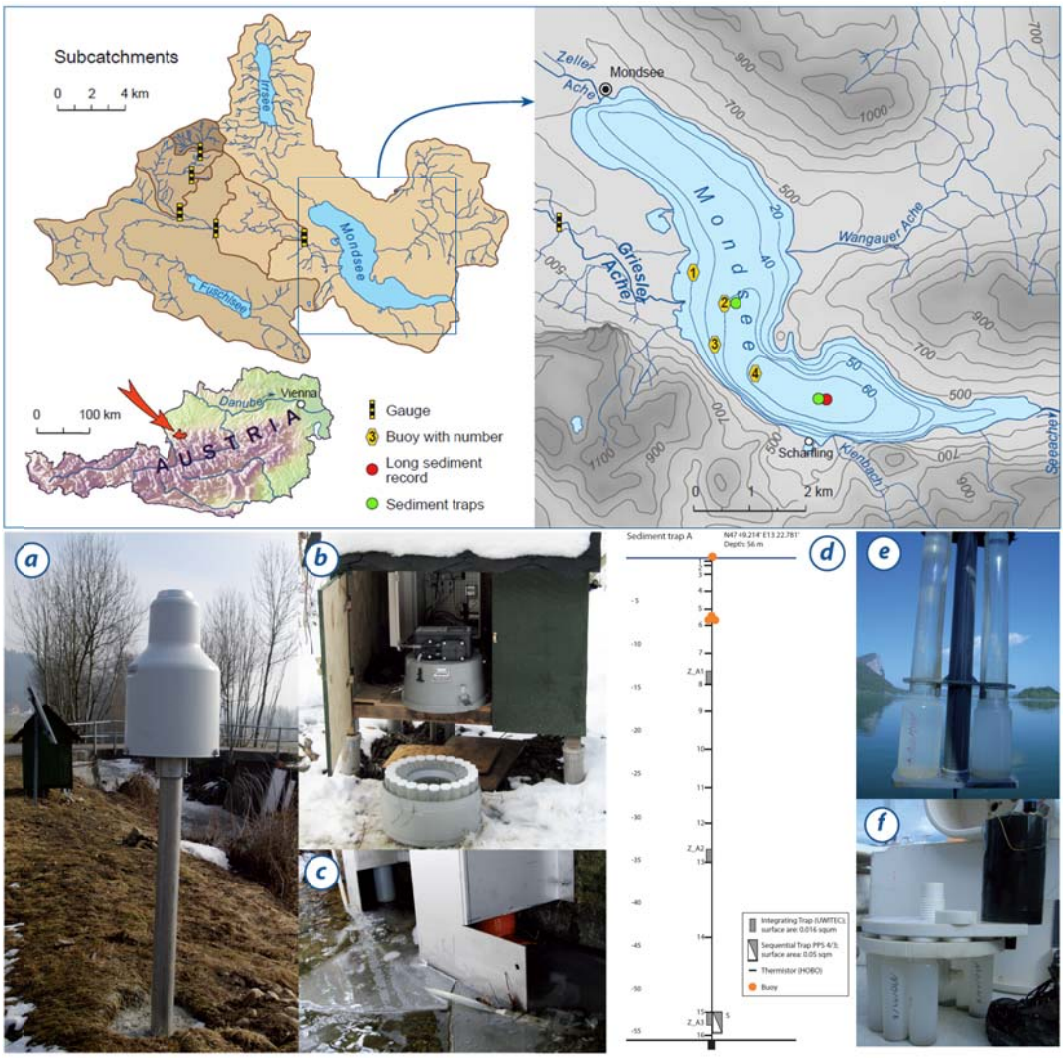

Figure 1.2. Monitoring set-up at Lake Mondsee: 5 river gauging stations with measurement devices for (a) precipitation, (b) automated water sampling, (c) water level, electrical conductivity, temperature and turbidity; (d) two sediment trap chains with (e) 3 integral traps in different water depths and one sequential trap 3m above lake floor. Monitoring buoys are described in detail by Mueller *et al.* (2013).

With the installation of the first instruments in December 2010 the monitoring collected data over a 3-year period until December 2013. Trapped sediment samples, river water sediment samples as well as soil and river bed samples taken in the catchment were analysed for sediment mass and composition by

- Carbon and nitrogen analyses
- Stable isotopic analyses of oxygen, carbon and nitrogen
- Microscopic investigations on smear slides
- X-ray diffraction and grain size analyses

The monitoring was planned, financed and installed within the framework of the joint project PROGRESS, part A.3 "*Extreme Events in Geoarchives*" (www.earth-in-progress.de) in close cooperation with Philip Mueller, who simultaneously earns his doctoral degree in the field of Hydrology. For the monitoring, my scientific tasks were to run the sediment traps and the sedimentological analyses.

1.3 Organization of the thesis

The thesis is conceptualized as a 'cumulative thesis' subdivided into six chapters. Following this introduction giving essential background information (chapter 1), chapters 2 to 4 represent the scientific work subdivided into three manuscripts (Table 1.1).

The first manuscript (chapter 2) entitled 'Flood event layers in recent sediments of Lago Maggiore (N. Italy) and their comparison with instrumental data' informs about the detection of even sub-mm thick detrital layers in lake sediments by combining microfacies and μ-XRF scanning techniques. Detailed intra-basin correlation of detrital layers and comparison to instrumental lake level and river runoff data allows distinguishing river runoff events from local erosion, as well as evaluating the relation between detrital layer thickness and flood amplitude.

The second manuscript (chapter 3) entitled 'Processes of flood-triggered detrital layer deposition in the varved Lake Mondsee sediment record revealed by a dual calibration approach' addresses spatial distribution patterns of detrital flood layers and the driving processes in Lake Mondsee. The comparison to instrumental precipitation and river runoff data allows identifying (i) empirical flood thresholds for detrital layer formation as well as (ii) missing layers or additional, non-flood triggered detrital layers at individual coring locations.

The third manuscript (chapter 4) entitled 'Hydrological and sedimentological processes of flood layer formation in Lake Mondsee' presents the results of the three-year monitoring of hydo-sedimentary dynamics in Lake Mondsee and its catchment revealing (i) river floods as the main precursor for detrital sediment input to Lake Mondsee and (ii) the influence of factors besides flood amplitude controlling amount and spatial distribution of detrital sediment flux in Lake Mondsee.

Summary and conclusions of the thesis including future perspectives are given in chapter 5. The references are listed in chapter 6.

Table 1.1. Manuscripts presented in the thesis.

Chapter	Manuscript title	Status
Chapter 2	*Lucas Kämpf, Achim Brauer, Peter Dulski, Andrea Lami, Aldo Marchetto, Stefano Gerli, Walter Ambrosetti and Piero Guilizzoni.* Flood event layers in recent sediments of Lago Maggiore (N. Italy) and their comparison with instrumental data	Freshwater Biology (2012) 57, 2076–2090 doi:10.1111/j.1365-2427.2012.02796.x
Chapter 3	*Lucas Kämpf, Achim Brauer, Tina Swierczynski, Markus Czymzik, Philip Mueller, Peter Dulski.* Processes of flood-triggered detrital layer deposition in the varved Lake Mondsee sediment record revealed by a dual calibration approach	Journal of Quaternary Science (2014) 29, 475–486 doi: 10.1002/jqs.2721

Chapter 4	*Lucas Kämpf, Philip Mueller, Hannes Höllerer, Birgit Plessen, Rudolf Naumann, Heiko Thoss, Andreas Güntner, Bruno Merz, Achim Brauer.* Hydrological and sedimentological processes of flood layer formation in Lake Mondsee	The Depositional Record (2015) 1, 18-37 doi: 10.1002/dep2.2

1.4 Authors contribution

Chapter 2: I performed the microfacies analyses and intra-basin correlation within five surface sediment cores and measured the µ-XRF data in two surface sediment cores in collaboration with Peter Dulski. I compared the sediment data with instrumental data on river runoff and lake level. I analyzed the data, reviewed the relevant literature and wrote the manuscript. The co-authors, reviewers and particularly Achim Brauer substantially helped to improve the final manuscript.

Chapter 3: I organized and lead the coring campaign at Lake Mondsee and performed the microfacies analyses, varve counting and intra-basin correlation within 13 surface sediment cores as well as µ-XRF measurements in collaboration with Peter Dulski. I developed the ideas about depositional processes at Lake Mondsee and the implications for the interpretation of the flood record. In addition, I conducted the evaluation and interpretation of the results, aided by discussions with the coauthors. I wrote the manuscript with major contributions of Achim Brauer.

Chapter 4: I planned the monitoring set up in collaboration with Philip Mueller and changed the sediment traps in a monthly rhythm over three years (from January 2011 to December 2013). I performed the carbon and nitrogen analyses for sediment trap samples in collaboration with Birgit Plessen, the grain size analyses in collaboration with Philip Mueller and Sebastian Lorenz as well as the XRD analyses in collaboration with Rudolf Naumann. I conducted the evaluation and interpretation of the results and I almost entirely wrote the manuscript with contributions of Philip Mueller, Andreas Güntner, Bruno Merz and Achim Brauer.

2 Flood event layers in recent sediments of Lago Maggiore (N. Italy) and their comparison with instrumental data

Lucas Kämpf[1], Achim Brauer[1], Peter Dulski[1], Andrea Lami[2], Aldo Marchetto[2], Stefano Gerli[2], Walter Ambrosetti[2] and Piero Guilizzoni[2]

[1] *GFZ German Research Centre for Geosciences, Section 5.2 Climate Dynamics and Landscape Evolution, 14473 Potsdam, Germany*

[2]*National Research Council, Institute of Ecosystem Study, 28922 Verbania Pallanza, Italy*

Published in Freshwater Biology

Abstract

A succession of 20 detrital layers was detected in five short cores from the Pallanza Basin in the western part of Lago Maggiore (Italy) by combining thin-section analyses and high-resolution micro X-ray fluorescence (μ-XRF) scanning techniques. The detrital layers range in thickness from 0.6 mm to 17.4 mm and appear most distinct in the upper 20-25 cm of each core, where eutrophication since the early 1960s resulted in the deposition of a dark, organic sediment matrix. The age-depth model of previously dated cores was transferred by precise intra-basin correlation of distinct marker layers, thus providing a reliable chronology for the 20 detrital layers covering the time period 1965-2006.

All detrital layers are related to regional floods as recorded by short-term lake level rises and peaks in discharge of the River Toce, the main tributary to the Pallanza Basin. Detailed intra-basin correlation of detrital layers allows us to distinguish river runoff events from local erosion, as well as evaluate the relation between detrital layer thickness and flood amplitude. Massive clay accumulation on top of the thickest detrital layers might have affected lake ecology by attenuating light and influencing metabolic activity.

In the clastic-dominated sediments deposited before 1965, detrital layers are less clearly discernible because of the predominantly clastic pelagic sediment matrix. The combination of thin section and µ-XRF techniques, however, shows the potential to establish even longer flood layer time series from Lago Maggiore sediments.

2.1 Introduction

Many of the most severe floods which caused damage and loss of life in Europe occurred in the Alps (Bacchi & Ranzi, 2003; Schmocker-Fackel & Naef, 2010). A particularly memorable event was the flood at Lago Maggiore in October 1868, when the water level rose to 6.94 m above the mean level. The strong impact of floods on human society and ecosystems raises the question of how the frequency and strength of such events will develop under the predicted changing climatic conditions (e.g. Milly *et al.*, 2002; Schmocker-Fackel & Naef, 2010; Min *et al.*, 2011).

Since instrumental data spanning the last 50 to 100 years are too short to represent natural climate variability, establishing long time series of flood frequencies from lake and fluvial sediment archives is a challenge for palaeoclimatic research (Knox, 2000; Chapron *et al.*, 2005; Thorndycraft & Benito 2006; Debret *et al.*, 2010). Lake sediments trap flood-triggered sediment transport by tributaries (Ludlam, 1974; Sturm & Matter, 1978; Hsü & Kelts, 1985; Lamoureux, 2000), resulting in long chronologies of detrital layers intercalated in pelagic background sediments (Gilli *et al.*, 2003; Chapron *et al.*, 2005; Czymzik *et al.*, 2010; Støren *et al.*, 2010). Palaeoflood frequencies are based on the occurrence intervals of detrital layers, but detailed comparisons with instrumental data have revealed that some floods are not reflected in the sediment records (Gilli *et al.*, 2003; Swierczynski *et al.* 2009; Czymzik *et al.* 2010). Hence, a detailed understanding of the processes of flood-triggered detrital layer deposition is required (Mangili *et al.*, 2005; Lamb *et al.*, 2010). Various approaches have been initiated including studies on single flood events (Schiefer, Menounos & Slaymaker, 2006; Kämpf *et al.*, 2012) as well as on monitoring flood-triggered sediment flux (Effler *et al.*, 2006; Cockburn & Lamoureux, 2008; Crookshanks & Gilbert, 2008).

The specific objective of this study is to use the stratigraphy of detrital layers in surface cores from Lago Maggiore to reconstruct the flood history of the last 40 years and compare it with instrumentally recorded data on lake level and discharge of the main tributary River Toce. Investigating the spatial distribution of detrital layers in multiple cores combined with instrumental flood data should provide a calibration for the sediment data. The main goal is improving the knowledge of the generation of flood-induced detrital layers in a mid-latitude pre-alpine lake.

2.2 Study site

Lago Maggiore (Fig. 2.1) lies just to the south of the Alps (deepest part at 45°57'N; 8°38'E), along the border between Italy and Switzerland at an altitude of 194 m a.s.l (mean lake level; above sea level). It is a large lake (212.5 km^2; volume 37.5 km^3) and also very deep (mean and maximum depths, 177 and 370 m, respectively) with a drainage area of about 6599 km^2. Lago Maggiore has been extensively studied with a limnological data set extending back to 1950, documenting the history of eutrophication during the period 1965 - 1980 followed by successful reoligotrophication in the 1990s (e.g. Manca, Calderoni & Mosello, 1992: Mosello, Calderoni & de Bernardi, 1997; Salmaso *et al.*, 2007; CIPAIS, 2007). An integrated network of meteorological stations around Lago Maggiore and in the catchment verifies a warming trend during the last 60 years (Ambrosetti & Barbanti, 1999). The recent trophic and pollution history of Lago Maggiore has also been reconstructed using biological and chemical proxies (e.g. Baudo *et al.*, 2002; Manca *et al.*, 2007; Marchetto *et al.*, 2004; Guilizzoni *et al.*, 2010; Guilizzoni *et al.*, 2012).

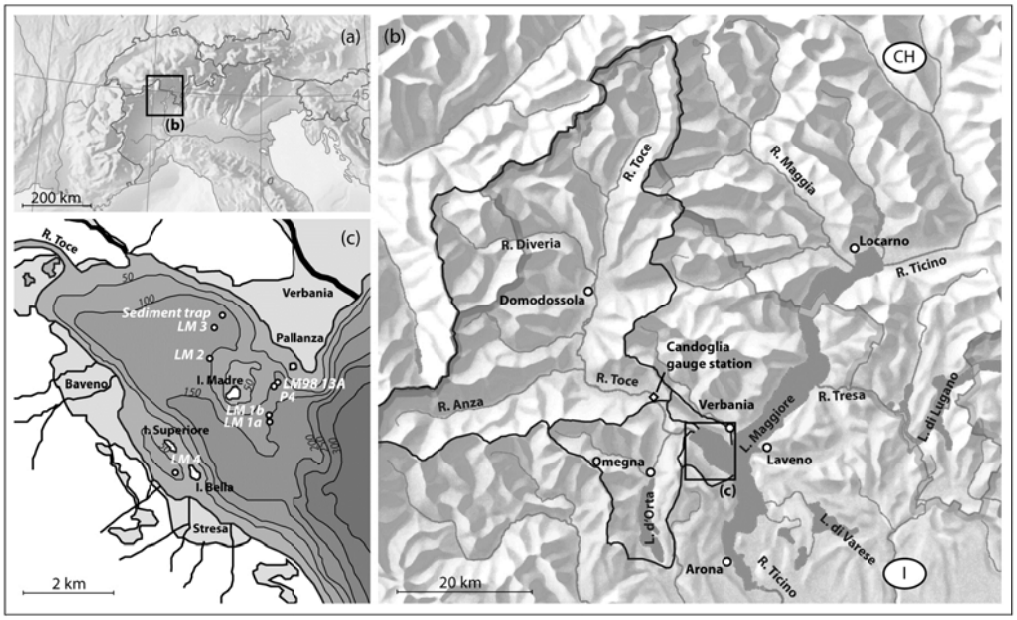

Figure. 2.1. (a) Location of Lago Maggiore. (b) Lago Maggiore and its catchment; background map © swisstopo; (c) Core locations within the Pallanza Basin (dots), including LMA06 cores (labelled with LM 1-4 in this study), P4 (Putyrskaya *et al*., 2009) and LM98 13A (Marchetto *et al*., 2004). Indicated is the position of the sediment trap investigated by Kulbe *et al*. (2008).

This study focuses on sediments from the Pallanza Basin in the western part of Lago Maggiore (152 m maximum water depth, Fig. 2.1c). The basin is surrounded by steep slopes (up to 20°) of the southern pre-alpine mountains, reaching elevations of 600 to 1480 m a.s.l. The main tributary of Pallanza basin is River Toce, draining an area of 1551 km² (Barbanti & Ambrosetti, 1989). The Toce watershed (Fig. 2.1b) is a typical glacial basin with steep hill slopes bounding a narrow valley located mainly in the north Piedmont region of Italy and partially in Switzerland (10% of the total area). The elevation of the watershed ranges from 194 m a.s.l. at the lake's outlet to approximately 4600 m a.s.l. at the Monte Rosa crest. The land cover is forest (70%), bare rocks (9%), agricultural (7%), natural grassland (6%), urban (4%), water (3%) and glaciers and perpetual snow (1%).

The catchment lithology has five main classes: gneiss (49%), micaceous schists (27%), calcareous schists (11%), granites (6%) and sedimentary rocks (sandstones and shales, 7%) (Barbanti & Ambrosetti, 1989; Carollo, Libera & Contardi, 1989; Montaldo, Ravazzani & Mancini, 2007).

The main flooding period in the Lago Maggiore area is from September to November. Major precipitation events are commonly caused by an interaction of large-scale circulation patterns and regional forcing mechanisms. North-westerly air flows, when crossing the Alpine barrier, cause a lee cyclogenesis over the Gulf of Genova inducing southerly winds (Bacchi & Ranzi, 2003). The Alps are a natural barrier, forcing the southerly moist flows to rise, which produces heavy and long-lasting precipitation (Bacchi & Ranzi, 2003; Rotunno & Ferretti, 2003). The Mediterranean Sea is the main moisture source area for southern Alpine precipitation (Sodemann & Zubler, 2010) and therefore the amount of water vapour strongly relates to the surface temperature of the Mediterranean Sea (Pinto *et al.*, 2001). The combination of these meteorological and geomorphological factors is such that the western site of the Southern Alps including the Toce catchment gives rise to some of the most severe flood events in Europe (Bacchi & Ranzi, 2003).

2.3 Methods

2.3.1 Coring

In 2006, five short cores were collected with a gravity corer (Type Ghilardi, 63 mm liner diameter, Kelts *et al.*, 1986) from the Pallanza Basin (Fig. 2.1c) because sediment sequences in that area do not show major disturbances (e.g. Baudo *et al.*, 2002; Marchetto *et al.*, 2004). Mass flow deposits observed in cores of the deepest part of the central basin of Lago Maggiore have caused major erosion leading to shortened and non-continuous sediment profiles.

Table 2.1. Data on gravity cores collected in the Pallanza Basin including the original core name and the name used in the text, position, water depth and core length. Cores P4 (Putyrskaya *et al.*, 2007) and LM98 13A (Marchetto et al., 2004) are used for dating the LMA06 cores (No LM 1-4). The transition between sediment units I and II (I/II, dated to 1965) and the mean sediment accumulation rate (SAR) between 1965 (I/II) and 2000 (K-4).

Original core name	Name used here	Sampling	Lon (E)	Lat (N)	Water depth (m)	Core length (cm)	Depth of I/II trans. (cm)	Mean SAR 1965–2000 (cm year^{-1})
LMA06 Ex13/10/1	LM 1a	2006	8°32.89′	45°54.37′	148.0	72.0	18.5	0.45
LMA06 Ex13/10/2	LM 1b	2006	8°32.89′	45°54.47′	134.0	107.0	22.0	0.55
LMA06 16/10/2	LM 2	2006	8°31.93′	45°55.11′	113.0	44.0	23.0	0.56
LMA06 17/10/1	LM 3	2006	8°31.94′	45°55.48′	120.0	62.0	27.0	0.67
LMA06 51/10/1	LM 4	2006	8°31.30′	45°53.75′	59.0	55.0	Not detected	0.60[a]
LM98/13A		1998	8°32.95′	45°54.80′	70.0	68.0	14.0	0.36[b]
P4		2004	8°33.02	45°54.84′	150.0	93.0	15.5	0.38
2 sequ. sediment traps (á 500 cm^3)		October 04–May 06	8°32.07′	45°55.61′	57.0/117.0	Sampling interval: 21 days (winter); 7 days (summer)		

(a) I/II was not detected in core LMA06 51/10/1 and SAR refers to the interval 1977-2000 (K-15 - K-4). (b) SAR in core LM98 13A is reported in Marchetto *et al.* (2004). Data on sediment cores have been compared with sediment trap data obtained by Kulbe *et al.* (2008).

The core locations (Table 2.1, Fig. 2.1c) are labelled as follows: location LM 1 (two cores, LM 1a+b) lies southeast of Isola Madre close to the opening to the main basin. Towards the inflow of River Toce, two cores were taken in the basin centre (LM 2) and nearby the northern bank (LM 3). LM 4 was retrieved close to the southern shore line in the south of Isola Superiore. Two additional cores close to position LM 1, LM98 13A (Marchetto *et al.*, 2007) and P4 (Putyrskaya, Klemt & Röllin, 2009), were collected in previous years and are considered in this study for chronological purpose. The recent parts of the sediment cores are compared with data obtained from a sediment trap mooring installed in the northern part of the Pallanza Basin (Fig. 2.1c) during two hydrological cycles from October 2004 to May 2006 (Kulbe *et al.*, 2008). Two integrating sediment traps (Technicap, 500 cm^2) in 57 m and 117 m water depth collected sediment on a 7-day (summer) and 21-day basis (winter), respectively. The position close to core LM 3 provided information on the dynamics of autochthonous particle formation (diatoms, pigments, Cladocera) as well as on influx of allochthonous particles and pollutants (DDT, PCB, HCB, Hg) from the nearby tributary River Toce (Kulbe *et al.*, 2008).

2.3.2 Microfacies and geochemical analysis

Detailed micro-facies analyses were carried out on the uppermost 18 - 27 cm of each core (total length: 44 - 107 cm, Table 2.1) and the upper 72 cm of core LM 1a. Overlapping samples (10 cm x 2 cm x 1 cm) were taken from the fresh sediment surface of a split core from which thin sections were prepared according to Brauer & Casanova (2001). The sediment composition and textural features were analyzed descriptively under 12.5-100x magnification using a petrographic microscope (Carl Zeiss Axiophot). Semi-quantitative geochemical data were obtained by micro X-ray fluorescence (µ-XRF) measurements on the sediment slabs from thin-section preparation of the cores LM 1a (0 - 52 cm) and LM 3 (0 - 26 cm) in 100 µm steps, allowing direct comparison of geochemical and micro-facies data (Brauer *et al.*, 2009). Analyses were carried out using an EDAX EAGLE III XL µ-XRF spectrometer (EDAX, Mahwah, New Jersey, USA) with a low-power Rh X-ray tube at 40 kV and 300 µA. All measurements were performed under vacuum on a single scan line with 123 µm spot size and a counting time of 30 s. The fluorescent radiation emitted from the sample was recorded by an energy dispersive Si (Li) detector and transformed into element information for each measuring point. The resulting intensities for major elements (aluminium (Al), silicon (Si), potassium (K), calcium (Ca), titanium (Ti), iron (Fe), sulphur (S)) are given as counts per second (cps), reflecting relative changes in element composition.

2.3.3 Dating

The chronology of sediment cores was established by correlation to previously dated cores LM98 13A and P4. The age-depth model of core LM98 13A is based on ^{210}Pb measurements and historically documented biological and chemical markers, comprising changes in diatom composition in 1963 and 1989 (*Cyclotella* vs *Stephanodiscus* and *vice versa*) and an increase in nutrients and pigments in 1963 (Marchetto *et al.*, 2004; Guilizzoni *et al.*, 2012). The results of modelling the vertical ^{137}Cs distribution in core P4 were published by Putyrskaya *et al.* (2009).

Cross-correlation to the five cores of this study was done using 11 marker layers for the time period 1965 - 2006.

2.3.4 Instrumental data

Lago Maggiore lake level values have been collected daily since 1868 (data from the Consorzio del Ticino and from the meteorological station of Pallanza (CNR-National Research Council), 1951-present). For the entire observational period until 2006 Ambrosetti, Barbanti & Rolla (2006) inferred a total of 67 floods by lake levels exceeding 195.5 m a.s.l. at Pallanza. Discharge data of the main tributary River Toce were calculated to monthly means from river stage data, measured by the Institute of Ecosystem Study (CNR-ISE) at Candoglia gauge station since 1977 (Fig. 2.1b). For some years (1980, 1982, 1989, 1990, 1992, 1995, 1997, 1998, 1999) daily discharge data were not available. However, since the available monthly means of discharge do not indicate major floods during these periods, an effect of these gaps in the time series on this study is excluded.

2.4 Results

2.4.1 Lithology

Two main lithological units (I and II) have been distinguished in the Pallanza Basin sediment record in four of the five cores (Table 2.1, Fig. 2.2). The lower sediment unit I is characterized by a light greyish colour and the predominantly homogeneous clastic sediments consisting mainly of silt-sized mica, quartz and feldspar grains with scattered sand-sized grains clearly reflected in elevated count rates of Al, Si, K, Ca and Ti (Fig. 2.2). Al shows the most distinct peaks for detrital horizons and thus is used as a representative proxy for detrital matter. This is likely due to the abundance of Al-bearing mica in the micaceous schists and gneiss of the catchment. Correlation coefficients of r^2 >0.60 of Al with Si, K, Ca and Ti indicate that all these elements are mainly of detrital origin (Table 2.2). The biogenic silica within diatom frustules is best described by the Si/Al ratio (Francus *et al.*, 2009), because Si reflects both siliciclastic matter and biogenic components. Low values of Si/Al in sediment unit I reflect low biogenic silica contents, proven by diatom counts in core LM 1b, and therefore a low internal productivity, which is in good agreement with limnological data (Guilizzoni *et al.*, 2012). Fe shows weak correlation with detrital elements indicated by r^2 values ranging between 0.22 (Fe *versus* Si) and 0.29 (Fe *versus* Ti). Thus, Fe mainly reflects the lake internal iron cycle including early diagenetic formation of iron sulphides especially in organic-dominated intervals (O-sections in Fig. 2.2). The organic matter in these sections is mainly composed of plant macro-remains and amorphous organics. The mostly homogeneous clastic sediment unit I is intercalated by 1-12 mm thick light greyish layers (L in Fig. 2.2), which are optically hardly discernible from matrix sediments. Elevated count rates of detrital elements like Al, Ti and K suggest a detrital origin of these layers. Nineteen detrital layers were detected in sediment unit I in core LM 1a down to 72 cm sediment depth (Fig. 2.2).

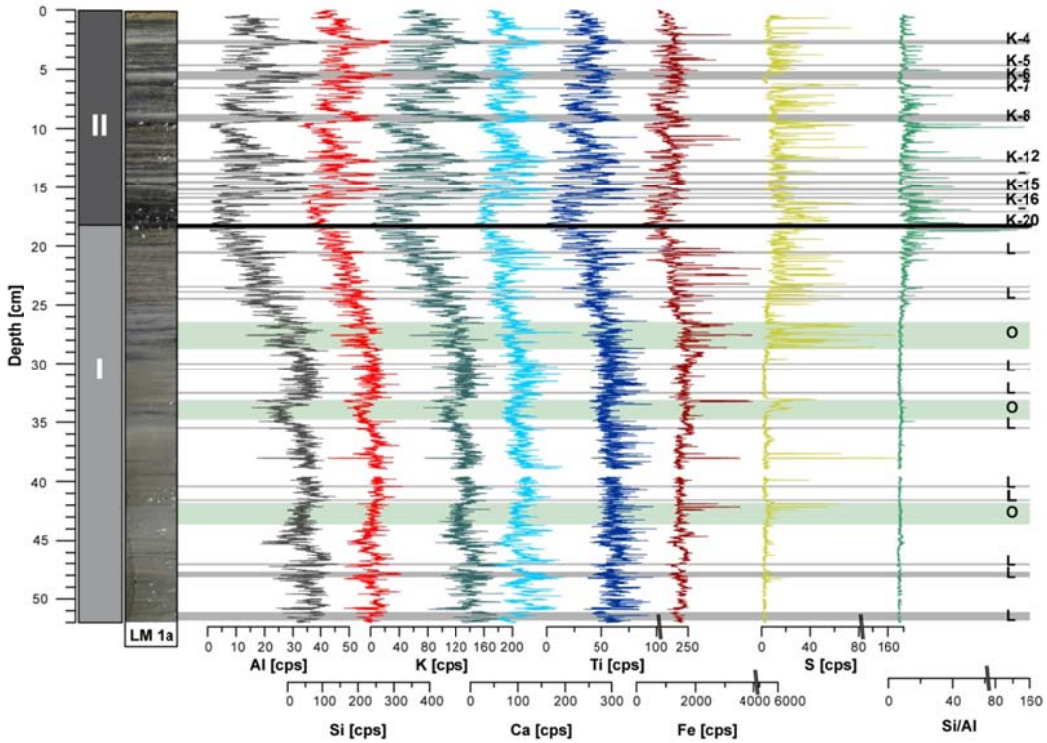

Figure 2.2. Lithology of the core LM 1a (0-52 cm) and micro X-ray fluorescence line scans of aluminium (Al), silicon (Si), potassium (K), calcium (Ca), titanium (Ti), iron (Fe), sulphur (S) and Si/Al ratios. Intensities are given in counts per second (cps). Grey bars mark detected detrital layers which are labelled with K in sediment unit II (correlated between different sediment cores) and with L in sediment unit I (not correlated). Bar thickness correspond to detrital layer thickness. Sediment unit I contains subsections enriched in organic matter which are labelled with O (green bars).

Table 2.2. Linear correlation (r^2-values) of major elements, measured with micro X-ray fluorescence line scanning (µ-XRF) at 100 µm resolution on impregnated sediment blocks from core LM 1a (0-52 cm sediment depth).

	Al	Si	S	K	Ca	Ti
Al						
Si	**0.91**					
S	0.21	0.25				
K	**0.89**	**0.81**	0.21			
Ca	**0.64**	**0.60**	0.13	**0.53**		
Ti	**0.68**	**0.63**	0.15	**0.68**	**0.56**	
Fe	0.26	0.22	0.04	0.27	0.23	0.29

Correlations between elements of predominantly detrital origin are written in bold.

A sharp boundary to the upper dark greyish sediment unit II occurs at various sediment depths between 18.5 cm at the distal site LM 1a and 27 cm close to the northern bank (LM 3, Fig. 2.3). The generally darker colour of sediment unit II is due to increased organic material as indicated by an increase in loss on ignition and total carbon in core LM 1b (Guilizzoni *et al.*, 2012) as well as higher abundances of diatom frustules observed in thin sections and determined in core LM 1b by Guilizzoni *et al.* (2012). Diatom frustules forming discrete layers ranging in thickness from 0.8 to 3.0 mm cause distinct peaks in the Si/Al profile (Fig. 2.2). Iron sulphides formed within the diatom layers induce peaks in Fe and S.

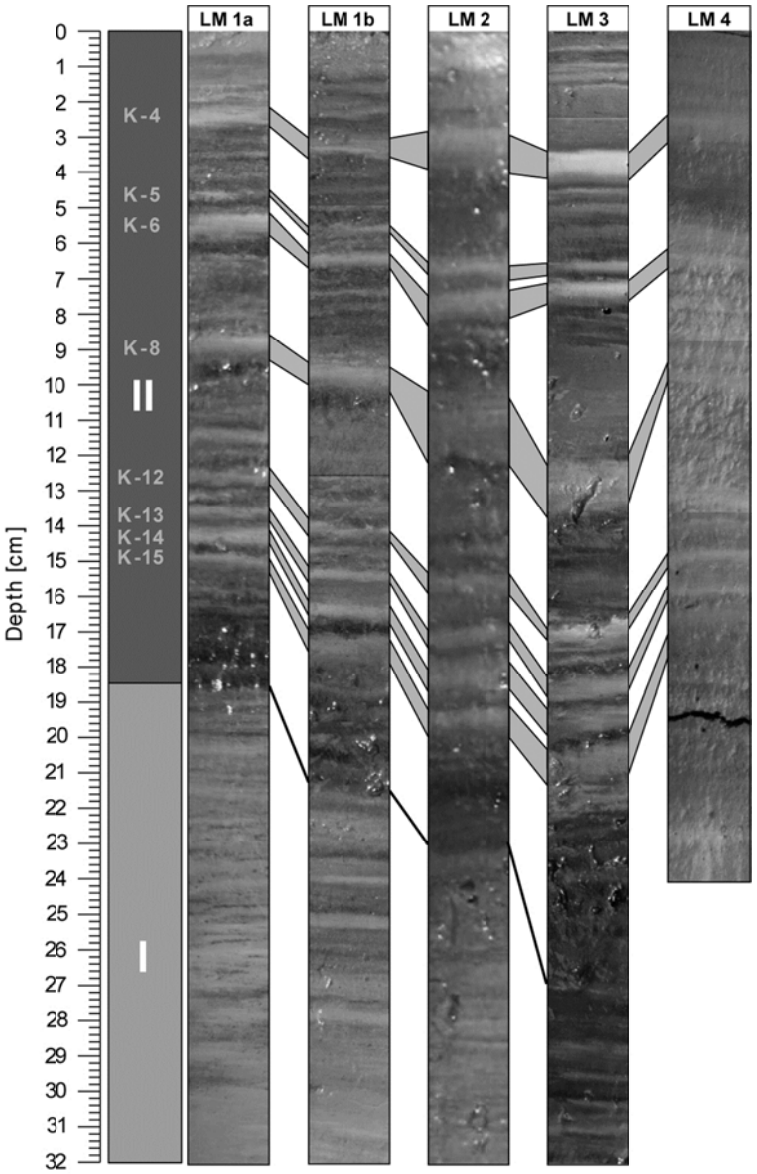

Figure 2.3. Intra-basin correlation of core sequences LM 1-4: linking eight distinct detrital marker layers in sediment unit II (K-4, K-5, K-6, K-8, K-12, K-13, K-14, K-15) and the boundary between sediment units I and II.

Sediment unit II is further characterized by an irregular sequence of 20 light-coloured detrital layers (K-1 - K-20). Eight of these layers (K-4, K-5, K-6, K-8, K-12, K-13, K-14, K-15) were macroscopically identified in various cores ranging in thickness from 1.5 to 17.4 mm (Fig. 2.3). All of these eight marker layers are characterized by a graded structure with maximum grain sizes up to 100 µm and abundant spherical quartz and feldspar grains in the basal part. Upwards within the layers mainly flat-shaped mica grains are accumulated. The top sections are formed either by fine silt or in some cases by clay. The lower boundary is sharp and the thickest layers (K-4, K-6 and K-8) show flame structures in the proximal core LM 2, due to micro-scale erosion (Mangili *et al.*, 2005). The succession of these layers exhibits a characteristic pattern, which is similar in each core (Fig. 2.3). In combination with the typical microfacies features this allows us to confidently correlate these layers in different cores (Sturm & Matter, 1978; Hsü & Kelts; 1985, Schiefer *et al.*, 2011).

Twelve thinner layers down to 0.6 mm thickness were detected with microscopic techniques only. In general, these layers are less distinctly graded and never have a clay top. Although they do not show comparable characteristics, these layers can be reliably correlated between different coring sites by their stratigraphic position within the succession of the eight main marker layers (Fig. 2.4).

Three thick layers occur each in one core only at sites closer to the banks (LM 3: depth: 2.9 cm/ thickness: 16.8 mm; 11.8 cm/ 28.8 mm; LM 4: 9.6 cm/ 6.4 mm). These local layers are matrix supported and contain minerogenic matter, abundant plant fragments and occasionally scattered iron sulphides inducing peaks in S counts (Fig. 2.4). In the basal part individual detrital grains >150 µm occur.

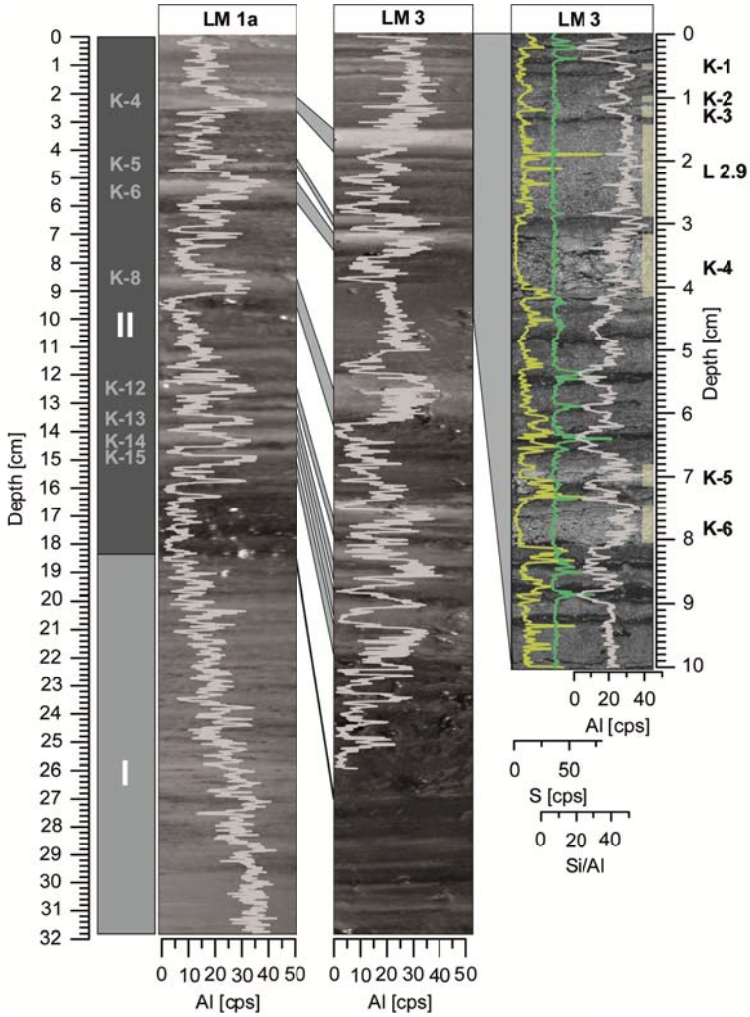

Figure 2.4. Core photographs of LM 1a (distal, southeast of Isola Marde) and LM 3 (proximal, near-shore) with an overlay of micro X-ray fluorescence line scans of Al and correlation of distinct marker layers K-4, K-5, K-6, K-8, K-12, K-13, K-14, K-15 and the transition between sediment units I and II. Right side: Thin-section scan from a standard flatbed scanner with polarising foil of the uppermost 10 cm of the near-shore core LM 3 showing detrital layers (K-1, K-2, K-3, K-4, K-5, K-6) and matrix-supported layers (L 2.9). Overlain are the Al line scan, reflecting intervals of enriched mineral matter, the sulphur (S) line scan (peaks indicate iron sulphides) and the Si/Al ratio, reflecting parts enriched in diatom frustuls.

2.4.2 Chronology

The chronology of the cores is based on detailed correlation of previously dated core sequences LM98 13A (^{210}Pb, biological and chemical markers, Marchetto *et al.*, 2004; Guilizzoni *et al.*, 2012) and P4 (^{137}Cs, Putyrskaya *et al.*, 2009) to the nearby core LM 1a (Fig. 2.1c), based on 11 well-defined marker layers (Fig. 2.5). Amongst these are (1) eight macroscopically visible discrete layers (K-4, K-5, K-6, K-8, K-12, K-13, K-14, K-15), (2) the distinct transition between sediment units I and II and (3) shifts in diatom assemblages due to changes in trophic status in 1963 (decrease in *Cyclotella* and increase in *Stephanodiscus*) and 1989 (*vice versa*) (Marchetto *et al.*, 2004, Guilizzoni *et al.*, 2012).

As a result an age-depth model was established for the cores LM 1a - LM 4. The age model of core LM 4 located close to the southern shore is based on fewer marker layers since the I/II transition and the marker layers K-5 and K-14 were not found.

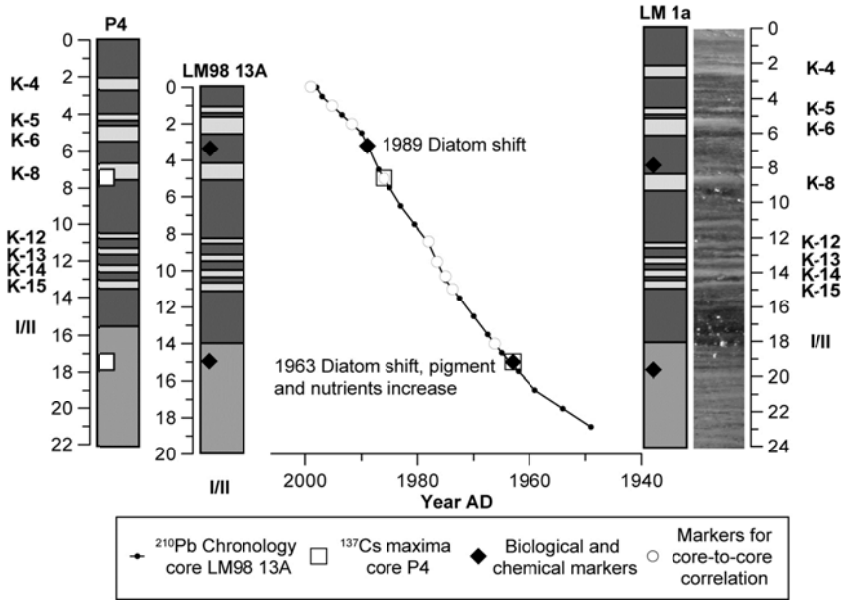

Figure 2.5. Chronology of LM 1-4 sediment cores based on correlation with previously dated cores: ^{210}Pb chronology of LM98 13A (CRS-model, small black dots, Marchetto *et al*., 2004), ^{137}Cs maxima 1963 and 1986 in core P4 (squares in the left core sequence, Putyrskaya *et al*., 2009), and two documented chemical and biological markers in LM98 13A (middle) and LM 1a (right core sequence) (black diamonds, Guilizzoni *et al*., 2012, Marchetto *et al*., 2004). Transferring the chronology to core LM 1a was done by using further nine distinctive lithological markers (circles in the age-depth-model): eight detrital layers (light layers in the profiles, thicknesses accord to LM 1) and the transition between sediment units I and II.

2.4.3 Spatial distribution of detrital layers

The grid of detrital layers reveals basin-wide distribution of detrital material. However, not all detrital layers are detected in each core sequence (Fig. 2.6). Cores LM 1b, located southeast of the island Isola Madre, and LM 3 close to the northern shore, include the most complete records with 19 detrital layers each. Sixteen detrital layers were found in the basin centre (LM 2), 14 at site LM 1a (nearby 1b) and eight in core LM 4 close to the southern shore.

Most of the detrital layers (75%) are thickest in the proximal cores LM 2 + 3, which are closest to the River Toce inlet. Layer thickness in the basin centre (LM 2) exceeds values in the more lateral core LM 3 in 62.5% of the cases. The decrease in layer thickness from proximal to distal sites is most prominent for the thickest layers K-4 and K-8 (LM 2 minus LM 1 = 7.0 - 12.0 mm) and gets smaller (2.0 - 5.0 mm) for thinner layers K-5, K-6, K-11, and K-12 to K-15. These layers occur in all cores except for K-12 (lacking in LM 1a+b), K-14 (LM 4) and K-11 which was detected solely in the proximal cores LM 2 and LM 3. Detrital matter of eleven thin layers, <3.0 mm at the proximal site LM 2, does not exhibit a clear spatial pattern (K-1 - K-3, K-7, K-9, K-10, K-16 - K-20). From these detrital layers only one appears in all cores (K-16). An exception for these general patterns is observed for local matrix-supported layers only occurring in near shore cores LM 3 and LM 4.

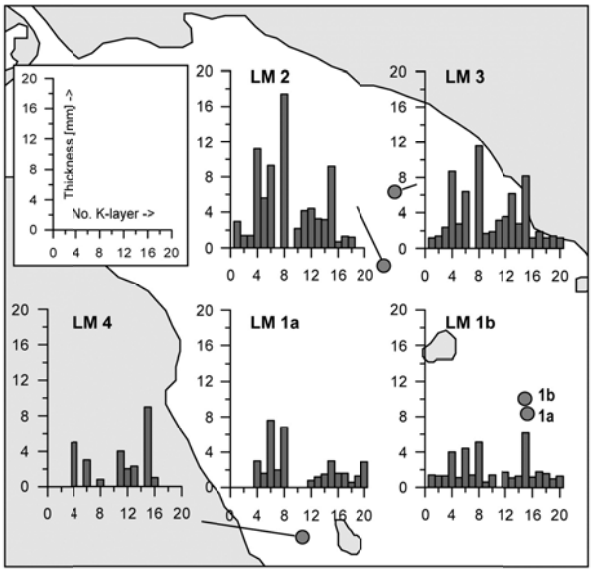

Figure 2.6. Thicknesses of detrital layers (K-1 - K-20) at the different coring sites in Pallanza Basin as measured in thin sections. Units are shown on the inset figure.

2.4.4 Comparison of the detrital layer record with instrumental data

Detrital layers and instrumental flood data are compared for the well-dated interval of sediment unit I since 1965 (Fig. 2.7). Using water level maxima >195.5 m a.s.l. at Pallanza as a flood indicator, a total of 22 floods were recorded in the period 1965 to 2006 (Ambrosetti *et al.*, 2006). The resulting mean recurrence interval of ca. two years is similar to the entire instrumental record since 1868 during which the lake level went beyond this level 67 times. Five of the six largest floods resulting in lake levels >197.0 m a.s.l. and 70% of all floods occurred in September-November.

During 1965 - 2006, 18 of the 20 detected detrital layers can be related to lake levels >195.5 m a.s.l. (Table 2.3, Fig. 2.7) suggesting that 82% of flood events, causing major lake level rise, are reflected in the sedimentary archive. Only two detrital layers (K-8: 194.9 m a.s.l., K-14: 195.4 m a.s.l.) cannot be correlated with the recorded dates of daily lake level maxima >195.5 m a.s.l.. Likewise, four lake level maxima >195.5 m a.s.l. are not represented by detrital layers.

An alternative definition of floods is through daily river discharge. For the period with available instrumental data from 1977-2006 maximum daily discharge of River Toce exceeded 600 m^3s^{-1} during 18 events matching with 86% of lake level maxima >195.5 m a.s.l. (Table 2.3). The recurrence time of ca. 1.7 years is slightly less than that of the lake level. In 1977 to 2006 15 detrital layers (K-1 - K-15) were identified in the sediment record of which 13 can be correlated to floods as defined by discharge maxima (72% of all events) (Table 2.3, Fig. 2.7). Two thin detrital layers K-9 and K-10 correspond to discharges below the threshold (241 m^3s^{-1}, 427 m^3s^{-1}), while for five discharge events >600 m^3s^{-1} no corresponding detrital layers have been found.

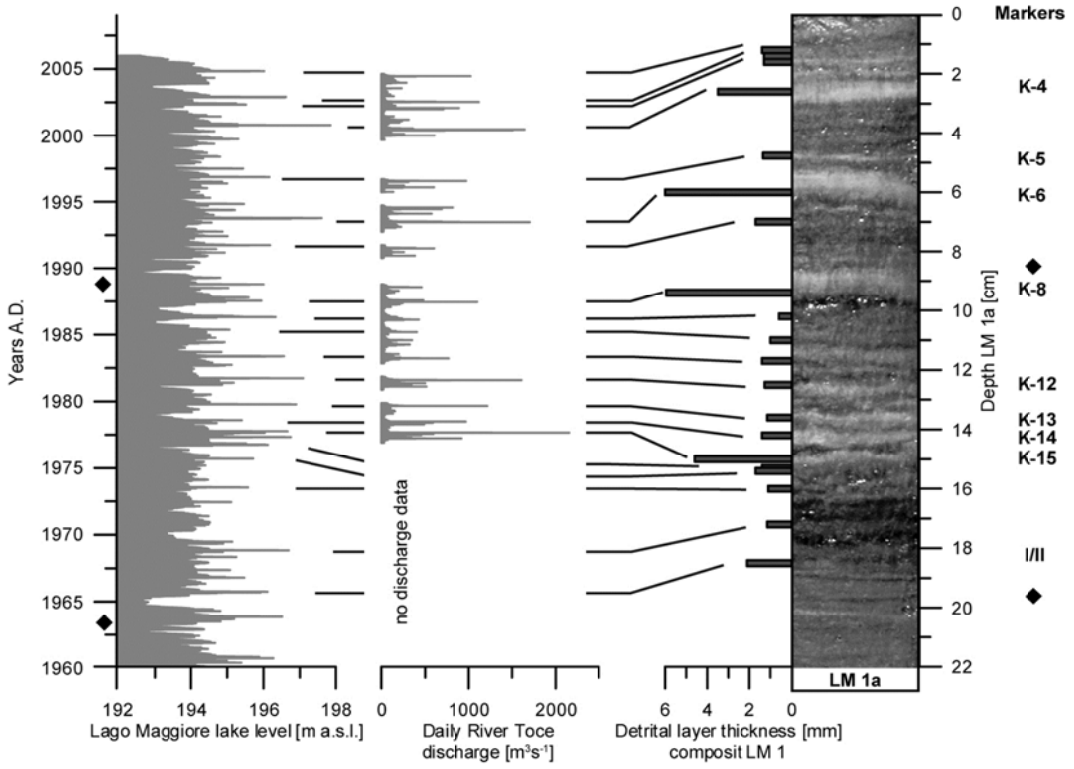

Figure 2.7. Alignment of the composite record of detrital layers in core sequences LM 1a+b (dark bars, right) with daily Lago Maggiore lake level and River Toce discharge data (light bars, left). The photo shows core LM 1a with the position of the 11 lithological markers used for dating the core sequences. Diamonds mark two distinct shifts in diatom composition documented in Marchetto *et al*. (2004) and Guilizzoni *et al*. (2012).

Combining both data sets reveals a number of 12 events with lake level and river discharge maxima exceeding the threshold values. Each flood event coincides to a detrital layer instead of one in May 1977 (lake level: 196.75 m a.s.l.; river discharge: 919.50 m^3s^{-1}).

Lake level and discharge maxima were compared with the thickness of detrital layers as measured in thin sections for each core (Fig. 2.8). No correlation is found between layer thickness and lake level maxima (r^2=0.00 - 0.08; p>0.45). For discharges, however, r^2 values vary considerably between different coring sites and are highest in the most complete core sequences LM 1b (distal): r^2=0.50 (N=14; p<0.01) and LM 3 (proximal): r^2=0.41 (N=14; p<0.01). A moderate correlation was found at the proximal site LM 2 (r^2=0.27; N=13; p<0.1). At the two distal sites with the fewest detrital layers significance sharply decreases below

the 90% level (p>>0.1) and correlations vary from a moderate value at site LM 4 (r^2=0.34; N=7) to no correlation at site LM 1a (r^2=0.03; N=9).

2.5 Discussion

2.5.1 Processes of detrital layer deposition

Detrital layers are thickest at sites LM 2 and LM 3, closest to the River Toce inlet (Fig. 2.1c) confirming the Toce as the main source of detrital sediment flux. Traces of micro-scale erosion at the base of two thick detrital layers K-6 (1993) and K-8 (1987) in the proximal core LM 2 indicate that during large floods the sediment-laden river water moves as a sub-surface high density turbidity current along the central axis of the basin (Sturm & Matter, 1978; Mulder & Alexander, 2001). This interpretation has been proven for layer K-1 (Table 2.3) by monitoring sediment flux during the October/November 2004 flood at a location close to LM 3 (Fig. 2.1c, Kulbe *et al.*, 2008) revealing strongly elevated flux rates in a near-bottom sediment trap. The observed thinning of detrital layers distally reflects the decrease in flow velocity of the turbidity current (Ludlam, 1974, Siegenthaler & Sturm, 1991). This effect is probably enhanced at the distal core locations LM 1a+b and LM 4 due to their leeward position south of Isola Madre and Isola Superiore, respectively.

Table 2.3. Data on 27 instrumentally recorded flood events 1965-2006 (left): date, water level at Pallanza and maximum daily discharge of River Toce. Right: thickness of 20 detrital layers correlated between different coring sites in Pallanza Basin and aligned to flood events 1965-2006.

Hydrological data			Detrital layers in short cores LMA06					
Date of maximum water level	Water level (m a.s.l.)	Maximum daily discharge ($m^3 s^{-1}$)	Name	LM 1a (mm)	LM 1b (mm)	LM 2 (mm)	LM 3 (mm)	LM 4 (mm)
03/11/2004	**196.02**	**1024.50**	K-1		1.4	3.0	1.2	
29/11/2002	**196.61**	**1117.74**	K-2		1.3	1.4	1.4	
07/06/2002	195.25	**889.26**						
05/05/2002	**195.52**	**707.00**	K-3		1.3	1.4	2.4	
16/10/2000	**197.86**	**2521.80**	K-4	3.0	4.0	11.2	8.7	5.0
30/04/2000	194.65	**605.20**						
14/11/1996	**196.16**	**973.10**	K-5	1.6	1.1	5.6	2.8	
07/11/1994	195.46	**813.10**						
24/09/1994	194.35	**687.10**						
14/10/1993	**197.61**	**1703.20**	K-6	7.6	4.4	9.3	6.4	3.0
01/10/1991	**196.18**	**600.96**	K-7	2.0	1.4			
15/10/1988	**196.00**	458.36						
17/10/1987	**195.59**	477.17						
25/08/1987	194.91	**1100.00**	K-8	6.8	5.2	17.4	11.6	0.8
20/07/1987	**195.94**	240.69	K-9		0.6		1.7	
27/04/1986	**196.33**	427.47	K-10		1.4	2.2	1.9	
23/05/1983	**196.57**	**766.60**	K-11			4.2	3.2	4.0
28/09/1981	**197.09**	**1607.00**	K-12	0.8	1.8	4.4	3.6	2.0
17/10/1979	**196.90**	**1216.00**	K-13	1.2	1.1	3.3	6.2	2.3
09/08/1978	195.40	**968.30**	K-14	1.5	1.3	3.2	2.8	
10/10/1977	**196.66**	**2153.10**	K-15	3.0	6.2	9.2	8.2	9.0
31/08/1977	**196.03**	590.90						
05/05/1977	**196.75**	**919.50**						
05/10/1976	**196.12**	no data	K-16	1.6	1.2	0.7	1.2	1.0
17/09/1975	**195.71**	no data	K-17	1.6	1.8	1.3	1.9	
18/07/1973	**195.57**	no data	K-18	0.6	1.6	1.2	1.2	
04/11/1968	**196.69**	no data	K-19	1.3	1.0		1.4	
02/10/1965	**196.11**	no data	K-20	2.9	1.3		1.2	

Flood events are written in bold, if exceeding the threshold of an event with a recurrence of ca. 2 years: lake levels >195.5 m a.s.l. (Ambrosetti *et al*., 2006) and daily mean discharges >600 $m^3 s^{-1}$.

During minor floods, the river water is less dense due to lower contents of suspended matter. After entering the lake the suspension likely moves as low-density over- or interflows (Mulder & Alexander, 2001, Sturm & Matter, 1978) causing a more random distribution of slowly sinking fine particles by lake internal currents and thus the absence of a clear proximal-distal pattern of thin detrital layers.

Three detrital layers appear only in one of the two cores close to the northern (LM 3) and southern shore (LM 4) (Fig. 2.3). The thickness (16.8-28.8 mm in LM 3) and specific microfacies of these layers (matrix-supported: sand-sized particles, organic plant macro-remains) indicates short-range transport of littoral sediments from the steep lateral slopes, probably driven by local debris flows (Hsü & Kelts, 1985; Anselmetti *et al.*, 2007; Swierczynski *et al.*, 2009). Thus, local processes including slope instability rather than regional flooding triggered the deposition of these layers.

2.5.2 Effects of flooding on the lake system

The impact of floods on the lake itself is strongly related to fluvial sediment transport considered to play important ecological and water quality roles by attenuating light and influencing metabolic activity (Effler *et al.*, 2006). These effects are, however, difficult to quantify (Guilizzoni *et al.*, 2012). Strongly decreasing concentrations of chlorophyll-*a* and filter-feeding zooplankton were observed after flood events in Lago Maggiore in the 1950s (Vollenweider, 1956) and in the 1970s (Ambrosetti *et al.*, 1980), most likely due to the increased turbidity (Guilizzoni *et al.*, 2012). Coarse silt and sand grains sink quickly and thus affect water clarity only to a minor degree, whereas clay particles have a stronger impact on the lake ecosystem due to their large active surface and long residence time in the upper water column. Fishermen report that clay covers their nets even several months after major flood events. High clay amounts are found on top of detrital layers triggered by large floods, e.g. in 1977, 1979, 1987, 1993 and 2000. Similar to total sediment load, fluxes of nutrients and pollutants are highest during flood events (Guilizzoni & Calderoni, 2007; Kulbe *et al.*, 2008) which might have a fertilizing effect resulting in ‘eutrophication pulses’ (Manca *et al.*, 2007). Such effects have been reported from lakes (e.g. Agren *et al.*, 2008) and coastal areas (e.g. Brodie *et al.*, 2010), but were not observed during the monitored Maggiore flood in November 2004 (Kulbe *et al.*, 2008).

2.5.3 Correlating the detrital layer record to instrumental data

Since the definition of thresholds for floods in instrumental time series implies a number of inherent uncertainties (Petrow & Merz, 2009), we compared the detrital layer record of the well-dated core section from 1965 to 2006 with two independent instrumental data sets, (1) daily lake levels recorded at Pallanza station and (2) maximum daily River Toce discharges recorded at Candoglia gauge station. Both instrumental data sets were combined (Table 2.3) to test the hypothesis of flood-triggered deposition of detrital layers. In total, 23 ‘instrumental floods’ occurred in the period of which both data sets are available

(1977-2006). Twelve of these appear in both time series, while five exceed threshold values only in the lake level data and six in river discharge data.

All 20 detrital layers identified in the sediment record during 1965-2006 can be correlated to flood events, thus proving flood-triggered deposition and excluding other causes like sediment reworking. For the period covered by both instrumental data series (1977-2006) we found that two detrital layers correlate to floods only in the lake level data (K-9, K-10) and two others (K-8, K-14) only to floods as defined by discharge data. This emphasizes the complex relations between instrumental floods and detrital layer deposition.The formation of detrital layers K-9 and K-10 during floods with maximum daily discharge below 600 m^3s^{-1} shows that factors other than maximum discharge, such as flood duration, must be considered as well. Layer K-10 is related to the April 1986 flood when river discharge was elevated for three weeks due to snow melt, but did not exceed daily discharge maxima >427 m^3s^{-1}. Interestingly, the detrital layers triggered by such type of floods are comparably thin and not deposited at all coring sites (Table 2.3).

Two thicker detrital layers (K-8, K-14) were deposited during floods with maximum daily discharge clearly above the defined threshold which, however, did not result in lake levels exceeding the threshold of 195.5 m a.s.l., but fell short of this value only by 0.6 and 0.1 m, respectively. One reason for this observation is the base lake level preceding a flood. In case of very low water levels before a major flood even intense river discharges might not be sufficient to raise the level above the threshold. Moreover, it must be taken into account that the lake level is not solely determined by River Toce discharges (catchment size: 1551 km^2) but also by the other tributaries of Lago Maggiore (total catchment size: 6599 km^2). Other factors include different response times of river discharge (fast) and lake level (slow) to extremes in precipitation.

2.5.4 Completeness of the detrital layer record

Besides proving that detrital layers are triggered by regional floods, interpreting lake sediments as flood archives requires knowledge of the 'completeness' of a detrital layer record, *i.e.* the number of floods which are not recorded in the sediment record as well as possible reasons for the lack of detrital deposition. From the 28 instrumental recorded floods during the period 1965-2006, 20 triggered the deposition of a detrital layer (71%). The eight most intense discharge events (>1000 m^3s^{-1}) all are reflected in the sediments. These results are very similar to earlier published data from Lake Ammersee at the northern alpine margin (Czymzik *et al.*, 2010). Five of the eight floods that did not lead to detrital layer formation can be explained by multiple flooding in one year (1977, 1987, 2000, 2002). It can be assumed that detrital matter of the first flood stayed in suspension and mixed with the suspended matter of subsequent floods 1-6 months later. Depending on lake water density fine to medium-sized silt grains can stay in suspension over several weeks to months, assuming a settling velocity of ca. 1-2 m d^{-1} (Bloesch & Sturm 1986; Perkins *et al.*, 2007). In addition, the strongest floods in October 1977, 1993 and 2000 triggered major turbidity currents that might have reworked surface deposits of preceding floods as indicated by two missing detrital layers below the thickest deposits K-6 and K-8 in the proximal core LM 2.

Finally, for three minor floods the lack of a corresponding detrital layer in any of the cores remained unexplained. These are two floods in September and November 1994 with maximum daily River Toce discharges not exceeding 820 m^3s^{-1} and lake levels up to 1.1 m below the threshold value and the October 1988 flood with maximum discharge below (458 m^3s^{-1}), but a lake level 0.5 m above the flood threshold.

'Missing' detrital layers, whether not deposited, not preserved or not detected, are metioned only in few lake-based palaeoflood studies (Siegenthaler & Sturm, 1991; Lamoureux, 2000; Gilli *et al.*, 2003; Swierczynski *et al.*, 2009; Støren *et al.*, 2010; Czymzik *et al.*, 2010; Schiefer *et al.*, 2011) but possible reasons for such observations mostly remain speculative.

2.5.5 Detrital layer thickness vs. flood amplitude

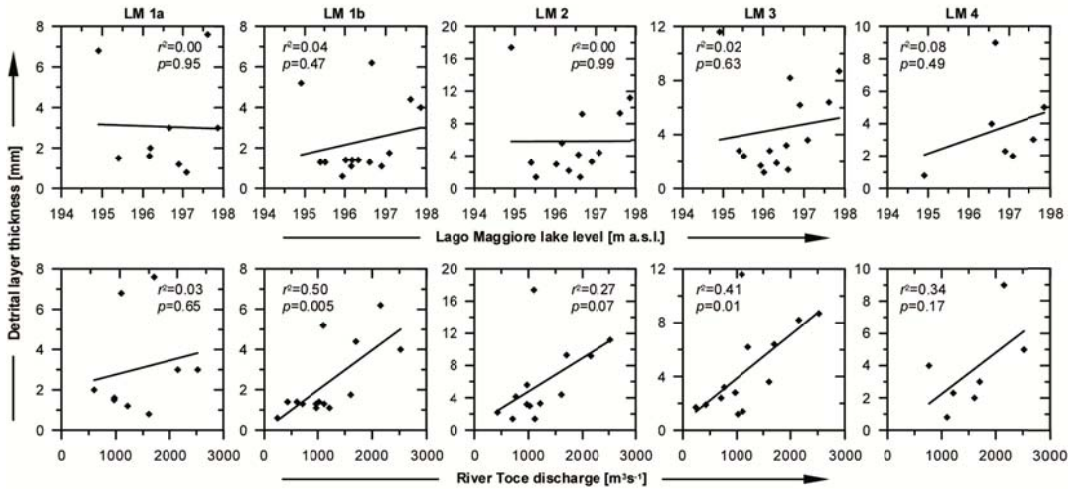

Figure 2.8. Correlation of maximum values of daily Lago Maggiore lake level and River Toce discharge with detrital layer thickness in cores of Pallanza Basin (K-1 – K-15, 1977-2006: LM 1a (N=9), LM 1b (N=14), LM 2 (N=13), LM 3 (N=14) and LM 4 (N=7).

Detrital layer thickness is highly variable in Pallanza Basin sediments raising the question of a possible relationship between layer thickness and flood size. The obvious hypothesis assumes that the amount of transported sediment is a measure of the amplitude of a flood (Lamoureux, 2000; Lamb, 2010; Schiefer *et al.*, 2011). In the Lago Maggiore record, detrital layer thickness moderately correlates with discharge data at locations with more than ten detrital layers related to instrumental floods (LM 1b, LM 2 and LM 3; r^2=0.27 - 0.50) and three of the four thickest detrital layers (K-4, K-6, K-15) in these cores are related to the three flood events with the highest discharge maxima (>1700 m^3s^{-1}) in 2000, 1993 and 1977. However, this obviously does not describe a linear relationship as evidenced by layer K-8. This is by far the thickest detrital layer in the record (Table 2.3), and was triggered by only the sixth-strongest flood event (Table 2.3) indicating that sediment delivery is not solely governed by peak discharges. The duration of a flood and processes in the sediment source area including the availability of erodible material (Lamoureux, 2000, Schiefer *et al.*, 2011), sediment storage in the catchment and local erosion events might also play a role. If the exceptional

K-8 layer is excluded, the correlation becomes much better especially in the proximal basin ($r^2_{LM\ 2}$=0.75, $r^2_{LM\ 3}$=0.67, $r^2_{LM\ 1b}$=0.66). Concerning only least intense floods <710 m^3s^{-1} no correlation is found at any site due to randomly distributed thin detrital layers (K-2, K-3, K-9, K-10), which relate to wide spreading of low density over- or interflows.

In summary, the observed stochastic relation between layer thickness and flood size depends on (1) factors controlling amounts of inflowing stream water and sediment (2) basin morphometry and the coring location within the lake with respect to the inflow and (3) individual events due to the small number of observed flood events ($N_{LM\ 1b,\ LM\ 2,\ LM\ 3}$ =13-14). At locations with fewer detrital layers no correlation can be found or is not reliable ($p_{LM\ 1a,\ LM4}$ >>0.10). Last but not least, local conditions at the coring sites can also influence the deposition and preservation of detrital layers as inferred from the differences observed for the detrital layer records of the two neighbouring sites LM 1a and LM 1b. This might explain why in some lake records a relation between flood amplitude and detrital layer thickness has been found (Schiefer *et al.*, 2006; 2011) while in others it has not been observed (Swierczynski *et al.*, 2009; Czymzik *et al.*, 2010).

2.5.6 Extending the flood layer record in time

Extending the detrital layer time series further back in time in the Lago Maggiore sediments faces two major difficulties, (1) the lack of a precise age model for the lower part of the lake sediment record, and, (2) higher minerogenic contents in the background sediment which confounds the recognition of thin detrital layers in particular. A gross attempt based on an age model derived from simple extrapolation reveals that the most distinct detrital layers at 24.4 cm, 32.5 cm, 40.5 cm and 52.0 cm depth in core LM 1a (L in Fig. 2.2) are likely related to measured flood events with lake level high stands >196.0 m a.s.l. in the years 1951, 1939, 1928 and 1907, respectively (Fig. 2.9). The most distinct, 12.0 mm thick detrital layer at 72.0 cm sediment depth in LM 1a (71.0 cm in LM 1b) likely relates to the well-known historical flood event in October 1868 that caused the highest lake level ever measured for Lago Maggiore (199.8 m a.s.l.).

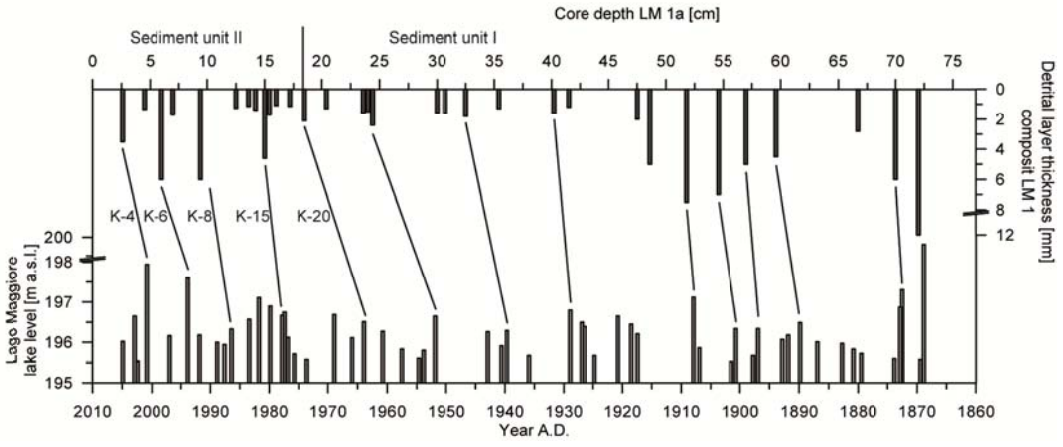

Figure 2.9. Alignment of the composite record of detrital layers in core sequences LM 1a+b (dark bars) to daily Lago Maggiore lake level high stands (light bars) back to 1868.

2.6 Conclusions

Sediments of Lago Maggiore have been shown to be a suitable archive for detailed flood frequency reconstruction. Therefore, it is necessary to apply an integrated approach combining instrumental monitoring data and detailed sediment analyses. Even thin flood layers can be detected by a new combination of micro-facies analyses on thin sections and μ-XRF element scanning. Deriving amplitudes of floods from sediment data is not straightforward and requires a good spatial coverage of cores within the lake basin to reconstruct sediment pathways.

So far, there is only little information on the impact of floods on lake ecosystems. For a better deciphering of the effects of floods and related sediment fluxes future project design should additionally include biomarker analyses (e.g. diatoms, pigments, Cladocera).

Acknowledgements. This study was supported by the EU Eurolimpacs project (GOCE-CT-2003-505540), by the Contract of the Swiss-Italian Commission for Lago Maggiore waters (CIPAIS) and by the Federal Ministry for Education and Research (BMBF) via the Potsdam Research Cluster for Georisk Analysis, Environmental Change and Sustainability (PROGRESS), part A.3 “Extreme events in geoarchives”. Angelo Rolla and Marzia Ciampittiello provided the data on River Toce discharges. We further thank Dieter Berger and Gabi Arnold for preparation of thin sections. Constructive comments from the editors and from two anonymous reviewers helped to improve the manuscript.

3 Processes of flood-triggered detrital layer deposition in the varved Lake Mondsee sediment record revealed by a dual calibration approach

Lucas Kämpf, Achim Brauer, Tina Swierczynski, Markus Czymzik, Philip Mueller, Peter Dulski

Helmholtz-Centre Potsdam – German Research Centre for Geosciences (GFZ), Telegrafenberg, 14473 Potsdam, Germany

Published in Journal of Quaternary Science

Abstract A succession of 23 sub-millimetre to maximum 12 mm thick, mostly flood-triggered detrital layers, deposited between 1976 and 2005, was analysed in 12 varved surface sediment cores from meso-scale peri-alpine Lake Mondsee applying microfacies and high-resolution micro-XRF analyses. Detailed intra-basin comparison of these layers enabled identification of (i) different source areas of detrital sediments, (ii) flood-triggered sediment flux and local erosion events, and (iii) seasonal differences of suspended flood sediment distribution within the lake basin.

Additional calibration of the detrital layer record with river discharge and precipitation data reveals different empirical thresholds for flood layer deposition for different parts of the basin. At proximal locations detrital layer deposition requires floods exceeding a daily discharge of 40 m^3s^{-1}, whereas at a 2 km more distal location an hourly discharge of 80 m^3s^{-1} and at least 2 days of discharge above 40 m^3s^{-1} is necessary. Furthermore, we observe a better correlation between layer thickness and flood amplitude in the depocentre than in distal and proximal areas of the basin. Although our results are partly site-specific, the applied dual calibration approach is suitable to precisely decipher flood layer formation processes and, thereby, improve the interpretation of long flood time series from lake sediments.

3.1 Introduction

Detrital layers in lake sediments are valuable recorders of extreme river floods (Siegenthaler and Sturm, 1991; Chapron *et al.*, 2005; Gilli *et al.*, 2013) and thus increasingly used to establish continuous long flood chronologies reaching several millennia back in time (Arnaud *et al.*, 2005; Lauterbach *et al.*, 2012; Czymzik *et al.*, 2013; Swierczynski *et al.*, 2013). The recurrence intervals of detrital layers provides information about palaeoflood frequencies (Czymzik *et al.*, 2010; Glur *et al.*, 2013), whereas flood intensities have been inferred from the thickness of individual deposits (Desloges and Gilbert, 1994; Brown *et al.*, 2000; Wilhelm *et al.*, 2013). Varved sediment records provide the unique opportunity to date detrital layers with seasonal precision (Mangili *et al.*, 2005) and, thereby, determine palaeoflood variability even at seasonal scale (Lamoureux, 2000; Czymzik *et al.*, 2010; Swierczynski *et al.*, 2012; Wirth *et al.*, 2013).

Despite the great potential especially of varved lake sediments for reconstructing long flood time series, there are still some confinements in interpreting detrital layer records due to a lack in understanding the complex chain of processes from an extreme rainfall event to the deposition of a fine layer of eroded catchment material on the lake floor. One important issue under discussion is the completeness of detrital layer flood time series. Detailed comparisons with instrumental hydrological data have revealed that detrital layer records can be biased by individual layers triggered by local erosion events rather than by floods (Kämpf *et al.*, 2012b; Swierczynski *et al.*, 2012; Simonneau *et al.*, 2013) and by individual flood events that are not recorded in the sediments (Lamoureux, 2000; Gilli *et al.*, 2003; Swierczynski *et al.*, 2009; Czymzik *et al.*, 2010; Schiefer *et al.*, 2011). Moreover, there is a lack of knowledge about the internal distribution of detrital sediments within lake basins, which, however, is important to determine the best coring location for flood reconstruction.

To better decipher processes of detrital flood layer deposition in lake sediments, several approaches have been initiated including in situ monitoring of flood triggered sediment fluxes (Cockburn and Lamoureux, 2008; Crookshanks and Gilbert, 2008) and detailed comparisons of single flood deposits with instrumental flood data (Gilbert *et al.*, 2006; Schiefer *et al.*, 2006; Kämpf *et al.*, 2012a). Here we present a new dual calibration approach for the detrital layer record from varved sediments of Lake Mondsee (Upper Austria) covering the Mid- to Late Holocene (Swierczynski *et al.*, 2013). This approach integrates (i) precise intra-basin correlation of detrital layers along transects from three near delta locations to a deep water distal site applying microscopic techniques, and, (ii) event-based calibration of detrital flood layers with precipitation and river discharge data over a 30-year period. The main goal of this study is to investigate the relations between hydrological conditions and detrital layer deposition and therewith to evaluate: (i) threshold values for detrital layer deposition, (ii) the completeness of flood layer records in dependence from their location within the lake basin and

(iii) the causes for flood events not leading to detrital layer deposition. Therewith we aim at an improved understanding of detrital layer deposition in Lake Mondsee and reconstruction of past flood variability with general relevance also for flood reconstructions from other lacustrine sediment records.

3.2 Study site

Lake Mondsee is located at the northern fringe of the European Alps in Upper Austria (47°48'N, 13°23'E) at an altitude of 481 m above sea level (a.s.l.). With a surface of 14 km^2 the lake represents a meso-scale peri-alpine lake which is by a factor of 2-3 smaller than the previously studied peri-alpine lakes Brienz, Bourget and Ammersee and even by a factor of 40 smaller than the largest peri-alpine lakes Geneva and Constance. Lake Mondsee has a maximum water depth of 68 m and is a meromictic hardwater lake with one mixing period in autumn/winter. A thermal stratification of the lake water column is established from May to September (Dokulil and Skolaut, 1986). Lake Mondsee has a specific shape which is different from other peri-alpine lakes and displays a significant kink in the generally elongated and NW-SE directed shape (Fig. 3.1c). In addition, the main tributary and source for suspended sediments, the Griesler Ache, flows into the lake from the West at the kink position where the lake basin is N-S directed so that the continuation of the water flow in the lake is not, as in the other peri-alpine lakes, directed straight to the outflow but makes a 90° turn.

The catchment (247 km^2) is subdivided into two major geological units by a main alpine thrust fault (van Husen, 1989) following the southern shoreline of the lake (Fig.1b). The northern catchment (ca. 75% of the total catchment) is formed by smooth peri-alpine hills of up to 1100 m a.s.l. which are built up by Cretaceous Flysch sediments (Sandstone, Argillite). The valleys are covered by moraines formed by latest Pleistocene glacier activity (van Husen, 1989). Three tributaries drain the northern catchment: the main inflow Griesler Ache in the West draining an area of 109 km^2 and forming a distinct delta as well as Zeller Ache in the North and Wangauer Ache in the East. The southern sub-catchment (ca. 25%) reaches a maximum elevation of 1700 m a.s.l. and belongs to the Northern Calcareous Alps. The base rock is composed of Jurassic and Triassic units of limestone and dolomite forming steep slopes at the southern lake shoreline which are drained by small torrents, e.g. the Kienbach creek with a catchment of 2.1 km^2 (Fig. 3.1c). The outflow of Lake Mondsee is located at the south-eastern end of the lake and drains the lake via the river Seeache into Lake Attersee (Fig. 3.1c).

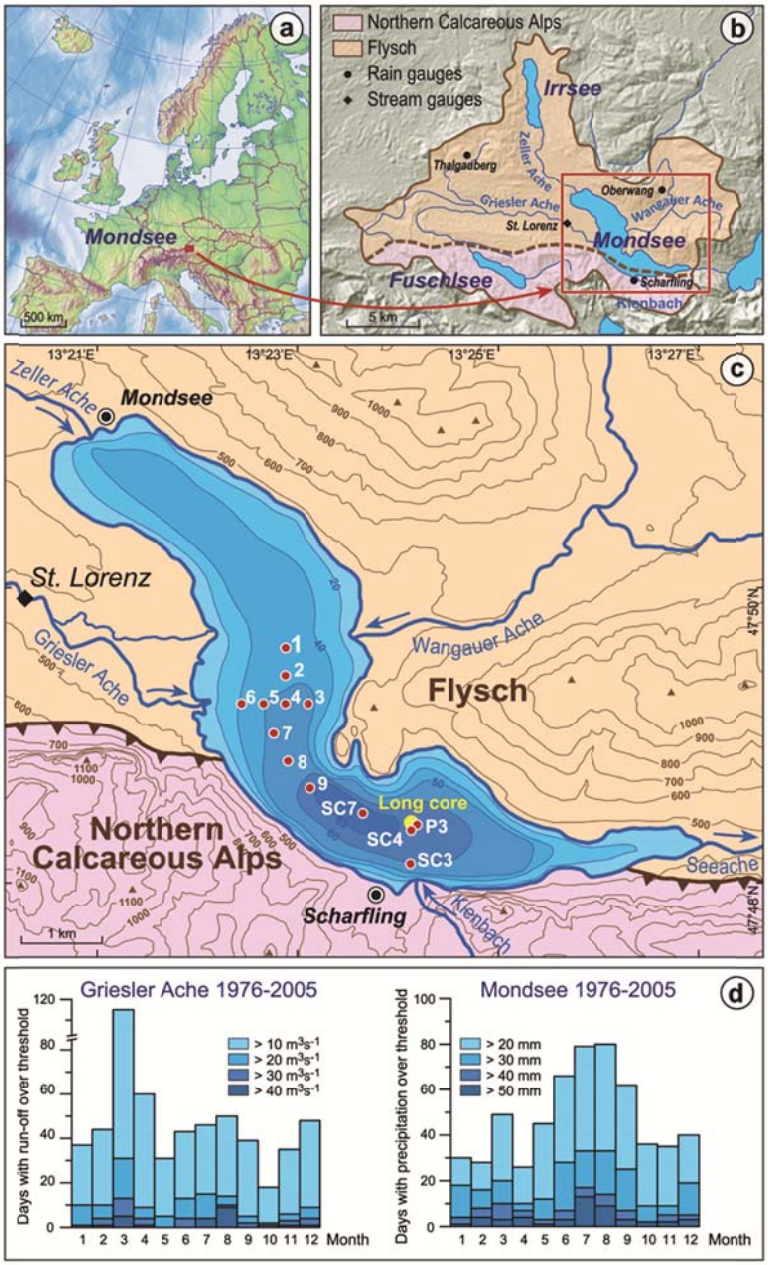

Figure 3.1. Lake Mondsee study site and climatic situation: (a) location, (b) Lake Mondsee catchment: dots indicate rain gauges and the stream gauge at Griesler Ache, (c) Bathymetric map of Lake Mondsee: dots indicate short cores retrieved in 2010 (1-9), 2007 (SC3-7), 2005 (P3 + long core profile), Fig. 3.1 a-c modified after Lauterbach *et al.* (2011), (d) monthly distribution of runoff events (left, Griesler Ache) and precipitation events (right, Mondsee).

The mean annual air temperature at climate station of Mondsee (reference period 1971-2000) is 8.7 °C with temperatures of -0.5 °C and +17.5 °C in January and July, respectively. The mean annual precipitation is 1550 mm and shows maxima during summer (Fig. 3.1d). Accordingly, floods mainly occur in summer and subordinated in early spring and rarely in winter. In summer, floods are triggered by short-term intense precipitation. The typical circulation pattern, reasonable for ca. 70% of the most extreme summer floods, is a low pressure cell or trough over Central to Western Europe (Tab. 3.2) generating a flow of very moist air from the Mediterranean Sea (Parajka *et al.*, 2010). This weather type is known as "Vb"-

type (Petrow *et al.*, 2009), and triggers the most extreme floods in Central Europe (Mudelsee *et al.*, 2004; Petrow *et al.*, 2009). The remaining events (ca. 30%) are related to northerly and westerly storm tracks (Tab. 3.2). Strong spring and winter floods are caused by precipitation events and associated rapid melting of snow. Frontal rainfall in that time is usually triggered by westerly circulation patterns (Tab. 3.2) carrying warm and moist air masses from the Atlantic Ocean (Petrow *et al.*, 2009; Parajka *et al.*, 2010).

3.3 Methods

13 short cores were recovered from Lake Mondsee (Fig. 3.1c) during three coring campaigns (2005, 2007, 2010) using a UWITEC Gravity Corer (60 and 90 mm in diameter). These cores are 72 to 160 cm long and have been collected in water depths between 34 m and 65 m (Tab. 3.4) following three transects along the steepest slope gradients in order to distinguish sediment source areas: (i) from the main inflow, Griesler Ache, to the long master core sequence used for establishing a long flood layer record (Swierczynski *et al.*, 2013); (ii) between the main (Griesler Ache) and the secondary (Wangauer Ache) tributary; (iii) from the Kienbach creek inflow draining the steep southern catchment into the southern part of the lake basin close to the location of the master core.

After cutting the sediment cores into two halves, lithological description and digital photographs on the split core surface were carried out. Overlapping samples for large-format (10 cm x 2 cm) thin sections for micro-facies analyses were taken from the fresh sediment surface. Thin sections were prepared according to the method described by Brauer and Casanova (2001). Microfacies analyses have been carried out under plain and polarized light conditions and magnifications between 20x and 400x, using a petrographic microscope (Olympus BX53). Thin-section images were obtained with a digital camera (Olympus DP72) and the software Olympus CellSens Dimension.

Micro- X-ray fluorescence (µ-XRF) scanning has been conducted to the upper 26 cm of cores MO/10/1, 4, 5, 7, 8, 9, MO/07/SC3 and MO/05/P3 using an EAGLE III XL µ-XRF spectrometer with a low power Rh X-ray tube at 40 kV and 300 µA. All measurements were performed under vacuum on a single scan line with 250 µm spot size, 200 µm step width and a counting time of 60 s. Each data point reflects the mean element intensity, expressed in counts per second (cps). Micro-facies data were interpreted in combination with element data obtained by µ-XRF scanning on those impregnated sediment slabs from which thin sections have been prepared. This allowed direct comparison of geochemical and micro-facies data (Brauer *et al.*, 2009).

The chronology of the sediment cores was established by varve counting, intra-basin correlation to the master core MO/05/P3, dated by varve counting and

additional ^{137}Cs measurements (Swierczynski *et al.*, 2009), as well as the identification of two marker diatom layers dated to 1983 and 1986 (Klee and Schmidt, 1987; Schmidt, 1991).

The sediment record was compared with regional flood data. Discharge in the main tributary, Griesler Ache, is recorded by the hydrographic service of Upper Austria at the St. Lorenz gauging station (Fig. 3.1b). Precipitation data are obtained from the rain gauges in Thalgauberg (Griesler Ache), supplied by the hydrographic service of Land Salzburg, Oberwang (Wangauer Ache) and Scharfling (Kienbach), measured by the hydrographic service of Upper Austria (Fig. 3.1b). We used hourly and daily data for the period 1976-2005 covered by hydrological and sedimentological datasets.

3.4 Results

3.4.1 Sedimentology

Mid- to Late Holocene sediments from Lake Mondsee sediments are formed by biochemical calcite varves comprising light and dark sub-layers (Lauterbach *et al.*, 2011). Light sub-layers are composed of fine calcite crystals (< 5 µm) clearly reflected in µ-XRF calcium peaks (Fig. 3.2). Dark sub-layers consist of clay to silt sized mixed organic-minerogenic material indicated by secondary peaks in titanium used as a proxy for detrital input from the northern Flysch catchment (Swierczynski *et al.*, 2012). Correlation coefficients of $r^2 = 0.70 - 0.75$ to aluminium, potassium and silica confirm the predominately detrital origin of all these elements. Sediment cores in the deep southern basin (MO/05/P3: 62 m, MO/07/SC4: 64 m water depth) are entirely varved. However, varve preservation in sediment sequences retrieved from shallower coring sites (< 60 m) is limited to the uppermost decimetres leading to a broad lithological division into a homogeneous lower sediment unit I and a varved sediment unit II (Fig. 3.2). The transition between both units is gradual and occurs between 18 cm sediment depth in the central basin (MO/10/9) and 37 cm proximal to the river inflow (MO/10/5) (Tab. S.1). The lamination in sediment unit I appears indistinct in the proximal basin (MO/10/5: 47 m) and is absent in sediment cores from shallower parts of the lake (MO/10/6: 34 m).

Sediment unit II was further divided into three sub-units based on sediment colour and varve micro-facies (Swierczynski *et al.*, 2009). Our investigation on detrital layers is confined to the uppermost part of sediment unit II (Fig. 3.2), ranging in thickness from 5.5 cm in the distal core MO/05/P3 to 16 cm in the proximal core MO/10/5 and containing 28 (MO/05/P3) to 33 (MO/10 cores) distinct varves. The only non-varved sediment core from the shallow delta area (MO/10/6) was not considered for further investigations.

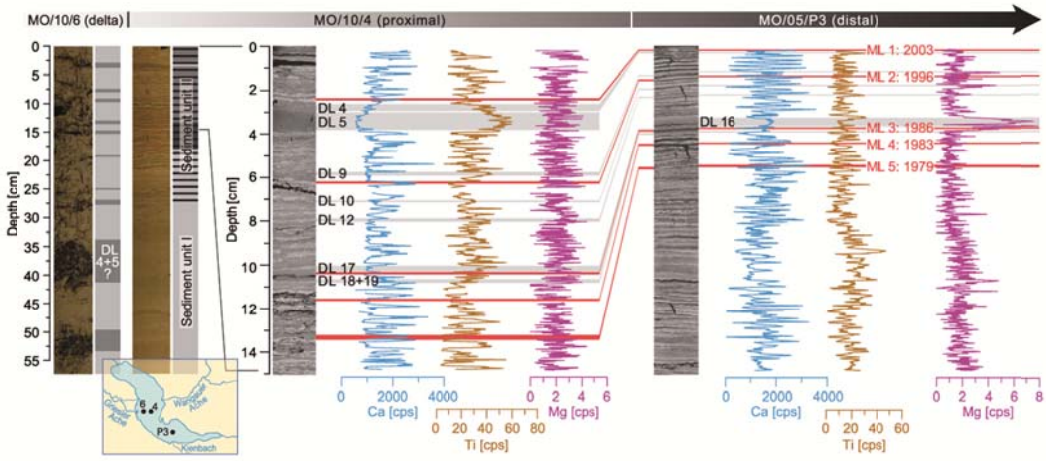

Figure 3.2. Lithology of Lake Mondsee sediments: MO/10/6 (310 m to the main inflow Griesler Ache/ 34 m water depth), MO/10/4 (820 m/ 55 m), MO/05/P3 (2850 m/ 62 m). Sediment unit II is shown in detail for cores MO/10/4 and MO/05/P3 by thin section scans and µ-XRF profiles of calcium (Ca) as proxy for endogenic calcite precipitation, titanium (Ti) as proxy for detrital input from the Flysch zone and magnesium (Mg) as proxy for detrital input from the Northern Calcareous Alps. Red bars indicate marker layers for core-to-core correlation (ML 1-5); grey bars indicate correlated detrital layers (DL).

3.4.2 Chronology

In order to establish precise calendar year chronologies for each sediment core, varve counting in thin sections has been independently carried out for each individual core sequence. Intra-basin correlation has been performed by using three distinct calcite layers (ML 1: 2003, ML 2: 1996, ML 5: 1979) and two diatom layers (ML 3: 1986, ML 4: 1983) marking well-documented shifts in diatom composition (Klee and Schmidt, 1987; Schmidt, 1991). Based on these markers all sediment cores have been correlated to the master core sequence MO/05/P3 indicating the top of the long sediment record (Lauterbach *et al.*, 2011; Swierczynski *et al.*, 2012). Varve counting is in agreement with ^{137}Cs peaks in core MO/05/P3 (Lauterbach *et al.*, 2011; Swierczynski *et al.*, 2012).

Varve formation (sediment unit II) in most of the Lake Mondsee sediment cores commences between 1953 and 1957 (Tab. 3.4) allowing determining the season of deposition of detrital layers by their micro-stratigraphic position within single varves (Fig. 3.4). Summer detrital layers are deposited within or directly on top of calcite layers. Detrital layers deposited within the mixed layer are formed in autumn to early spring and are labelled as winter detrital layers. This allows allocating 17 summer detrital layers and 10 winter detrital layers for the investigated time period between 1976 and 2005 (Fig. 3.3, Tab. 3.1).

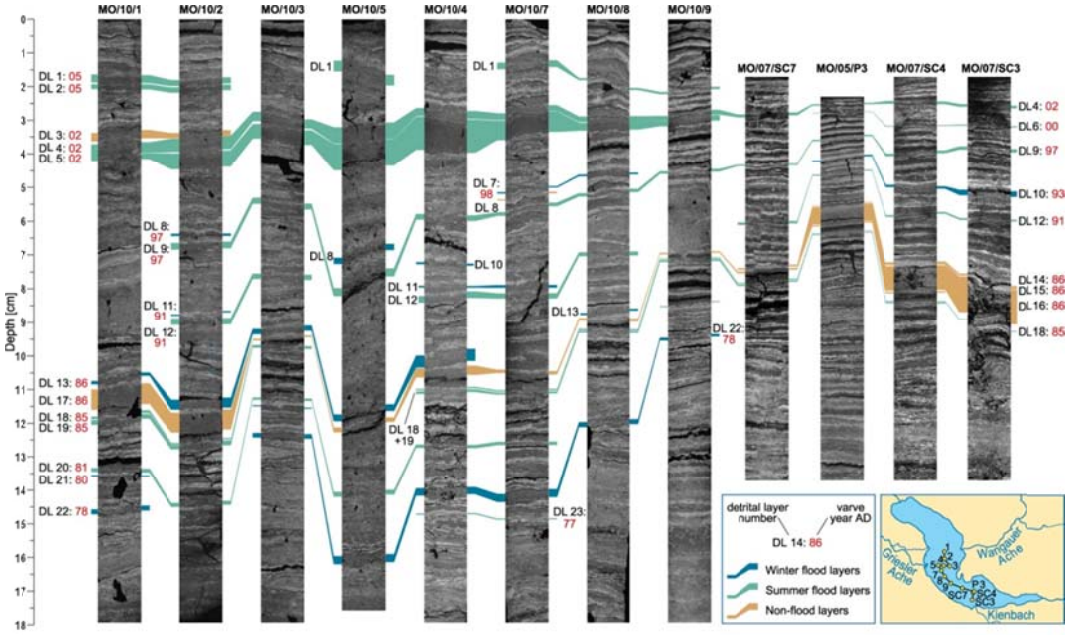

Figure 3.3. Intra-basin correlation of detrital layers in Lake Mondsee sediments (thin section scans) for the investigated period 1976-2005.

3.4.3 Detrital layer microfacies

27 detrital layers ranging in thickness from 0.1 to 12 mm have been detected in the investigated sediment cores labelled from top to down in the sediment sequences. Detrital layers can be clearly differentiated from calcite varves due to their composition of allochthonous minerogenic and, partly, organic matter originating from the catchment which is further reflected by distinct peaks in either titanium, a proxy for detrital matter from the northern Flysch catchment, or magnesium reflecting the southern catchment built up of limestone and dolomite or of both (Fig. 3.2).

Three main detrital microfacies have been distinguished (Tab. 3.1): (i) Graded layers (40% of all layers), (ii) silt/clay layers (30%) and (iii) matrix supported layers (30%). Graded layers range in thickness from 0.4-10 mm and are mainly composed of clastic material (quartz, feldspar, dolomite and calcite) and terrestrial plant debris. A typical feature in six graded layers is a normal upward fining (Fig. 3.4c+g). Four graded layers exhibit a more complex texture like an inversely graded basal bed overlain by a normal graded bed (layers DL 9, 12, 19; Fig. 3.4b+e) or a succession of two normal gradings (layer DL 4; Fig. 3.4g). Variations in maximum grain sizes observed in the basal layer part can be used to further distinguish between fine-grained (max. grain sizes < 10 µm; labelled with G-f in Tab. 3.1) and coarse grained layers (> 30 µm; G-c).

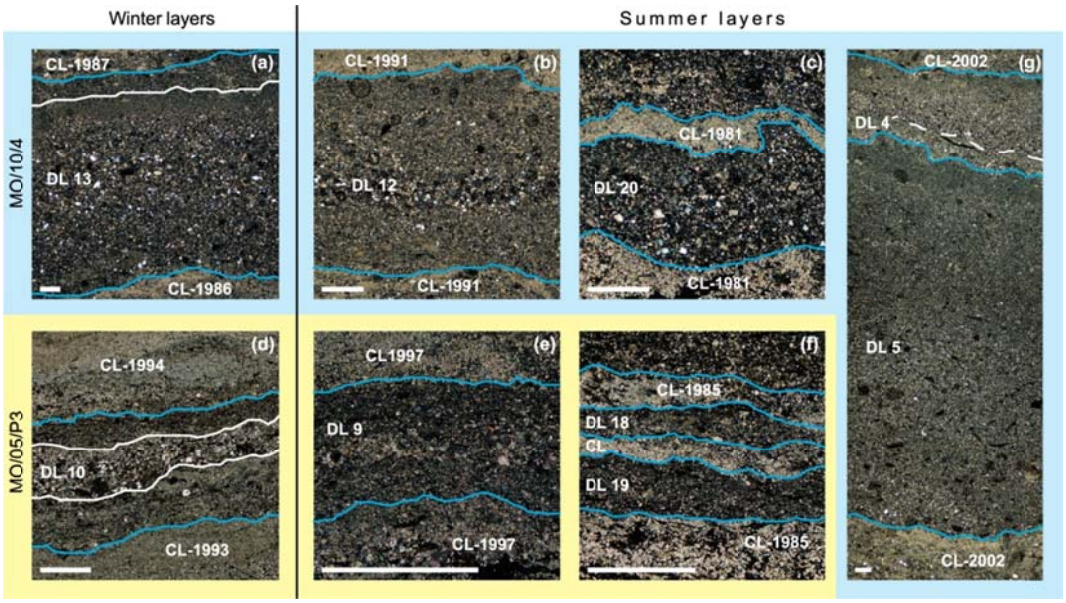

Figure 3.4. Detrital microfacies in the proximal core MO/10/4 (blue) and the distal master core MO/05/P3 (yellow): matrix supported layers: (a) DL 13, (d) DL 10; normally graded layers: (c) DL 20, (g) DL 5; two normally graded beds: (g) DL 4, separated by the dotted white line; inverse below normal grading: (b) DL 12, (e) DL 9; (f) Silt/clay layers: DL 18+19. White lines indicate detrital layer boundaries (DL + No.), blue lines indicate calcite layer boundaries (CL + varve year). White bars are equivalent to 0.4 mm.

Table 3.1. Detrital layers in the investigated uppermost part of Lake Mondsee sediments including layer thickness (in mm) and microfacies (MF).

Varve year + season	DL No.	MO 10/1		MO 10/2		MO 10/3		MO 10/5		MO 10/4		MO 10/7		MO 10/8		MO 10/9		MO 07/ SC7		MO 05/P3		MO 07/ SC4		MO 07/ SC3	
		[mm]	MF	[mm]	MF	[mm]	MF	[mm]	MF	[mm]	MF	[mm]	MF	[mm]	MF	[mm]	MF	[mm]	MF	[mm]	MF	[mm]	MF	[mm]	MF
2005 su	1	2.4	M	1.8	M	n. d.		3.2	M	-		2.0	G-f	0.6	S	0.7	G-f	0.4	S	-		n. d.		n. d.	
2005 su	2	1.5	M	1.6	G	n. d.		n. d.		-		n. d.		n. d.		n. d.		n. d.		-		n. d.		n. d.	
2002 wi	3	2.6	M	1.6	M	n. d.		n. d.		n. d.		n. d.		n. d.		n. d.		n. d.		n. d.		n. d.		n. d.	
2002 su	4	3.2	G-c	4.0	G-c	2.8	G-c	4.8	G-c	2.4	G-c	2.0	G-c	1.6	G	1.4	G	0.8	G-f	0.4	S	0.8	G-f	0.8	G-f
2002 su	5	1.8	G-f	4.8	G-f	4.4	G-f	8.0	G-f	10.0	G-f	6.5	G-f	2.4	G-f	1.6	G-f	n. d.		n. d.		n. d.		n. d.	
2000 su	6	n. d.		n. d.		n. d.		n. d.		n. d.		n. d.		n. d.		n. d.		n. d.		0.1	M	0.2	M	0.3	M
1998 wi	7	-		n. d.		n. d.		n. d.		-		0.4	M	0.5	M	n. d.		n. d.		n. d.		n. d.		n. d.	
1998 su	DL	-		n. d.		n. d.		n. d.		-		0.4		n. d.		n. d.		n. d.		n. d.		n. d.		n. d.	
1997 wi	8	-		0.7	M	n. d.		1.8	M	n. d.		0.6	M	n. d.		n. d.		n. d.		n. d.		n. d.		n. d.	
1997 su	9	-		2.0	G-c	1.8	G-c	2.4	G-c	1.7	G-c	1.1	G-c	1.0	G-c	0.8	S	0.4	S	0.4	G	0.8	G	1.0	G
1993 wi	10	-		n. d.		n. d.		-		0.6	M	n. d.		n. d.		-		n. d.		0.4	M	0.7	M	1.6	M
1991 wi	11	-		0.4	M	n. d.		-		0.5	M	0.8	M	n. d.		-		n. d.		n. d.		n. d.		n. d.	
1991 su	12	-		1.8	G-c	1.6	G-f	-		2.0	G-c	1.6	G-c	1.2	G-c	-		0.7	S	0.3	S	0.5	S	0.5	G-f
1990 wi	DL	-		3.5	G-c	n. d.		-		n. d.		n. d.		n. d.		-		n. d.		n. d.		n. d.		n. d.	
1989 wi	DL	-		0.6	M	n. d.		-		n. d.		n. d.		n. d.		-		n. d.		n. d.		n. d.		n. d.	
1986 wi	13	1.0	M	3.0	M	1.6	M	2.0	M	3.6	G-c	n. d.		0.6	M	-		n. d.		n. d.		n. d.		n. d.	
1986 su	14	n. d.		n. d.		n. d.		n. d.		n. d.		n. d.		n. d.		n. d.		n. d.		n. d.		0.5	M	0.4	M
1986 su	15	n. d.		n. d.		n. d.		n. d.		n. d.		n. d.		n. d.		n. d.		n. d.		0.2	M	0.2	M	0.5	M
1986 su	16	n. d.		n. d.		n. d.		n. d.		n. d.		n. d.		n. d.		n. d.		0.5	G-c	5.2	M	8.0	M	12.0	M
1986 su	17	6.2	G-f	6.0	G-f	0.5	S	0.5	S	2.8	S	1.0	S	0.8	S	0.4	S	0.5	S	0.3	S	0.4	S		
1985 su	18	0.8	G-f	0.4	S	n. d.		-		0.4	S	0.4	S	0.4	S	0.3	S	0.2	S	0.1	S	0.2	S	0.2	S
1985 su	DL	n. d.		n. d.		n. d.		-		n. d.		n. d.		n. d.		n. d.		n. d.		n. d.		n. d.		0.2	M
1985 su	19	1.4	G-f	1.4	G-f	0.8	G-f	-		0.8	G-f	0.6	S	0.5	S	0.5	S	0.4	S	0.2	S	0.3	S	n. d.	
1981 su	20	1.2	G-f	1.2	M	0.7	G-f	1.5	M	1.0	G-c	1.0	G-c	-		0.3	S	n. d.		n. d.		n. d.		0.5	S
1980 wi	21	0.5	M	n. d.		0.3	S	n. d.		n. d.		0.7	M	-		n. d.		n. d.		n. d.		n. d.		n. d.	
1978 wi	22	1.5	G-c	n. d.		1.4	G-c	2.4	G-c	2.2	G-c	2.4	G-c	1.5	G-c	0.8	S	n. d.		n. d.		n. d.		n. d.	
1977 su	23	-		-		n. d.		n. d.		0.4	S	0.4	S	-		-		n. d.		n. d.		n. d.		n. d.	

(M) Matrix supported layers, (S) silt-clay layers, (G) graded layers in combination with more specific microfacies features: very fine-grained (-f, max. grain size < 10 µm), very coarse-grained (-c, max. grain size > 30 µm). The absence of detrital layer deposition is indicated by the abbreviation n. d., dashes (-) point to disturbed sediment sequences or highly clastic background sedimentation and therefore possibly hidden detrital layers.

Silt/clay layers differ from graded layers mainly by the almost entirely minerogenic composition with grains rarely exceeding 10 µm in diameter and the lack of clear textural organization. The thickness of these layers varies between 0.1 and 6.2 mm. Some of the thinner (<0.5 mm) silt/clay layers appear as individual detrital grains aligned along the bedding (Fig. 3.4f) rather than as distinct layers.

Matrix supported layers range in thickness from 0.1 to 12 mm and contain minerogenic matter sizing between 30 and, partly, > 100 µm and terrestrial plant debris incorporated within a matrix of amorphous organic matter and clumped aggregates of endogenic calcite (Fig. 3.4a+d).

3.4.4 Detrital layer geochemistry

Detrital layer geochemistry differs within the lake basin (Fig. 3.5). In the northern part of the lake basin (Fig. 3.5a) detrital layers exhibit high values in Ti count rates (proxy for siliciclastic matter) and low values of Mg (proxy for dolomitic components). The predominantly siliciclastic composition corroborates the Flysch zone (Fig. 3.1) as main source of detrital material. In contrast, the element composition of detrital layers in the southern part of the basin (Fig. 3.5b) is more complex. Four layers exhibit clear peaks in Ti, thus pointing to the Flysch zone as main source region (DL 4, 12, 18, 19), whereas two layers show increased Mg counts indicating the Northern Calcareous Alps as sediment source (DL 10, 16). One layer shows both higher Ti and Mg values indicating a mixture of material from both sources (DL 9).

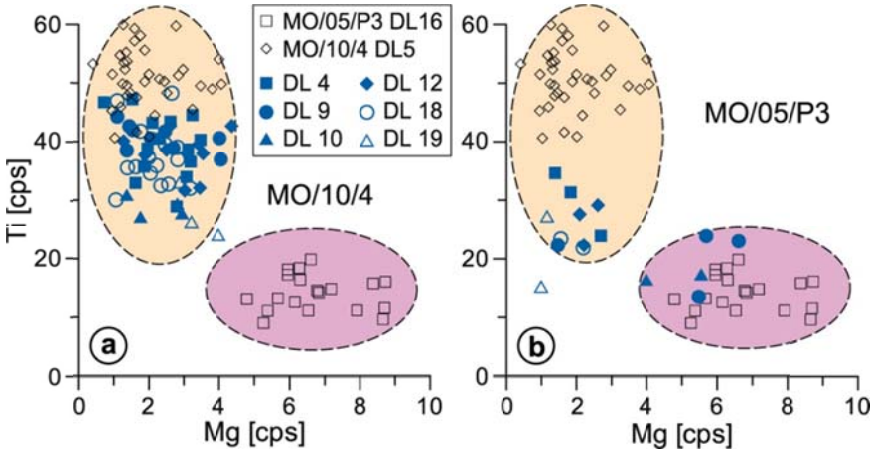

Figure 3.5. Micro-XRF counts of Ti and Mg within flood layers (blue symbols): (a) in the proximal sediment core MO/10/4 and (b) in the distal master core MO/05/P4. Reference layers for source identification (black symbols) are DL 5 triggered by a local flood in the northern Flysch sub-catchment and DL 16 triggered by a debris flow event in the southern sub-catchment in the Northern Calcareous Alps. Circles indicate areas representative for the two sub-catchments; yellow: Flysch Zone, pink: Northern Calcareous Alps.

3.4.5 Intra-basin distribution of detrital layers

Based on independent varve counting in all 12 investigated sediment cores, intra-basin correlation of detrital layers has been performed (Fig. 3.3) to identify the spatial distribution of each individual detrital layer within the lake basin and disentangle between the three potential point sources for suspended sediment supply, the Griesler and Wangauer Ache discharging from the West and from the East into the northern part of the basin where the shape of the lake makes a kink and the Kienbach creek discharging from the South into the southern part of the basin.

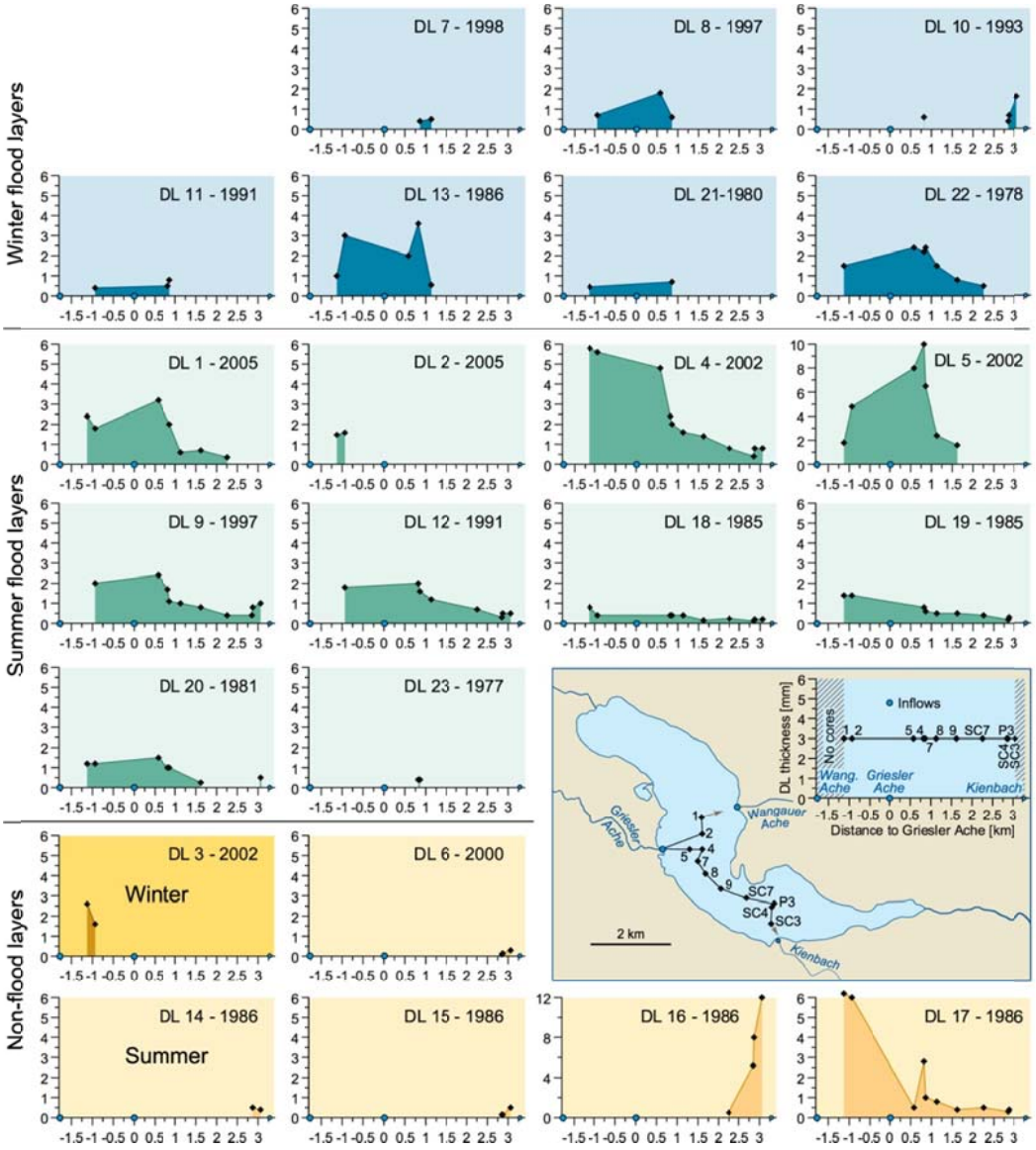

Figure 3.6. Spatial distribution of detrital layers within Lake Mondsee: layers triggered by floods in winter and summer and layers not related to floods. Sampling points are arranged along transects as shown in the map.

The investigated sediment interval from 1976 to 2005 includes 27 detrital layers (Tab. 3.1). Four layers with a thickness from 0.2 to 4.5 mm were only found each in one sediment core at the most proximal locations close to the river inflows (MO/10/2: 2 layers, MO/10/7 and MO/07/SC3: 1 layer each) and likely reflect local reworking of unconsolidated delta material. The remaining 23 detrital layers have been correlated within the investigated part of the basin (Fig. 3.3).

Sediment cores located near the inflow of the main tributary Griesler Ache (ca. 0.8 km) contain the highest number and thickest detrital layers (MO/10/4: 13 layers, max. 10 mm, MO/10/7: 15 layers, max. 6.5 mm) indicating the Griesler Ache as the main source of detrital material. Towards the depocentre of the lake the number of detrital layers decreases and these layers commonly are thinner (MO/07/SC7 (2.3 km): 8 layers, max. 0.8 mm). Besides this common proximal-distal pattern of sediment flux, four detrital layers (DL 4, 9, 10, 12) show a slightly increasing thickness towards the Kienbach inflow suggesting an additional sediment flux occurring from the Kienbach creek in the South contemporaneously to the sediment flux from the main tributary (Fig. 3.6). Further four detrital layers (DL 6, 14-16), which are all matrix-supported, have been only deposited in the southern part of the basin indicating the Kienbach creek as the exclusive sediment source (Fig. 3.6).

The distribution of suspended detrital matter within the lake basin after a flood apparently is dependent from the season in which the flood occurred. Whereas six of the seven winter floods are only recorded in cores within 1.5 km distance from the Griesler Ache and Wangauer Ache river mouths mainly as matrix-supported layers (90%), summer flood layers are much wider distributed within the lake basin (Fig. 3.6). From the 11 summer layers found in proximal cores near the Griesler Ache inflow (MO/10/4+7), eight layers are distributed over a distance of 1.6 km (MO/10/9) and six layers even further South to the location of the long master core in 2.9 km distance. The microfacies of these layers changes from graded layers at proximal sites (82% in MO/10/4+7) to silt/clay layers at distal sites (50% in MO/10/8, 63% in MO/10/9, 91% in MO/07/SC7). Three of the very fine-grained silt/clay layers in the distal master core (DL 12, 18, 19) could only be identified as detrital layers by correlation with the proximal core sequences. These layers have been added to the previously published long flood layer chronology (Swierczynski *et al.*, 2012 and 2013).

3.4.6 Detrital layers vs. instrumental data

To investigate the effects of river discharge on detrital layer formation, all 23 detrital layers occurring between 1976 and 2005 in at least two of the sediment cores have been compared to discharge data of the gauged main tributary river, Griesler Ache, and precipitation data of the three sub-catchments of Lake Mondsee (Fig. 3.7). This event-based comparison with instrumental data is

possible due to the determination of the flood seasons in the sediment record by micro-stratigraphical methods. 17 detrital layers (74%) correspond to events of elevated runoff in the Griesler Ache ranging in maximum daily discharge (Q_d) from 24 to 83 m^3s^{-1}. 12 of these layers (70%) correlate to strong floods exceeding 40 m^3s^{-1}. This runoff value was exceeded 13 times in the studied time interval and in all except one case this discharge resulted in the deposition of a detrital layer (92%). The likelihood for detrital layer deposition sharply decreases for lower flood amplitudes and is only 12% for floods with a daily discharge of 30-40 m^3s^{-1}.

Ten of the 17 floods, led to detrital layer deposition, occurred in summer of which 90% relate to intense precipitation (P) > 80 mm d^{-1} and associated hourly peak discharges (Q_h) > 60 m^3s^{-1} (Tab. 3.2). Detrital layers which formed after summer floods commonly are widely distributed in six to 12 sediment cores, except for one flood in July 1977 of which corresponding detrital layers have been found only in two proximal cores (Fig. 3.6). Five of the remaining seven floods occurred in spring (March-April) and two in winter (Tab. 3.2) all related to rain events exceeding 50 mm d^{-1} and commonly less extreme peak discharges (57% < 60 m^3s^{-1}) leading to detrital layer deposition in two to six cores.

For six detrital layers which occur in few cores either close to the Kienbach creek in the South (DL 6, 14-16) or close to the Wangauer Ache in the North (DL 3), neither coinciding discharge events in the Griesler Ache nor precipitation events in any sub-catchment have been measured. Therefore, local erosion or reworking processes rather than regional-scale flood events are assumed to have caused the formation of these layers. This has been proven for layer DL 16, which was triggered by a documented debris flow in the Kienbach valley (Swierczynski *et al.*, 2009). Among these detrital layers, which are not related to floods, only DL 17 exhibits a wider distribution in the lake basin and has been found in 11 cores. The thickness distribution of this layer within the basin points to the Wangauer Ache as source (Fig. 3.6). In summary, 17 of 23 detrital layers correspond to floods of the Griesler Ache (Fig. 3.7), and six layers are related to local events.

Besides detrital layers triggered by other processes than regional floods, flood layer records might be biased by missing flood layers, i.e. floods that did not result in deposition of a detrital layer. For the studied interval, only one major Griesler Ache flood in November 1979 (Q_d = 41.9 m^3s^{-1}) did not result in detrital layer deposition in any of the sediment cores (Tab. 3.2). However, the completeness of individual sediment cores with respect to flood layer deposition distinctly varies within the lake basin. Some layers are not perceptible in individual sediment cores, either due to predominantly clastic background sedimentation at the most proximal sites (e.g. MO/10/5) or sediment intervals with a less well preserved varve structure (Tab. 3.1). Such individual gaps were bridged by integrating neighbouring sediment cores to form composite profiles providing a more representative flood layer record (Fig. 3.7).

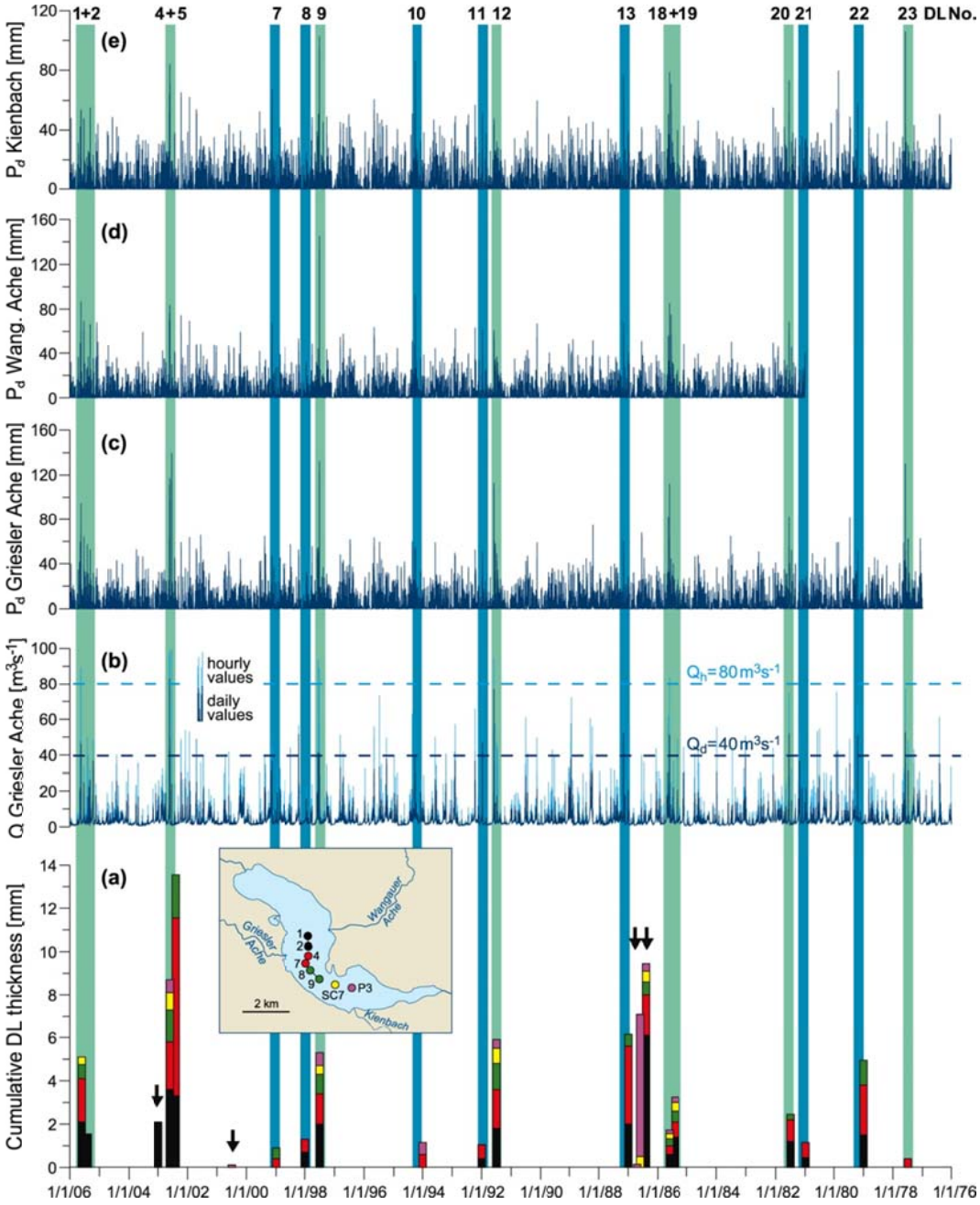

Figure 3.7. Mondsee detrital layer record compared to instrumental time series 1976-2005: (a) Layer thickness in five composite profiles (see map), (b) Griesler Ache daily and hourly discharge, (c-e) precipitation in the three main sub-catchments (Griesler Ache: Thalgauberg rain gauge, Wangauer Ache: Oberwang, Kienbach: Scharfling. Vertical bars: coincidence of detrital layer deposition and floods in winter (blue) and summer (green); black arrows: detrital layers not related to floods; horizontal dashed lines: empirical runoff thresholds for triggering detrital layers in Lake Mondsee.

Sediment cores in the proximal part of the basin, 0.9 km apart from the Griesler Ache inflow (MO/10/4+7), contain 16 of the total 17 flood layers, whereas towards distal direction the number of identified floods decreases: 11 layers (65%) are transported over a distance of 1.5 km (MO/10/8+9) and six layers (35%) to the master core in the distal southern part of the basin in a distance of 2.9 km to the Griesler Ache inflow. Four of the six floods, recorded in the master core, are the

strongest summer floods in the investigation period in terms of intensity ($Q_h > 80$ m^3s^{-1}) and duration ($Q_d > 40$ m^3s^{-1} for at least 2 days). The other two flood layers in the master record were triggered by a summer flood below the threshold (DL 18; $Q_d = 30.3$ m^3s^{-1}) and a local spring precipitation event in the Kienbach catchment (DL 10; $P = 86.2$ mm d^{-1}).

3.5 Discussion

Detrital layers in lake sediments commonly are considered as flood indicators (Siegenthaler and Sturm, 1991; Gilli *et al.*, 2013). However, there is still a lack of knowledge about the completeness of palaeoflood records and how discharge and precipitation control the formation and thickness of flood layers (Gilli *et al.*, 2013). An important aspect for interpreting the number and thickness of detrital layers deposited after flood events certainly is the coring location with respect to the inflowing suspended matter (Czymzik *et al.*, 2013). Here, we address these issues in a detailed case study for the Lake Mondsee sediment record by a comprehensive methodological approach combining multiple-core analyses with a calibration of detrital layers based on instrumental flood data. The precise chronology of varved sediment records gives the unique opportunity of such an individual event-based comparison of sedimentological and instrumental flood records (Schiefer *et al.*, 2006; Chutko and Lamoureux, 2008; Czymzik *et al.*, 2010). Reconstruction of flood layer distribution within the lake basin through multiple core analyses provides complementary information about depositional processes (Sturm and Matter, 1978; Gilbert *et al.*, 2006; Schiefer, 2006; Schiefer *et al.*, 2011; Kämpf *et al.*, 2012a) and, in combination with sediment geochemistry, about sediment source areas (Swierczynski *et al.*, 2009; Simonneau *et al.*, 2013).

An important factor for interpreting detrital layers as flood deposits is the process of suspended sediment distribution within the basin either though underflows (hyperpycnal flows) or interflows (mesopycnal flows). Based on our detailed intra-basin correlation we assume that graded and matrix supported layers represent hyperpycnal flow deposits whereas silt/clay layers which are mostly very thin and almost evenly distributed over the lake basin represent mesopycnal flow deposits. Hyperpycnal flow deposits are rarely found in the depocentre of Lake Mondsee (MO/07/SC7 in Tab. 3.1); only one graded layer occurs during the studied time interval, whereas all other detrital layers appear as silt/clay layers. However, since all silt/clay layers in the depocentre can be unambiguously correlated to graded layers in proximal cores by their micro-stratigraphic position within the varved sediment sequence, we infer a separation of the suspended sediment plumes triggered by regional flooding into hyperpycnal flows confined to the near delta area (c. 1.5 km) and mesopycnal flows which are distributed to more distal parts of the lake basin. In this respect Lake Mondsee is different from

larger peri-alpine lakes like, for example, lakes Bourget and Brienz, where thick turbidites resulting from underflows have been found in the entire depocentre (Sturm and Matter, 1978; Arnaud *et al.*, 2005; Chapron *et al.*, 2005). Besides the smaller size of Lake Mondsee and its main tributary, the specific shape of the lake basin and the location of the main inflow with respect to the main water flow direction, as above described in the section study site, likely influences the amount of suspended matter influx and its distribution within the lake basin.

Table 3.2. Comparison of the detrital layer record and instrumental time series for the investigation period 1976-2005. Instrumental data include maximum daily and hourly runoff in the main tributary, Griesler Ache, daily precipitation sums in the catchments of the main and secondary tributaries and weather regime data from Gerstengarbe and Werner (2005).

Sediment data					Hydrological data								
Varve year	Varve season	DL No.	N Cores	Cum. Thickness [mm]	Date of max. runoff	Daily runoff [m^3s^{-1}]	Hourly runoff [m^3s^{-1}]	Flood duration [d] [> 40 m^3s^{-1}]	[> 20 m^3s^{-1}]	Max. daily precipitation Thalgauberg [mm]	Oberwang [mm]	Scharfling [mm]	Weather type
2005	su	1	7	11.1	8/16/2005	**46.3**	**89.6**	1	1	**94.7**	**87.0**	54.0	WZ
2005	su	2	2	3.1	7/11/2005	24.8	33.6	0	1	64.4	69.5	48.0	TRM
2002	*wi*	*3*	*2*	4.2	*11/4/2002*	*20.5*	*32.6*	*0*	*1*	*32.7*	*42.5*	*32.8*	
2002	su	4	12	25.0	8/12/2002	**83.2**	**112.8**	2	3	**117.2**	**83.5**	**84.0**	TM
2002	su	5	8	39.5	7/16/2002	24.2	**99.6**	0	1	**139.5**	30.0	19.5	TRM
2000	*su*	*6*	*3*	0.6	*8/7/2000*	*17.8*	*45.2*	*0*	*0*	*50.8*	*46.6*	*44.3*	
1998	wi	7	2	0.9	2/21/1999	36.8	52.0	0	3	46.9	67.5	67.0	NWZ
1997	wi	8	3	3.1	3/17/1998	**51.7**	56.9	1	3	52.8	53.5	35.2	NWZ
1997	su	9	11	13.4	7/6/1997	**41.0**	**89.0**	2	3	**132.4**	**145.0**	**102.7**	TRW
1993	wi	10	4	3.3	4/18/1994	**40.4**	**62.5**	1	1	54.5	**92.8**	**86.2**	TM
1991	wi	11	3	1.7	12/23/1991	**46.8**	**82.6**	1	2	51.2	61.5	51.6	WZ
1991	su	12	9	10.2	8/2/1991	**76.8**	**94.8**	3	4	**113.0**	61.0	47.7	HFA
1986	wi	13	6	11.8	3/1/1987	**52.7**	**81.4**	3	4	60.0	68.0	76.4	WW
1986	*su*	*14*	*2*	0.9	-								
1986	*su*	*15*	*3*	0.8	-								
1986	*su*	*16*	*4*	25.7	*7/18/1986*	*11.0*	*43.8*	*0*	*0*	*68.0*	*51.3*	*42.0*	
1986	*su*	*17*	*11*	19.4	*6/18/1986*	*4.3*	*39.1*	*0*	*0*	*45.2*	*31.5*	*19.8*	
1985	su	18	10	3.4	8/26/1985	30.3	**62.0**	0	2	**82.2**	56.2	50.8	TRM
1985	su	19	10	6.9	8/6/1985	**51.5**	**84.1**	2	2	**112.4**	**85.5**	78.7	TRM
1981	su	20	8	7.4	7/19/1981	**51.8**	**74.8**	2	3	**82.2**	69.0	73.0	TRM
1980	wi	21	3	1.5	3/12/1981	36.7	53.1	0	4	25.2	25.3	30.0	SWZ
				-	11/27/1979	**41.9**	**75.5**	1	2	59.1	no data	54.2	BM
1978	wi	22	7	12.2	3/12/1979	**51.3**	**69.4**	2	2	52.1	no data	57.5	WZ
1977	su	23	2	0.8	7/31/1977	**52.7**	**77.0**	1	2	**130.2**	no data	**106.0**	NEZ

Extreme values of hydrological parameters are written in bold (daily runoff > 40 m3s-1, hourly runoff > 60 m3s-1, daily precipitation > 80 mm), detrital layers not related to floods are written in italic. Abbreviations for sediment data: DL No.: detrital layer number, N cores: amount of cores containing the layer, Cum. Thickness: cumulative detrital layer thickness added up over all cores, acronyms for weather types (Gerstengarbe and Werner, 2005): WZ: westerly cyclonic, TRM: low pressure trough over Central Europe, TM: low pressure cell over Central Europe, NWZ: north-westerly cyclonic, HFA: high pressure cell over Fennoscandia anticyclonic, WW: angular westerly, SWZ: south-westerly cyclonic, BM: high pressure ridge over Central Europe, NEZ: north-easterly cyclonic.

3.5.1 Reconstructing flood frequencies

The comparison with instrumental flood data revealed an empirical discharge threshold for detrital layer deposition in Lake Mondsee sediments of about 40 m^3s^{-1} mean daily discharge (Fig. 3.7). Above this threshold detrital layers are formed in at least two sediment cores in the lake basin. However, we observe clear variations of this threshold for different locations within the lake due to the

different distance from the inflow of suspended matter. In the distal lake basin the threshold is even better defined by maximum peak discharge and flood duration rather than by mean daily discharge. The long master core predominately records floods exceeding 80 m^3s^{-1} peak discharge and a daily mean of 40 m^3s^{-1} lasting for at least two days. In addition, we found that not all detrital flood layers have been formed at all core locations, not only because of different distances from the inflow source, but also due to variable distribution of suspended sediment loads within the lake. In summary, flood layer time series obtained from single cores indeed might be biased by so-called 'missing' flood layers so that such flood reconstructions must be considered as minimum flood estimates.

Possible explanations for missing layers include erosion by hyperpycnal flows (Mangili *et al.*, 2005; Schiefer, 2006) and sediment focusing by meandering (Gilbert *et al.*, 2006) or spatially limited hyperpycnal flows (Lamoureux, 1999). Alternative explanations are related to an uneven distribution of suspended matter within the basin especially during mesopycnal flow transport. A previously underestimated factor in this respect is the season of flooding. For Lake Mondsee we demonstrate that summer detrital layers are much wider distributed within the basin compared to winter flood layers which are spatially confined to sites proximal to the inflow even during strong winter floods (Fig. 3.6). This might be explained by summer stratification favouring long-distance transport of fine-grained suspended matter in the upper water column to the depocentre by mesopycnal flows (Sturm and Matter, 1978; Desloges and Gilbert, 1994; Schiefer, 2006; Hodder *et al.*, 2007). Moreover, lake internal currents, recorded during an ongoing monitoring study in Lake Mondsee (Mueller *et al.*, 2013), could have a potential effect on mesopycnal flows (Sturm and Matter, 1978; Giovanoli and Lambert, 1985; Schiefer, 2006). Although the generation of lake internal currents might be specific in Lake Mondsee (Mueller *et al.*, 2013) because of the characteristic basin morphology and the position of the discharging river inflows, an influence of internal currents for sediment distribution must be considered for all larger lake systems.

In addition to missing layers as a bias for interpreting long palaeoflood time series, there is also the possibility of additional detrital layers, which are not related to regional floods and thus may lead to an overestimation of flood numbers. In Lake Mondsee, such non flood-triggered layers are formed by two different mechanisms: (i) debris flows deriving from the steep-sided Kienbach valley in the southern sub-catchment (Swierczynski *et al.*, 2009) and (ii) reworking of unconsolidated sediment from the deltas and slopes through wave action and sediment instabilities. Debris flow deposits can be clearly distinguished from flood layers based on the exclusively dolomitic sediment composition (Fig. 3.5) and coarser detrital grain sizes. Reworked detrital material deposited around the river deltas commonly did not form distinct layers and, therefore, can be also distinguished from flood deposits. Only in one case, a distinct and widespread detrital layer with a similar appearance like other flood layers (DL 17, Fig. 3.6)

has formed without a corresponding discharge peak in the Griesler Ache. This layer is not distinguishable from common flood layers. Intra-basin correlation enabled to trace this layer to the Wangauer Ache stream. Since no enhanced precipitation is recorded in the Wangauer Ache catchment during that time (Fig. 3.7), we assume a local erosion event either in the stream bed or from the subaquatic slopes.

Based on the abovementioned evidences, we can state that the long master core located in the distal southern basin completely records the strongest summer floods defined as peak discharge (80 m^3s^{-1}) and flood duration (2 days > 40 m^3s^{-1}). In addition to the earlier published flood layer record based on only the master core (Swierczynski *et al.*, 2012 and 2013), we were able to identify three extremely thin flood layers (DL 12, 18, 19) through the multi-core approach. The amounts of detrital material transported to this distal site were so low, that we could identify them only through tracing flood material from the proximal site. The preferential deposition of summer flood layers can be explained by the effect of lake stratification favouring wide distribution of suspended matter through mesopycnal flows. Local erosion events can be, in most cases, clearly distinguished from flood deposits by multiple core micro-facies and micro-XRF analyses. Obviously, the empirical threshold must be considered as an approximation since also two low amplitude floods triggered the formation of detrital layers.

3.5.2 Reconstructing flood amplitudes

Besides establishing long time series of flood frequencies, it is challenging to reconstruct also amplitudes of palaeofloods. First attempts applied flood layer thickness as proxy for flood amplitudes (Brown *et al.*, 2000; Wilhelm *et al.*, 2013; Wirth *et al.*, 2013) based on the concept that sediment flux in the lake is directly related to river discharge as has been demonstrated in several pro-glacial lakes (Desloges and Gilbert, 1994; Schiefer *et al.*, 2006; Hodder *et al.*, 2007; Chutko and Lamoureux, 2008; Schiefer *et al.*, 2011). Although in agreement with this concept, most of the thickest flood layers in the Mondsee sediment record (1 to 5 mm; Fig. 3.7) indeed were triggered by the strongest flood events (1991, 1997, 2002), our calibration demonstrates that the assumed relation between flood amplitude and layer thickness is not generally valid but shows clear differences depending from the particular core position within the lake basin. This is obvious from highly variable linear correlation coefficients (Tab. 3.3). Reasons for these variations are non-linear components influencing layer thickness in different ways. For example, layer thickness in the distal southern part of the lake does not correlate to flood amplitudes ($r^2(Q_h) = 0.22$), because of additional sediment supply from the local Kienbach creek (Figs. 5 and 6) into this part of the basin. The proximal zone is generally more susceptible for local sediment mobilization

events in the catchment or from the slopes which can cause thick detrital layers (DL 5, 16, 17) as has been also shown for other lake sediment records (Czymzik *et al.*, 2010; Kämpf *et al.*, 2012b). For the Lake Mondsee record, a significant linear correlation of layer thickness and flood amplitude is only revealed for the depocentre ($r^2(Q_h) = 0.77$), which is far enough from additional local sediment sources and receives sediment supply only after the strongest floods crossing a certain threshold.

Table 3.3. Linear correlation of detrital layer thickness from composite sediment profiles with daily (Q_d) and hourly runoff maxima (Q_h) in the main tributary Griesler Ache.

	MO/10/1+2	MO/10/4+7	MO/10/8+9	MO/07/SC7	MO/ P3+SC4
n flood layers	14	16	11	6	6
r^2 (Q_d)	0.08	0.03	0.02	0.96	0.13
p (Q_d)	>0.1	>0.1	>0.1	0.001	>0.1
r^2 (Q_h)	0.48	0.28	0.46	0.76	0.22
p (Q_h)	0.04	>0.1	0.08	0.04	>0.1

In addition to processes observed at Lake Mondsee, other processes are assumed to influence flood layer thickness including soil moisture and vegetation cover which affect runoff generation (Merz and Blöschl, 2009) and erosivity of soil and surface sediments and thereby, the amount of suspended material transported in the streams (Dugan *et al.*, 2009; López-Tarazón *et al.*, 2010). Although these factors can also vary on short time scales, they commonly work on longer time scales through soil evolution, climatic controlled land-cover changes and human impact (Giguet-Covex *et al.*, 2011; Arnaud *et al.*, 2012), and thus result in a complex non-linear relation of flood amplitude and layer thickness in centennial to millennial scale lake sediment records. Due to the limited calibration period of the present study, these long-term processes are out of the observational range and cannot be addressed here.

In summary, the relation between detrital layer thickness and flood amplitude depends on a complex interaction of linear and non-linear factors controlling discharge and suspended sediment transport in tributary streams and sediment distribution within the lake and shows a distinct spatial heterogeneity within the lake basin. Deciphering these processes can be at least partly achieved by multiple sediment core analyses and calibration of sediment with meteorological and hydrological data.

3.6 Conclusions

The applied dual calibration approach for flood layer deposition in a lake sediments combining multi-core micro-facies analyses and calibration with instrumental data turned out suitable to decipher processes controlling flood layer formation, thereby, fostering an improved interpretation of long flood layer time

series derived from lake sediments. This approach allowed identifying missing layers or additional, non-flood triggered detrital layers at individual core locations. In addition, empirical flood amplitude thresholds for the formation of flood layers have been assessed and proven to be specific for different coring locations. This, in turn, is important information for defining the most suitable coring locations for future lake sediment investigations aiming at flood reconstructions. Our study further demonstrates that the season in which a flood occurs influences the distribution of detrital material within the lake basin, possibly because of the state of lake water stratification and/or internal water currents. However, these assumptions remain speculative and need to be tested by extending the observation through in-lake monitoring of suspended matter distribution and deposition.

The results of this study provide a more robust interpretation of the long flood time series from Lake Mondsee and allow to better estimate uncertainties. In more general, we contribute to the discussion if and how flood layer thickness can be applied as proxy for flood amplitude by demonstrating that in certain circumstances a relationship between layer thickness and flood amplitude exists. However, this relationship can be strongly overprinted by non-linear components and is spatially different even within one lake basin. Therefore, reconstructing flood amplitudes still remains a major challenge for palaeoflood research in lake sediments. Even if our results obviously are in parts site-specific, we consider the dual calibration approach for flood layers as a suitable tool also for other lake records. Ideally, it should be complemented by observation of in-situ sedimentation through in-lake monitoring.

Acknowledgements. This study contributes to the Potsdam Research Cluster for Georisk Analysis, Environmental Change and Sustainability (PROGRESS) part A.3 ‘Extreme events in geoarchives’ funded by the German Federal Ministry for Education and Research (BMBF). We especially thank Richard Niederreiter (UWITEC) and Hannes Höllerer (University of Innsbruck) for their help during sediment sampling, Michael Köhler (MK Factory), Dieter Berger and Gabriele Arnold (both Helmholtz Centre Potsdam GFZ) for the preparation of thin sections and Brigitte Richert (Helmholtz Centre Potsdam GFZ) for performing µ-XRF measurements. Andreas Hendrich and Manuela Dziggel helped with the figures. Precipitation and discharge data sets were supplied by the hydrographic services of Upper Austria and Land Salzburg. Temperature data for the climate station of Mondsee were provided by the Central Institute for Meteorology and Geodynamics Austria (ZAMG). We thank Dr. Kyle Hodder and an anonymous reviewer for constructive comments which helped to improve the manuscript.

Supporting Material

Table 3.4. Data on surface sediment cores from Lake Mondsee including the onset (sediment depth and time) of varve formation at individual coring sites.

Core name	Sampling	Lon (E)	Lat (N)	Water depth [m]	Core length [cm]	Trans. I/II Depth [cm]	Onset of varves [varve yr AD]
MO/10/1	Oct 2010	13°22'47.28"	47°49'34.02"	48.0	133.0	26.5	1957
MO/10/2	Oct 2010	13°22'46.68"	47°49'21.48"	52.0	134.0	28.0	1953
MO/10/3	Oct 2010	13°23'01.38"	47°49'10.32"	55.0	158.0	28.0	1954
MO/10/4	Oct 2010	13°22'47.10"	47°49'09.66"	55.0	143.0	27.5	1953
MO/10/5	Oct 2010	13°22'31.86"	47°49'09.90"	47.0	149.5	37.0	1953
MO/10/6	Oct 2010	13°22'17.70"	47°49'12.12"	34.0	141.5	-	-
MO/10/7	Oct 2010	13°22'40.56"	47°49'00.18"	54.0	148.0	28.0	1953
MO/10/8	Oct 2010	13°22'48.96"	47°48'46.74"	54.0	143.5	22.0	1957
MO/10/9	Oct 2010	13°23'06.72"	47°48'36.36"	59.0	160.0	18.0	1957
MO/07/SC7	Mar 2007	13°23'33.78"	47°48'30.42"	65.0	72.0	19.7	< 1953
MO/07/SC4	Mar 2007	13°24'01.68"	47°48'22.74"	64.0	68.0	18.2	< 1953
MO/05/P3	Jun 2005	13°24'05.46"	47°48'24.72"	62.0	97.0	11.9	< 1953
MO/07/SC3	Mar 2007	13°23' 59.46"	47°48'10.02"	60.0	70.5	17.5	1957

4 Hydrological and sedimentological processes of flood layer formation in Lake Mondsee

Lucas Kämpf[1,2], Philip Mueller[3], Hannes Höllerer[4], Birgit Plessen[1], Rudolf Naumann[5], Heiko Thoss[3], Andreas Güntner[3], Bruno Merz[3], Achim Brauer[1]

[1]GFZ German Research Centre for Geosciences, Section 5.2 Climate Dynamics and Landscape Evolution

[2]TU Dresden, Faculty of Environmental Sciences, Institute for Soil Science and Site Ecology

[3]GFZ German Research Centre for Geosciences, Section 5.4 Hydrology

[4]University of Innsbruck, Research Institute for Limnology Mondsee

[5]GFZ German Research Centre for Ge osciences, Section 4.2 Inorganic and Isotope Geochemistry

Published in The Depositional Record

Abstract Detrital layers in lake sediments are recorders of extreme flood events. However, their use for establishing time series of past floods is limited by lacks in understanding processes of detrital layer formation.

Therefore, we monitored hydro-sedimentary dynamics in Lake Mondsee (Upper Austria) and its main tributary, Griesler Ache, over a three-year period from January 2011 to December 2013. Precipitation, discharge and turbidity were recorded continuously at the river outlet to the lake and compared to sediment fluxes trapped with 3 to 12 day resolution at two locations in the lake basin, in a distance of 0.9 (proximal) and 2.8 km (distal) to the Griesler Ache inflow.

Within the three-year observation period, 26 river floods of different magnitude (10-110 m^3s^{-1}) have been recorded resulting in variable sediment fluxes to the lake (4-760 g $m^{-2}d^{-1}$) including the 'century-scale' flood event in June 2013. The

comparison of hydrological and sedimentological data revealed (i) a rapid sedimentation within three days after the peak runoff in the proximal and within six to ten days in the distal lake basin, (ii) empirical flood thresholds for triggering sediment flux at the lake floor increasing from the proximal (20 m^3s^{-1}) to the distal lake basin (30 m^3s^{-1}), and (iii) various factors that control the detrital sediment transport in the lake. The amount of sediment transported to the lake is controlled by runoff and catchment sediment availability. The distribution of detrital sediment within the lake basin is mainly driven by mesopycnal interflows and closely linked to flood duration and the season in which a flood occurred.

The combined hydro-sedimentary monitoring revealed detailed insights into processes of flood layer formation in a meso-scale peri-Alpine lake and, thereby, improves the interpretation of the depositional record of flood layers.

4.1 Introduction

Lakes form ideal sediment traps in the landscape continuously recording land surface processes in the catchment including extreme events (Hsü and Kelts 1985). Discrete flood-triggered sediment fluxes of detrital catchment material into lakes result in the formation of discrete detrital layers at the lake floor (Sturm and Matter 1978; Siegenthaler and Sturm 1991). Therefore, detrital layers in lake sediments are increasingly used to establish long flood chronologies especially in the Alpine (Støren *et al.* 2010; Glur *et al.* 2013; Wirth *et al.* 2013b; Wilhelm *et al.* 2013), peri-Alpine (Arnaud *et al.* 2005; Swierczynski *et al.* 2013; Czymzik *et al.* 2013) and Arctic realms (Francus *et al.* 2002; Lamoureux *et al.* 2006; Lapointe *et al.* 2012). The recurrence intervals of detrital layers provide information about palaeoflood frequencies (Czymzik *et al.* 2010; Swierczynski *et al.* 2012; Schlolaut *et al.* 2014), whereas flood intensities have been inferred from the thickness (Schiefer *et al.* 2011; Wilhelm *et al.* 2013) of individual deposits.

Varved sediment records provide, in addition, the unique opportunity to date detrital layers with seasonal precision (Mangili *et al.* 2005) and, thereby, (i) determine palaeoflood variability even at seasonal scale (Swierczynski *et al.* 2012; Wirth *et al.* 2013a) and (ii) calibrate the sub-recent detrital layer record with instrumental flood data (Francus *et al.* 2002; Chutko and Lamoureux 2008; Czymzik *et al.* 2010).

Commonly, flood reconstruction from lake sediments assume the completeness of the depositional record in the sense that each flood resulted in a well-preserved detrital layer. However, a test of the hypothesis of completeness of the depositional record is still lacking. First detailed comparisons of detrital layer records with instrumental data even questioned the assumption of completeness by providing evidence for both, floods that did not result in detrital layer deposition and detrital layers, which were not triggered by strong floods (Czymzik

et al. 2010; Kämpf *et al.* 2012b). A possible reason might be that the amount and spatial distribution of detrital sediment within a lake basin triggered by flood events might vary (Lamoureux 1999; Jenny *et al.* 2014) probably even depending on the season in which a flood occurred (Kämpf *et al.* 2014). A better knowledge of the hydrological and sedimentary processes of detrital layer formation is required to reduce the bias in interpretation and, thereby, improve the use of depositional records as palaeoflood archives.

To gain a more sophisticated process understanding of detrital layer formation different attempts have been initiated comprising detailed analyses of single flood deposits (Gilbert *et al.* 2006; Kämpf *et al.* 2012a) and *in situ* monitoring of flood triggered sediment fluxes (Best *et al.* 2005; Crookshanks and Gilbert 2008; Dugan *et al.* 2009). Most observational studies of detrital sediment fluxes in lakes have been performed in arctic and high mountain lakes with predominantly clastic sedimentation. Despite of the growing number of flood reconstructions from Alpine and peri-Alpine lakes (e.g. Wirth *et al.*, 2013b), in-depth monitoring studies in such lakes with mainly autochthonous sediments (biochemically precipitated calcite and organic components) are still lacking.

Here we present results of a three-year integrated lake and catchment monitoring of flood and sediment dynamics in the peri-Alpine Lake Mondsee. The study period comprises the 'century-scale' flood event in June 2013 (Blöschl *et al.* 2013). We chose Lake Mondsee for this in-depth monitoring since it provides a varved sediment record and a flood layer record covering the last 7100 years (Swierczynski *et al.* 2013) as well as a good data base of meteorological and hydrological data. In addition, a first calibration of sub-recent detrital layers with instrumental flood data is available (Kämpf *et al.* 2014). Ultimately, we will contribute new knowledge about flood layer formation in a meso-scale peri-Alpine lake, which is expected to generally improve flood reconstructions from depositional records of lakes.

4.2 Study site

Lake Mondsee is located at the northern fringe of the European Alps in Upper Austria (47°48'N, 13°23'E) at an altitude of 481 m above sea level (a.s.l.) (Fig. 4.1). With a surface area of 14 km^2 and a maximum water depth of 68 m Lake Mondsee is a meso-scale peri-Alpine lake characterized by a specific morphometry displaying a significant kink in the generally elongated and NW-SE directed shape (Fig. 4.1). Lake Mondsee is a meromictic hardwater lake (Dokulil and Skolaut 1986) with one mixing period in autumn/winter and thermal stratification between May and September (Fig. 4.2). Episodically, the lake is completely ice-covered which happened once during the observation period in February to March 2012.

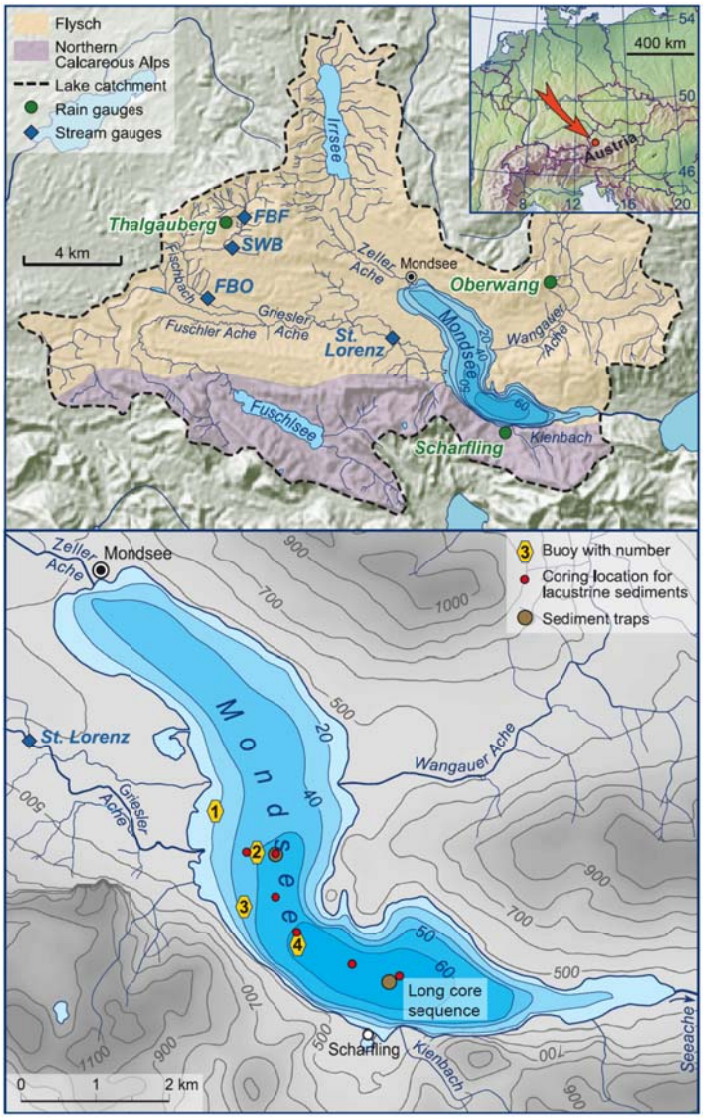

Figure 4.1. Lake Mondsee catchment and monitoring set-up including (i) 4 stream gauges equipped with devices for measuring precipitation, water level, air and water temperature, electrical conductivity, turbidity and automated water sampling, (ii) 4 monitoring buoys within the lake for multilevel water current and turbidity monitoring (Mueller *et al.*, 2013) and (iii) 2 sediment trap chains equipped with 3 integral traps in different water depths, 1 sequential trap at the lake floor and thermistors in different water depths. Additional rain gauges in the catchment conducted by the hydrographic services of Upper Austria and Salzburg are also indicated. Five surface sediment cores were recovered along a transect from the Griesler Ache inflow towards a long sediment core in the distal lake basin (Swierczynski *et al.*, 2013).

The catchment (247 km^2) is subdivided into two major geological units by a main Alpine thrust fault (van Husen 1989) following the southern shoreline of the lake (Fig. 4.1). The northern catchment (ca. 75% of the total catchment) is formed by peri-Alpine hills of up to 1100 m a.s.l. which are built up by Cretaceous Flysch sediments (Sandstone, Argillite). The valleys are covered by moraines formed by latest Pleistocene glacier activity (van Husen 1989). Three tributaries drain the northern catchment: the Griesler Ache in the West, the Zeller Ache in the North, and the Wangauer Ache in the East. Regarding its size and runoff variability

(A_0=110 km^2; MQ=4 m^3s^{-1}; HHQ =137 m^3s^{-1}, ref. BMLFUW [2011]), the Griesler Ache is the largest tributary to Lake Mondsee and the main source for suspended sediments during floods (Kämpf *et al.* 2014). The southern sub-catchment (ca. 25%) reaches a maximum elevation of 1700 m a.s.l. and is part of the Northern Calcareous Alps. The base rock is composed of Jurassic and Triassic units of limestone and dolomite forming steep slopes at the southern lake shoreline which are drained by small torrents like, for example, the Kienbach creek with a catchment of 2.1 km^2 (Fig. 4.1). Lake Mondsee drains via the river Seeache into Lake Attersee at the south-eastern end of the lake (Fig. 4.1).

4.3 Methods

A monitoring network was installed in Lake Mondsee and its catchment between 2011 and 2012, comprising five river gauges along the main tributary to Lake Mondsee, the Griesler Ache, as well as four monitoring buoys and two sediment trap chains within the lake (Fig. 4.1). The combination of river gauges and monitoring buoys was designed to track hydro-sedimentary dynamics, i.e. runoff generation and sediment transport, continuously from the head catchments to the lake (Mueller *et al.* 2013).

4.3.1 Catchment monitoring

Precipitation in the Griesler Ache catchment is recorded since June 2011 using OTT Pluvio rain gauges (OTT Hydromet, http://www.ott.com) at the gauging stations St. Lorenz located close to Lake Mondsee (482 m a.s.l., 4 km distance to inflow), Fischbach Outlet (FBO, 552 m, 10 km) located at the confluence of the Griesler Ache and the Fischbach, which is the largest tributary to the Griesler Ache, and at two stations in the Fischbach head-catchment, Streuwiesenbach (SWB, 777 m, 11 km) and Fischbach Forest (FBF, 786 m, 12 km). In addition we used data from three precipitation gauges at Thalgauberg in the Griesler Ache catchment (730 m a.s.l., 11 km distance to inflow) (operated by the Hydrographic Survey of Salzburg), Scharfling in the Kienbach catchment (482 m, 0.7 km) and Oberwang in the Wangauer Ache catchment (595 m, 5 km) (both operated by the Hydrographic Survey of Upper Austria). Runoff data were obtained from the stream gauge of St. Lorenz (Hydrographic Survey of Upper Austria), located 4 km upstream of the Griesler Ache inflow to Lake Mondsee (Fig. 4.1). For monitoring sediment transport in the river, the station was additionally equipped with a FTS DTS-12 turbidity sensor (Forest Technology Systems Inc., http://www.ftsenvironmental.com) and an ISCO 3700 automatic pumping sampler (Teledyne ISCO, http://www.isco.com). Depending on the actual values of discharge and turbidity, 3-24 river water samples (1 l) were taken automatically

for each of 21 flood events since June 2011 following the turbidity-threshold-sampling (Lewis 1996).

4.3.2 Lake monitoring

Two moorings were installed in Lake Mondsee, each equipped with one sequencing sediment trap (S-trap) and three integrating sediment traps (I-traps). The locations follow a transect from the inflow of the Griesler Ache river to the location of a long sediment record used for establishing a flood layer chronology over the last 7100 years (Swierczynski *et al.* 2013), with one mooring in a distance of 900 m to the river mouth (proximal trap: 47°49.21’ N, 13°22.78’ E, water depth: 56 m) and the other in a distance of 2800 m (distal trap: 47°48.32' N, 13°23.92' E, water depth: 63 m). We compared the sediment trap data with detrital layers investigated in surface sediment cores that were previously retrieved close to the trap locations in the proximal (sediment core MO/10/4: 47°49.16’ N 13°22.79’ E) and distal lake basin (MO/05/P3: 47°48.41' N, 13°24.09' E, ref. Kämpf *et al.* [2014]).

The I-traps (UWITEC, http://www.uwitec.at) have two collecting cylinders with an active area of 127 cm^2 in total. The two sequencing traps are equipped with a computer programmable sample bottle carrousel and differ in size: with 500 cm^2 we chose a trap with a smaller active for the proximal location (PPS 4/3, 12 sample bottles, Technicap, http://www.technicap.com) and a larger one for the distal location (1250 cm^2, PPS 3/3, 12 sample bottles) due to expected higher sediment accumulation ratios closer to the inflow of the Griesler Ache (Swierczynski *et al.* 2009). The S- and one of the I-traps were deployed approximately 3 m above the lake bed surface in a water depth of 53 m (prox.) and 60 m (dist.). The other two I-traps were moored in the upper water column (14 m) and between the upper and lower traps (prox.: 33 m, dist.: 30 m). 12 temperature loggers (Hobo U22 Water Temp Pro, Hobo, http://www.onsetcomp.com) were attached to the proximal mooring at water depths of 1, 3, 5, 8, 11, 14, 18, 22, 33, 43, 53 and 55 m and 4 loggers to the distal mooring at water depths of 1, 14, 30 and 60 m.

The moorings were first deployed at 13 January 2011. The S-trap at the distal mooring was added on 04 April 2012. The traps were recovered in a monthly rhythm between April and November until 03 April 2014. Thus, I-traps collect material on a basis of 21 to 41 days between April and November and of 41 to 123 days between December and March. The individual S-trap samples cover a time interval of 3-4 days between April and November and 4-12 days between December and March.

This study reports data from samples collected between January 2011 and December 2013 giving a total of 28 I-trap samples from the upper (14 m) and

lower (prox.: 53 m, dist.: 60 m) water column at each location as well as 269 S-trap samples at the proximal and 158 samples at the distal location. The S-trap time series exhibit three gaps: (i) between March and April 2012 (37 days) caused by persistent ice cover, (ii) between September and October 2012 (21 days) due to technical reasons, and (iii) in June 2013 (6 days) due to very high lake water level that inhibited trap recovery. The third gap was bridged by deploying two additional I-traps close to the mooring locations.

4.3.3 Sediment analyses

The sample bottles of the river water samplers and sediment traps were stored at 4°C after recovery for at least 48 h to ensure that all suspended particles had settled. The samples were freeze dried and the total dry weight was determined. For trap samples, the daily sediment flux (in g $m^{-2}d^{-1}$) was calculated for each sample. For river water samples, the measured suspended sediment concentration (SSC in g l^{-1}) was used for setting up SSC rating curves of the turbidity sensor at the gauge of St. Lorenz (Supplementary Fig. 4.2). The rating curves were established individually for the three strongest recorded floods by applying polynomial regression (Lewis and Eads 2009).

Total carbon (TC), nitrogen (TN) and organic carbon (TOC) were determined for each S-trap sample using an elemental analyser Euro Vector EA (EuroEA 3000, www.eurovector.it). For TC and TN, around 5 mg of powdered sample was loaded in tin capsules and combusted in the elemental analyser. TOC was determined on in-situ decalcified samples. Around 3 mg of sample was weighted into Ag-capsules, treated with 20 % HCl, heated for 3 h at 75°C, and finally wrapped and measured as described above. Replicate determinations showed a standard deviation better than 0.2%. Organic matter (OM) was calculated as OM=2×TOC (Meyers and Teranes 2001) and total inorganic carbon (TIC) as TIC=TC-TOC. The $CaCO_3$ content was calculated stoichiometrically by multiplying the TIC by 8.33, assuming that all inorganic carbon is bound as calcium carbonate. We are aware that minor dolomite contributions from catchment rocks (Supplementary Fig. 4.1) in the detrital carbonate fraction might cause little inaccuracies.

Grain size was measured for 13 selected trap samples with high sediment flux rates using a laser particle sizer (Fritsch Analysette, Fritsch, http://www.fritsch.de). The samples were sieved at 1 mm and dispersed in an ultrasonic bath before measuring. Image data were automatically transferred to particle distribution by the software Fritsch MaScontrol applying the Fraunhofer model.

The mineralogical composition was determined for those trap samples that were also analysed for their grain size distribution and for four samples of river bed

material as well as two detrital layers in sediment cores using a PANanlytical Empyrean X-ray diffractometer equipped with a Cu tube (http://www.panalytical.com). The samples were powdered before measuring.

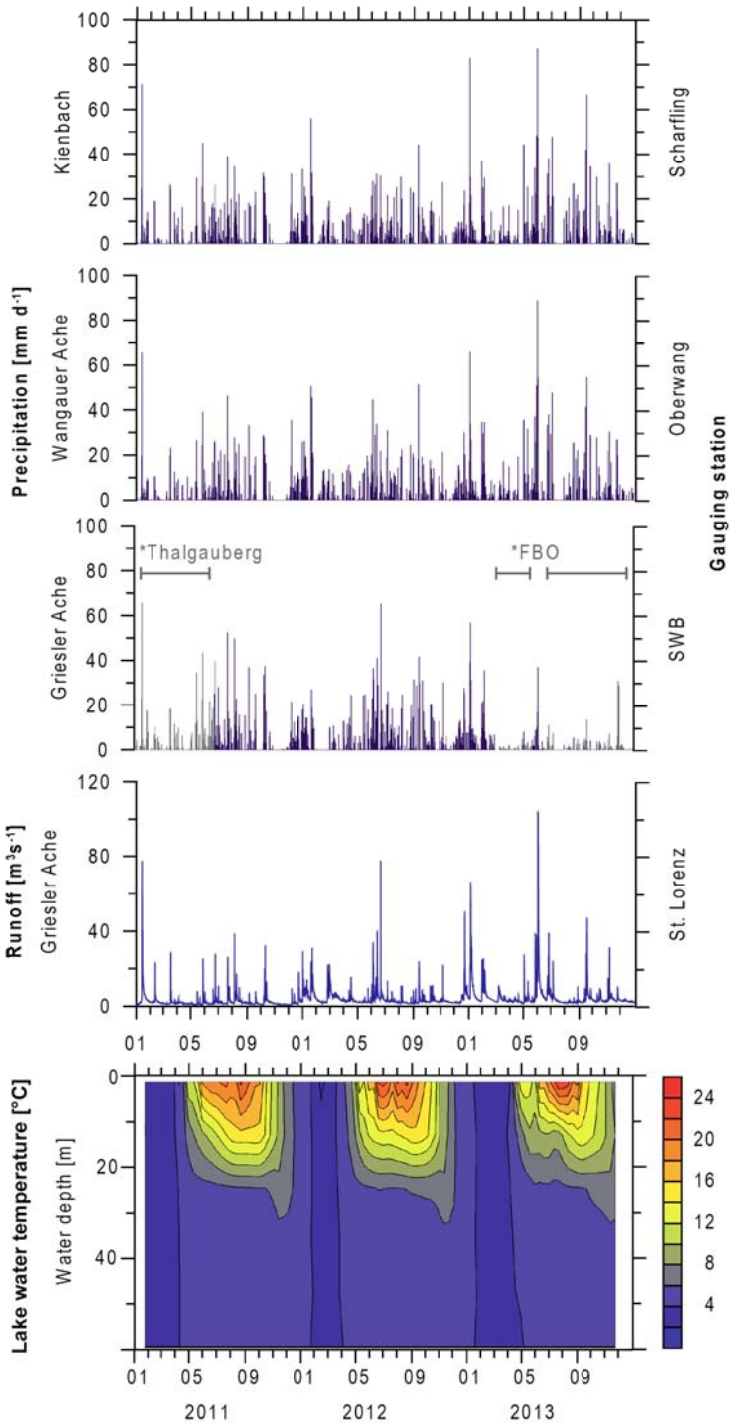

Figure 4.2. Hydroclimatic data 2011-2013: daily precipitation sums from different catchments: Kienbach (Scharfling rain gauge), Wangauer Ache (Oberwang), and Griesler Ache (Streuwiesenbach [SWB], gaps in the time series were filled with data from Thalgauberg and Fischbach Outlet [FBO] rain gauges); hourly runoff of the Griesler Ache River at St. Lorenz gauging station and water column temperature at the proximal trap site. Locations of the gauging stations can be found in Fig. 4.4.1.

4.4 Results

4.4.1 Hydro-climatic conditions at Lake Mondsee 2011-2013

Mean annual precipitation in the Mondsee catchment during the observation period from January 2011 to December 2013 was 1600 mm and thus, in the range of the long-term mean (1981-2011, ref. BMLFUW [2011]). Large rainfall amounts (> 40 mm d^{-1}) were recorded during 20 days (2011; 4, 2012: 7, 2013: 9) and primarily took place between May and September (15 days) and, secondarily, in winter (5 days >40 mm). With 90 mm d^{-1} the maximum precipitation was recorded at the Oberwang rain gauge on 01 June 2013 (Fig. 4.2).

The mean runoff between January 2011 and December 2013 was 4.1 m^3s^{-1} that is close to the long-term mean of 3.9 m^3s^{-1} (1961-2011, ref. BMLFUW [2011]). Runoff events > 30 m^3s^{-1} occurred 14 times in the observation period (2011: 3, 2012: 4, 2013: 7) and, like precipitation events, cumulated in summer (May-Sep: 8, Oct-Nov: 2, Dec-Feb: 4). The largest flood in the monitoring period reached a maximum hourly discharge of 104 m^3s^{-1} (02 June 2013) and was one of the strongest recorded floods in that region with an estimated return period of around 100 years (Eybl *et al.* 2013).

4.4.2 Variability in sediment flux I: total sediment composition

Sediment flux in Lake Mondsee was trapped over the period from January 2011 to December 2013 at two different sites within the lake basin (Fig. 4.4.1), one located in a position proximal to the inflow of the main tributary river (distance: 900 m) and one in a distal position (2800 m). The total sediment flux including both, allochthonous and autochthonous components, was by median 4 g $m^{-2}d^{-1}$ (prox.: 4.2 g $m^{-2}d^{-1}$, dist.: 3.6 g $m^{-2}d^{-1}$) and exhibited (i) a seasonal variability with higher flux rates in summer (5-6 g $m^{-2}d^{-1}$ in May-Sep) and lower flux rates in autumn and winter (1-1.5 g $m^{-2}d^{-1}$ in Oct-Jan) and (ii) short-term peaks of up to 758 g $m^{-2}d^{-1}$ in the proximal and up to 59 g $m^{-2}d^{-1}$ in the distal lake basin (Figs. 4.3a+b).

The seasonal variability of the trapped sediment flux is also expressed by distinct changes in sediment composition (Figs. 4.3c+d). Calcite contents varied from 20-40% (October to April) to 60-95% (May to September) with maximum values between July and August (Fig. 4.4.3c). The higher calcite contents in summer reflect biochemical precipitation of calcite in epilimnic waters which is a typical seasonal process in mid-latitude hardwater lakes (Koschel *et al.* 1983).

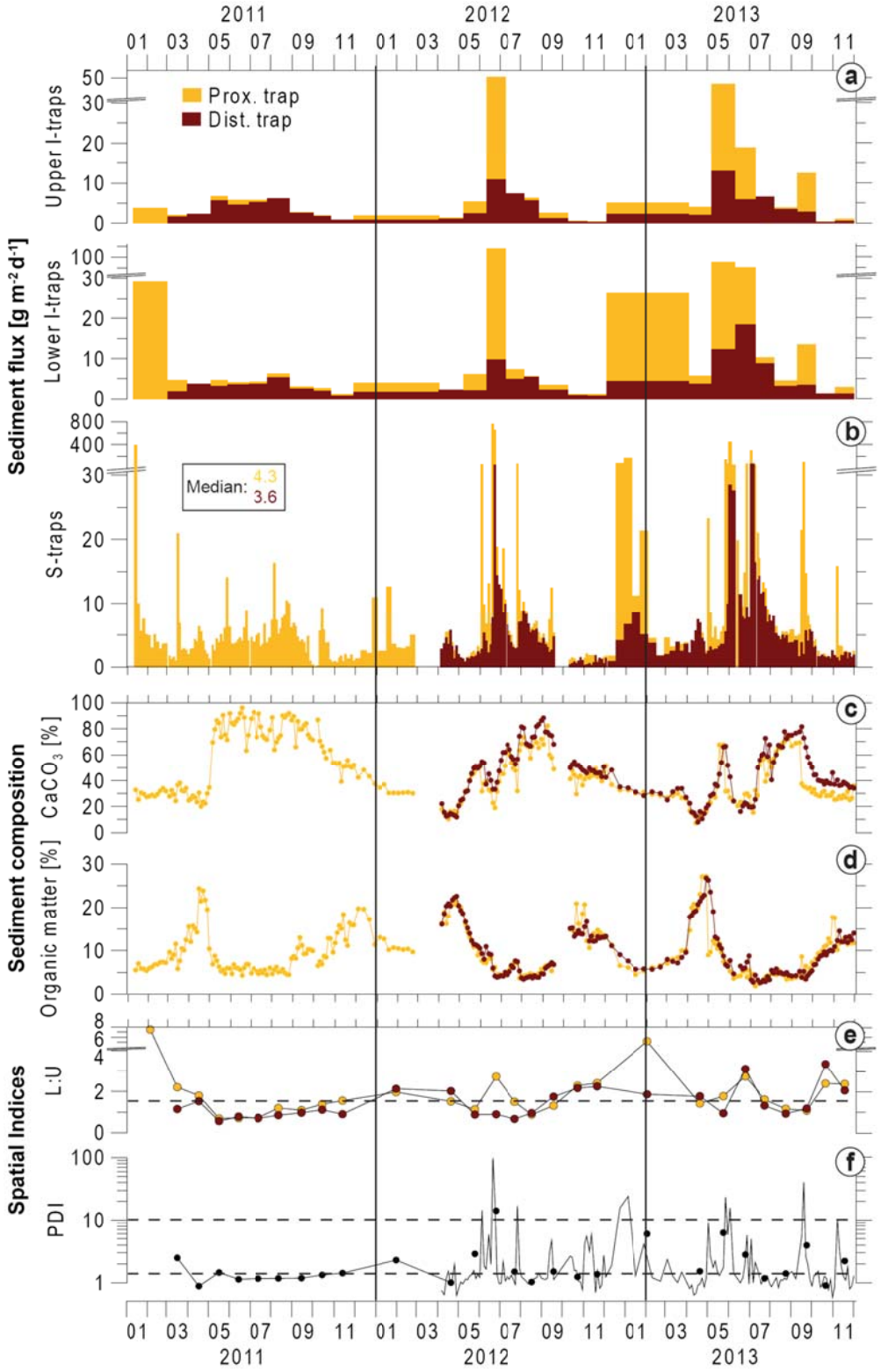

Figure 4.3. Sediment fluxes in Lake Mondsee at the proximal and distal location (01/2011-11/2013): (a) monthly values in integrating traps in the upper (14 m water depth) and lower water column (3 m above lake floor, A: 53 m, B: 60 m); (b) 3-12 day values in sequential traps in the lower water column and contents of (c) calcite and (d) organic matter (Prox.: 2011-2013, dist.: 2012-2013). Spatial sediment flux patterns are expressed by ratios of sediment flux between: (e) lower and upper traps (L:U) and (f) proximal and distal traps (PDI), dots in (f) indicate monthly values calculated from I-traps.

The contents of organic matter in trapped sediment, calculated from the measured TOC contents, varied between 5 and 25% and exhibited a clear maximum in April and a second, lower maximum of 15-20% in late autumn (October-December) when bulk sediment fluxes were lowest (Figs. 4.3b+d). The maximum in April was predominantly made up of diatom frustules, whereas in autumn amorphous organic matter and diatoms were abundant as revealed by smear slide investigations. Between October and March, the sediment was mainly composed of dolomitic and siliciclastic matter derived from either the shorelines by wave activity and/or directly from the catchment surface by runoff processes. The observed seasonal variations in sediment flux lead to the formation of characteristic diatom, calcite and mixed sub-layers preserved and described in the varved sediment record of Lake Mondsee (Lauterbach *et al.* 2011; Swierczynski *et al.* 2012).

4.4.3 Variability in sediment flux II: spatial distribution

We characterized the spatial sediment distribution in the lake water body by both its vertical and horizontal variability in order to decipher pathways and mechanisms of lake internal sediment transport. The vertical variability is expressed by the flux ratio of the lower and upper traps (L:U, ref. Cockburn and Lamoureux [2008]) calculated for the 28 I-trap samples representing monthly means (Fig. 4.3e). From these samples, 51% (prox.: 13 samples, dist.: 16 samples) ranged between 0.6 and 1.5 indicating comparable flux rates throughout the water column and 38% of the values ranged between 1.5 and 2.5 (prox.: 12 samples, dist.: 9 samples) representing a mixture of vertical and lateral sediment fluxes. L:U values > 2.5 rarely occurred (11%, prox.: 4 samples, dist.: 2 samples), reflecting sediment flux predominately in the lower water column mainly driven by hyperpycnal underflows (Cockburn and Lamoureux 2008). It has to be considered that the vertical sediment flux ratios likely represent minimum estimates of sedimentation during times of underflows, as the traps were designed to capture mainly sediment that settled vertically through the water column and were allocated 3 m above the lake bottom likely leading to an underestimation of material transported by underflows. The vertical sediment distribution indicates seasonally changing sediment pathways. In summer (May-Sep), the L:U ratio was < 1.5 for 90% of all values indicating predominately downward sediment flux from the upper water column. In fall to spring the L:U ratio was > 1.5 for 90% of all values pointing to the contribution of lateral sediment transport from the shoreline and/or the tributary streams during winter.

The lateral sediment distribution is expressed by the flux ratio of the proximal and the distal site (Proximal-Distal Index [PDI], ref. Lamoureux [1999]). PDI values were calculated for the lowermost I-traps and sequential traps (Fig. 4.3f) revealing 64% of the values ranging between 0.6 and 1.5 representing a uniform

sedimentation pattern and 36% of the values at the proximal site exceeding those at the distal site by factors > 1.5 proving sediment input from the main tributary river and decreasing sediment deposition towards distal direction through settling of particles. In few cases (6%) the PDI values exceed 10 indicating localized sediment fluxes to the proximal lake basin.

To identify events with strongly increased sedimentation in the sediment flux time series, we defined high sediment flux values as peaks which (i) exceeded the median sediment flux of 4 g $m^{-2}d^{-1}$, and (ii) showed an increase to the previous sample of more than 50%. This resulted in 32 sediment flux peaks occurring during 35 months of observation at the proximal trap location (2011-2013) and 14 peaks during 20 months of observation at the distal trap location (2012-2013) (Fig. 4.4). 12 of these 14 peaks occurred synchronously at both locations or delayed by one sample at the distal location. Four peaks occurred only in one part of the basin; two at the proximal and two at the distal trap. For peak sediment flux events at both trap sites the spatial distribution of detrital material is variable expressed in PDI values ranging between 2 and 25.

4.4.4 Sediment flux versus runoff

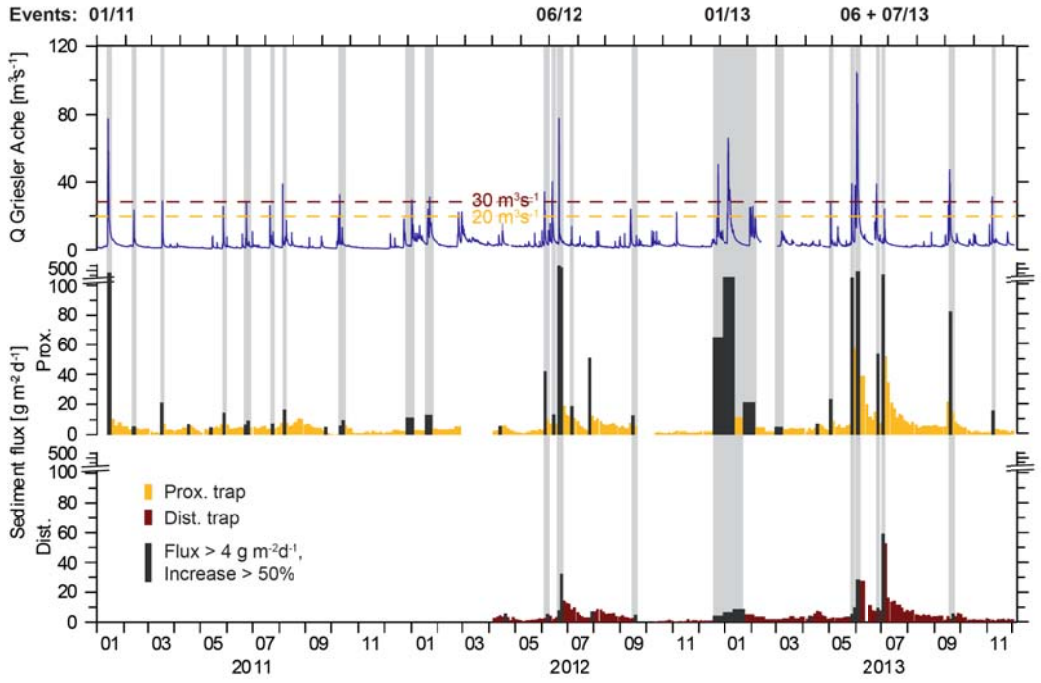

Figure 4.4. Comparison of trapped sediment flux in Lake Mondsee with runoff in the Griesler Ache River. Black coloured samples mark peaks in sediment flux as defined by exceeding the median sediment flux (4 g $m^{-2}d^{-1}$) and an increase to the previous sample of 50%. Grey bars mark sediment flux peaks coincided with elevated runoff and precipitation. Dashed lines indicate thresholds for triggering peaks in sediment flux: 20 m^3s^{-1} in the proximal and 30 m^3s^{-1} in the distal lake basin. The five runoff events that triggered the highest sediment flux to the lake basin (>100 g $m^{-2}d^{-1}$ at the proximal trap) are named at the top.

The three-year time series of trapped sediment flux was compared to runoff data from the outlet gauge of the main tributary river, the Griesler Ache, in order to test if a relation exists between river floods and the spatio-temporal sediment distribution within the lake (Fig. 4.4). Most of the defined peaks in sediment flux (prox.: 26 of 32; flux: 5-758 g $m^{-2}d^{-1}$; dist.: 11 of 14; 4-59 g $m^{-2}d^{-1}$) coincided with elevated river runoff ranging from 10 to 104 m^3s^{-1}. For one peak in sediment flux (July 2012), no discharge data were available so that this event was excluded from further analyses. Five peaks of the proximal (16% of all sediment flux peaks) and two peaks of the distal trap (15%) did not relate to elevated runoff. Interestingly, peaks not related to runoff events occurred independently either at the proximal or at the distal site (Fig. 4.4).

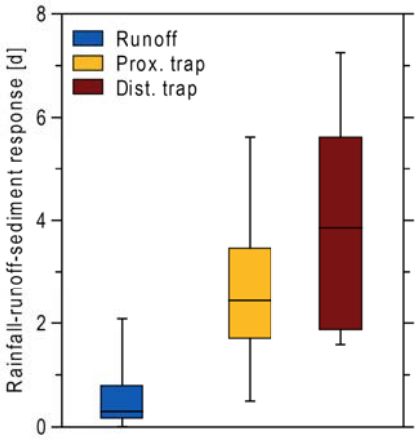

Figure 4.5. Time lag between peaks in precipitation and runoff as well as between peaks in runoff and sediment flux at the proximal and distal traps (end of sampling interval) of (prox.: n=25, dist.: n=7).

Comparing flood magnitudes in terms of their hourly peak river discharge reveals that 10% of low magnitude floods in the range of 10 to 20 m^3s^{-1} triggered a measurable peak in sediment flux in the proximal lake basin, whereas for floods > 20 m^3s^{-1} already 96% resulted in a distinct sediment flux at this location (Fig. 4.4). At the distal location elevated sediment flux was observed for floods < 20 m^3s^{-1}, but 80 % of floods > 30 m^3s^{-1} resulted in a peak. Two peaks in sediment flux at the distal location were related to floods between 20 and 30 m^3s^{-1}. The sediment flux peaks in the proximal lake basin occurred within three days after the discharge peak, i.e. within the same sampling interval (Fig. 4.5). In the distal lake basin the period of highest sediment flux mostly expanded over two sampling intervals (3-6 days).

Besides the coincidence of flood occurrence and enhanced sediment flux, we compared the amount of sediment deposited over the whole flooding period with peak runoff values and observed an exponential relation (Fig. 4.6a). The correlation coefficient decreases from the proximal ($r^2_{prox.}$=0.62) to the distal lake

basin ($r^2_{dist.}$=0.31) and is strongly affected by one event (07/13, Fig. 4.4), when a very high sediment deposition (prox.: 1258 g m^{-2}, dist: 468 g m^{-2}) but only a low maximum discharge were recorded (24 m^3s^{-1}). If this event is excluded, the correlation becomes better and more similar at both sites ($r^2_{prox.}$=0.76, $r^2_{dist.}$=0.80).

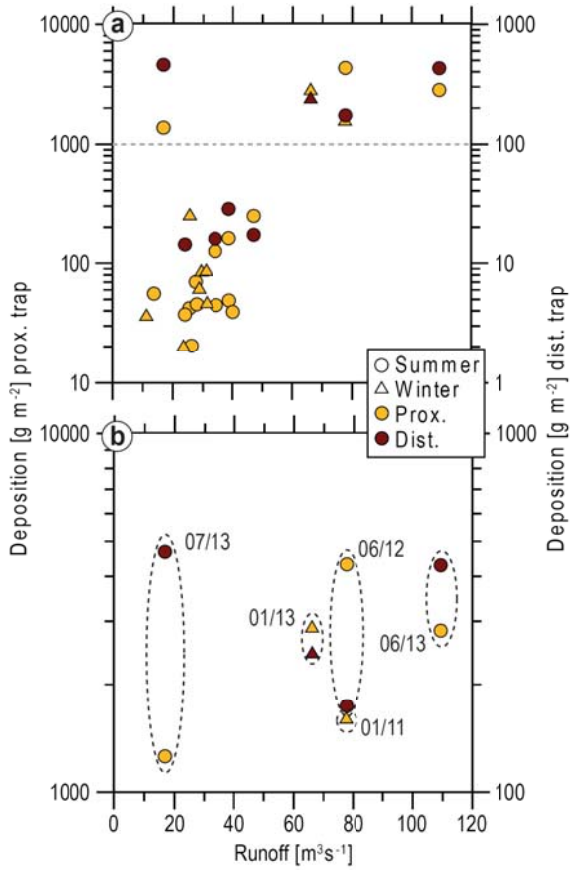

Figure 4.6. (a) Correlation of peak runoff (hourly values) and sediment deposition during the monitoring period 2011-2013 applying an exponential regression. Statistics: Prox.: n=25, r^2=0.76, p<0.01, Dist.: n=7, r^2=0.80, p<0.01; 07/13 event excluded from statistics. (b) Enlarged view of plot (a) for the five strongest sediment flux events that likely resulted in detrital layer formation.

4.4.5 Hydro-sedimentary dynamics during major floods

In total, 26 floods resulting in enhanced sediment flux to the lake floor were recorded in the three-year monitoring period. For five of these floods the sediment yield exceeded 1000 g m^{-2} at the proximal site (1258 - 4320 g m^{-2}) that were triggered by precipitation of more than 40 mm d^{-1} and resulting runoff peaks ranging from 24 to 104 m^3s^{-1} (Tab. 1). At the distal site the sediment yield was significantly lower (174 - 468 g m^{-2}).

Three of the five floods with highest sediment yields occurred in summer and two in winter (Tab. 1). The 01/11 flood lasted for three days with a maximum precipitation of more than 65 mm d^{-1} in all three gauged catchments (Fig. 4.2).

The 01/13 event was characterized by a persistent wet phase over two months with two main precipitation periods of three and four days, respectively, and maxima of 57 to 83 mm d^{-1} (Fig. 4.8). Whereas the two winter floods were both triggered by precipitation events that covered the whole catchment area, the three strongest summer floods were triggered by regional and local scale rainfall events (Fig. 4.2). The latter were convective events of high intensity and short duration (< 1 day) affecting only parts of the catchment, like the 06/12 event in the Fischbach sub-catchment (max. rainfall at station SWB: 65 mm d^{-1}) and the 07/13 event in the Wangauer Ache catchment (Oberwang: 48 mm d^{-1}). In contrast, the 06/13 event was triggered by a series of synoptic scale low pressure systems (Blöschl *et al.* 2013), resulting in strong precipitation over the whole catchment area lasting for two weeks (Tab.1).

The stream-flow rose within one to ten hours after the main precipitation events (Figs. 7+8). In January 2011, the flood hydrograph peaked at 78 m^3s^{-1} and was larger than 10 m^3s^{-1} for three days. The two runoff peaks between December 2012 and January 2013 were characterized by maximum discharges of 50 and 66 m^3s^{-1} and durations of three and seven days. The local rainfall events in June 2012 and July 2013 triggered peak flows of 78 m^3s^{-1} during the 06/12 event and 24 m^3s^{-1} during the 07/13 event. The comparably low peak flow in the Griesler Ache during the 07/13 event is due to the local character of the precipitation event which mainly covered the catchment of the Wangauer Ache which is not part of our monitoring network (Tab.1, Fig. 4.1). The June 2013 flood was exceptional for the entire observation period and reached by far the highest maximum discharge values (104 m^3s^{-1}) and the longest duration (9 days > 10 m^3s^{-1}). The flood resulted in a lake level rise of more than 1.5 m and flooding of the city of Mondsee.

Suspended sediment concentration in the river (SSC), as recorded by turbidity measurements and automatic water samples, reached highest values during the 06/13 event (SSC_{max}=61 g l^{-1} in samples, 103 g l^{-1} rated from turbidity) and was lowest during the 01/13 event (SSC_{max}=1.1 g l^{-1} in samples, 1.6 g l^{-1} rated from turbidity). During all events, SSC increased with increasing discharge and reached maxima during the rising limb of the flood hydrograph and already declined one to two hours before the flood peak (Figs. 7+8).

The sediment depositions in the lake occurred with time lags of one to four days after the peak runoff at the proximal location and of up to ten days at the distal trap (Figs. 7+8). The total sediment deposition in the proximal basin was highest during the 06/12 event (4320 g m^{-2}) and lowest during the 07/13 event (1258 g m^{-2}), whereas at the distal site the opposite has been observed, i.e. highest sediment deposition during the 07/13 event (468 g m^{-2}) and lowest during the 06/12 event (174 g m^{-2}).

Table 4.1. Table 1: Hydro-sedimentary data on the five largest sediment transfer events to Lake Mondsee within the monitoring period 2011-2013. Note that the 07/13 event is a very rare local event transporting sediments from a different sub-catchment (Wangauer Ache) that is not included in the monitoring program.

		01/11	06/12	01/13	06/13	07/13
Catchment data	**Precipitation**					
	Affected catchment area	Regional	Fischbach	Regional	Regional	Wangauer A.
	Date	10-15 Jan	20 Jun	09 Dec-12 Jan	19 May-06 Jun	03-05 Jul
	Days > 10 mm	2	1	3+3+4	1+2+4	2
	Maximum [mm d^{-1}]	71	65	83	90	48
	Sum [mm]	104	82	350	320	75
	Discharge Griesler Ache					
	Days > 10 m^3s^{-1}	3	1	3+7	1+8	1
	Max. hourly discharge [m^3s^{-1}]	78	78	66	104	24
	Max. daily discharge [m^3s^{-1}]	56	21	43	79	11
	Max. turbidity [NTU]	no data	1730	1078	1410	no data
	Max. measured SSC [g l^{-1}]	no data	19	1	62	no data
	Max. rated SSC [g l^{-1}]	no data	20	2	103	no data
Lake data	**Prox. trap**					
	Max. sediment flux [g $m^{-2}d^{-1}$]	391	758	163	452	54
	Sediment deposition [g m^{-2}]	1603	4320	2880	2825	1258
	$D:Q_{prox.}$	no data	0.1	0.3	0.2	< 0.1
	$L:U_{prox.}$	8	3	5	2	3
	Dist. Trap					
	Max. sediment flux [g $m^{-2}d^{-1}$]	no data	32	9	29	16
	Sediment deposition [g m^{-2}]	no data	174	245	430	468
	$D:Q_{dist.}$	no data	0.1	0.2	0.5	< 0.1
	$L:U_{dist.}$	no data	1	2	1	3
	PDI	no data	25	12	7	3

The sources of detrital sediment are determined by their mineralogical composition (Tab. 2). The sediments originating from the Flysch catchment predominately consist of siliciclastic material made up of quartz, mica and feldspars, whereas the Northern Calcareous Alps are predominantly composed of dolomite (Supplementary Fig. 4.1). This allows us to use the dolomite/quartz ratio (D:Q) to distinguish between the two main sediment source areas (Tab. 2). Riverbed material of the main tributaries Griesler and Wangauer Ache exhibit similar D:Q ratios of 0.2. This value is in accordance with most values measured in sediment trap samples in the lake, ranging between 0.2 and 0.5, indicating these catchments as main sources for detrital sediments. The lowest D:Q values < 0.2 are measured for the Fischbach bed load reflecting a clear dominance of Flysch sediments in this sub-catchment that exclusively drains a Flysch area (Supplementary Fig. 4.1). Similar values are measured in sediments trapped after the local 06/12 and 07/13 events. The highest D:Q values > 1.0 were measured for the bed load of the Kienbach creek reflecting a dominance of material originating from the Northern Calcareous Alps. Sediments trapped in the distal trap after the 06/13 flood exhibit D:Q values between 0.5 and 1.0 pointing to sediment transport from both, the Flysch and the Limestone catchments.

Sediment trap samples of the five events with highest sediment yields were further analysed for their grain size distribution (Fig. 4.9). The resulting distributions exhibit unimodal (prox.: 4 samples, dist.: 2 samples) and bimodal patterns (prox.: 1 samples, dist.: 4 samples) with maxima around 10-60 µm for unimodal and at 2-4 µm and 10-60 µm for bimodal functions, respectively. Thus, samples with a bimodal grain size distribution contain a higher portion of fine silt and clay particles. Fine-grained particles were generally more abundant in samples trapped (i) in summer, (ii) after the main sediment flux event and (iii) in the distal lake basin. The only exception is the June 2013 flood event (Fig. 4.9c), when trapped samples in the distal lake basin exhibited a unimodal function and a coarser maximum (36 µm) than in the proximal lake basin (24 µm).

4.5 Discussion

Detrital layers in lake sediments commonly are interpreted as flood recorders. However, the potential of these geoarchives for extending instrumental flood records back in time is still not fully exploited due to our limited knowledge about (i) how the amount and spatial distribution of detrital sediment are related to flood parameters and (ii) to which extent this relation is affected by local factors in the catchment and the lake. These are considered as potential bias for establishing palaeoflood time series from lake sediment records (e.g. Schiefer *et al.* 2006, 2011; Dugan *et al.* 2009).

The three-year monitoring at Lake Mondsee provides a comprehensive set of hydro-sedimentary data from the lake and its catchment comprising 26 floods with very different magnitudes (return periods ranging from << 1 year to 100 years), seasonal occurrence and sediment response (4 to 758 g $m^{-2}d^{-1}$). This reveals new insights into processes of flood layer deposition with unprecedented detail including a variety of influencing factors like peak runoff and season, sediment availability or the type of precipitation event giving the basis for an improved evaluation of the depositional record of Lake Mondsee. Our monitoring data have been related to the available sub-recent depositional record covering the time period from 1976 to 2005 (Fig. 4.11) (Kämpf *et al.* 2014) since it was not yet possible to obtain undisturbed sediment cores of the last three years due to the too high water content of the topmost sediments.

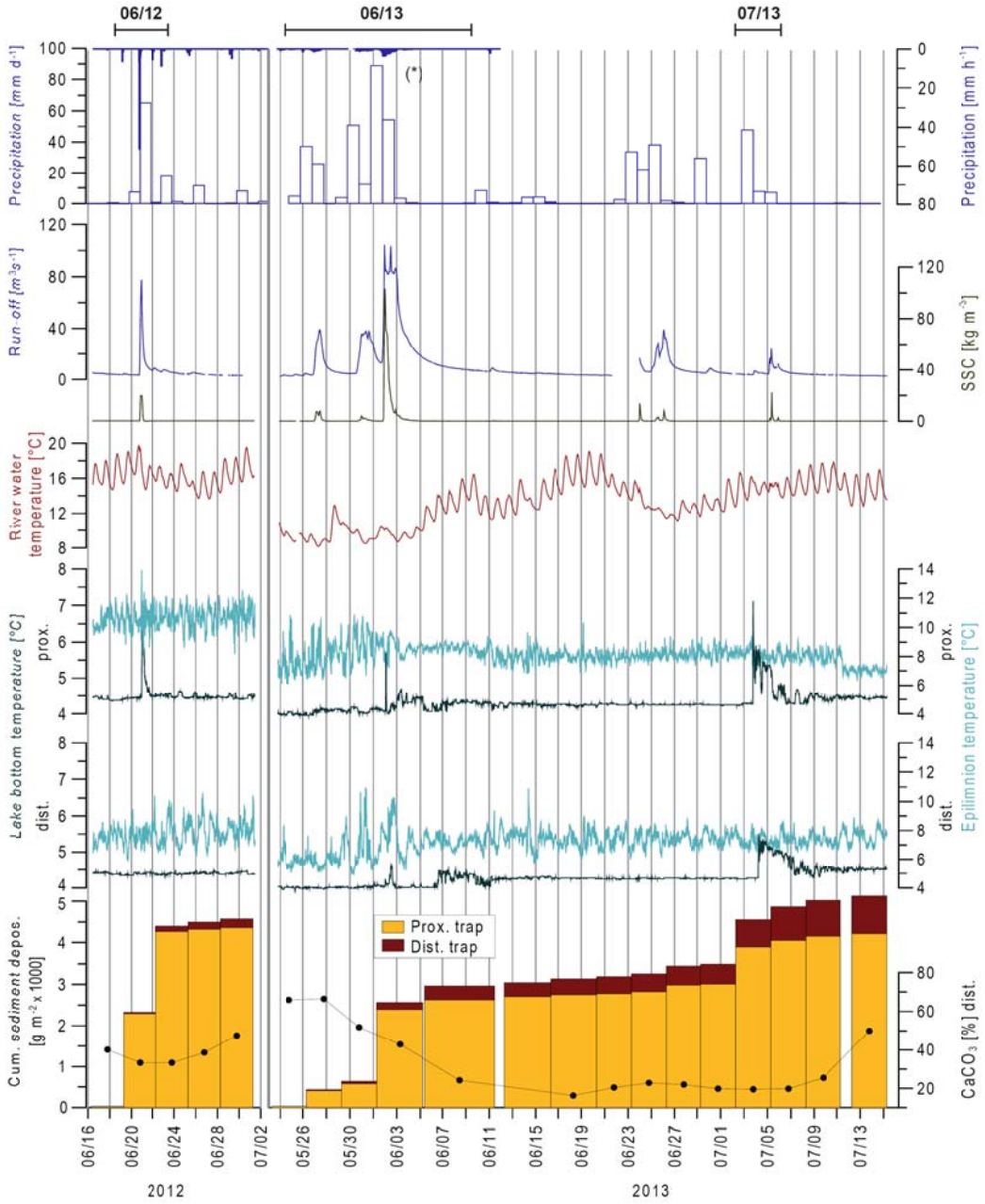

Figure 4.7. Precipitation, run-off, river sediment concentration, river and lake water temperature and trapped sediment deposition 3 m above the lake bottom at the proximal and distal trap location during the largest summer floods. (*) Daily precipitation data from 2013 measured at the Oberwang gauging station. The distance between vertical grey lines represents 2 days.

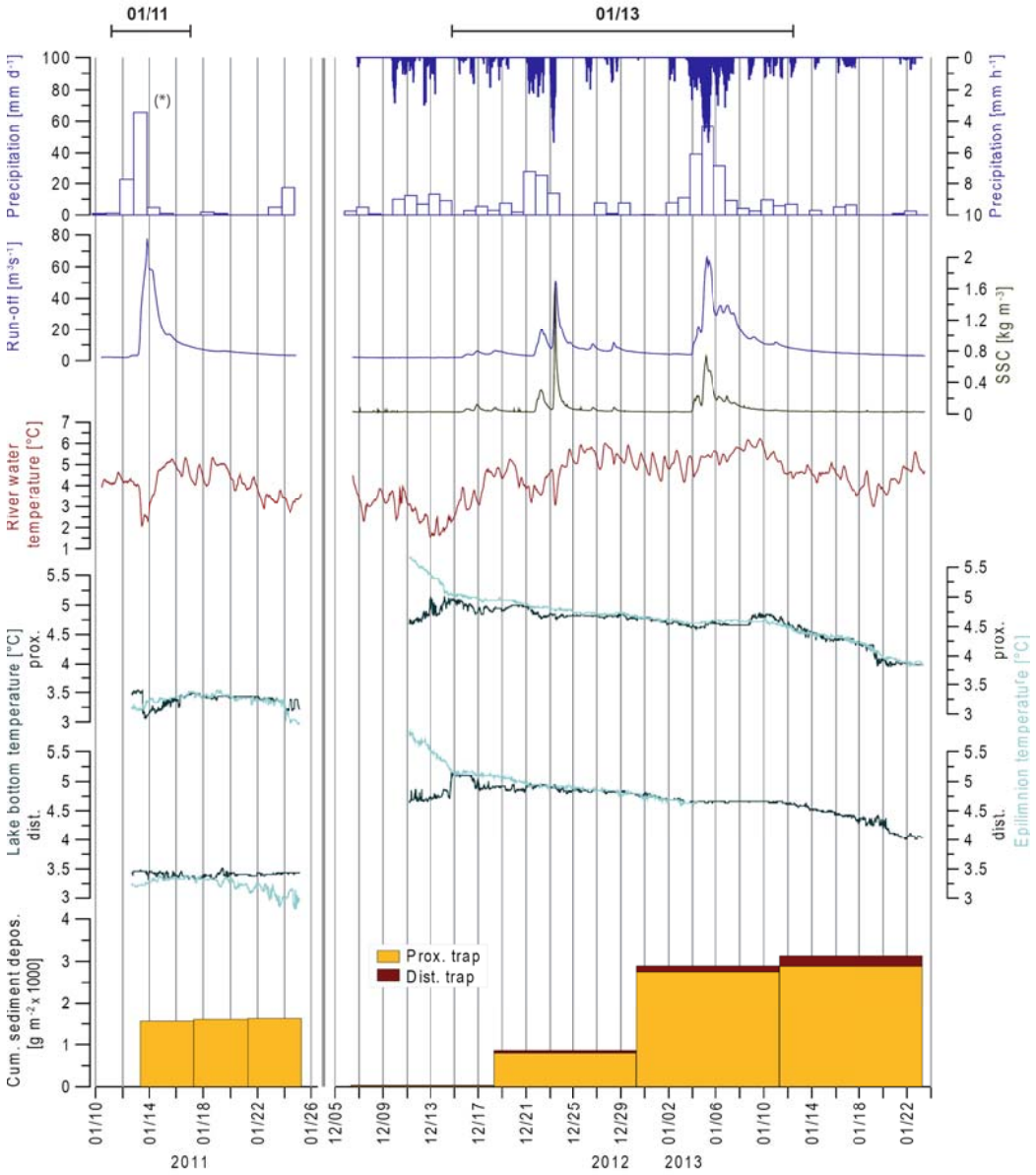

Figure 4.8. Precipitation, run-off, river sediment concentration, river and lake water temperature and trapped sediment deposition 3 m above the lake bottom at the proximal and distal trap location during the largest winter floods. (*) Precipitation data from the 01/11 event measured at Thalgauberg gauging station. The distance between vertical grey lines represents 2 days.

4.5.1 Parameters controlling flood-related sediment flux

Runoff magnitude

A general link between runoff events in the Griesler Ache and sediment flux into the lake is evidenced by the measured sediment response to 26 flood events. Moreover, we found different empiric runoff thresholds for both sites, above which suspended sediment is transported to the respective location: 20 m^3s^{-1} for the proximal and 30 m^3s^{-1} for the distal site (Fig. 4.4). Lower amplitude floods caused a measurable sediment flux only in two exceptional cases.

In addition to the coincidence of peaks in the runoff and sediment trap time series, we observed a significant exponential relation between peak runoff and the amount of trapped sediment in the proximal (r^2=0.76) and distal lake basin (r^2=0.80) if the local 07/13 event with predominant sediment flux from the ungauged secondary stream Wangauer Ache is excluded (Fig. 4.6a).

Hitherto, we only discussed the relation between runoff and sediment transport. More important for interpreting the depositional record, however, is an assessment of the amount of sediment flux that is necessary to produce a recognizable detrital layer in the sediment record. We can calculate this minimum sediment yield from the thickness of the finest detected detrital layers found in the sediments (0.2 mm; Kämpf *et al.* 2014) and a mean dry density of 1.5 g cm^{-3}. The resulting minimum sediment yield of approximately 300 g m^{-2} was exceeded by four of the 26 observed floods at the proximal site that were triggered by runoff peaks ranging from 66 to 104 m^3s^{-1} and precipitation > 65 mm d^{-1} (Fig. 4.4, Tab. 1). At the distal site, where the long flood record has been established (Swierczynski *et al.* 2013), only the strongest of these four events likely resulted in sufficient sediment transport to form a detrital layer (June 2013, max. runoff: 104 m^3s^{-1}). Hence, based on the amount of sediment deposition we predict the formation of one flood triggered detrital layer at the distal location (June 2013) and four layers at the proximal site (January 2011, June 2012, January, June 2013). Another event in July 2013 that also supplied sediment amounts > 300 g m^{-2} to the proximal and distal locations (Fig. 4.7) is not included in the further discussion since this event was caused by local precipitation in the Wangauer Ache catchment, which is not part of our monitoring network (Fig. 4.1).

The flood discharge values, which according to the observational data should have caused detrital layer formation, are for both locations in the same range as empirical discharge thresholds for detrital layers revealed from the depositional record (Kämpf *et al.* 2014). These are >60 m^3s^{-1} for the proximal site (observation: 66 m^3s^{-1}, 78 m^3s^{-1}, 104 m^3s^{-1}) and >80 m^3s^{-1} for the distal site (observation: 104 m^3s^{-1}). The good agreement between these independently obtained data further supports the existence of discharge thresholds for flood layer deposition and makes us confident that these thresholds can be reasonable well determined.

Despite the existence of thresholds in discharge for detrital layer formation we do not observe a correlation between runoff and sediment yield for the strongest floods (Fig. 4.6b). This suggests that the availability of fine-grained sediment in the rivers and variable sediment distribution within the lake basin also play a crucial role for detrital layer formation and will be discussed in the following.

Table 4.2. Mineralogical composition [%] of sediment trap samples obtained during major flood events (I= integral trap), river bed material and two detrital layers in the sub-recent sediment record. The ratio of dolomite and quartz contents (D:Q) was used to discriminate the Flysch (quartz-rich) and limestone (dolomite-rich) dominated sub-catchments (see also Supplementary Fig. 4.1).

	Sample	Calcite	Chlorite	Dolomite	Kaolinite	Illite	Orthoclase	Albite	Quartz	Smectite	D:Q
Sediment traps	13/6 prox.	26	4	6	2	10	3	4	28	16	**0.2**
	13/6 prox._I_upper	32	4	5		9	2	3	27	18	**0.2**
	13/6 prox._I_lower	27	4	6		10	3	5	29	17	**0.2**
	13/7 prox.	25	5	2	4	12	3	4	31	15	**0.1**
	13/1 prox.	25	3	9	2	7	3	7	35	10	**0.3**
	12/6 prox.	21	5	4	3	11	3	5	31	17	**0.1**
	13/6 dist.	43	4	18		10	2	2	20		**0.9**
	13/6 dist._I_upper	41	3	4		9	2	2	20	20	**0.2**
	13/6 dist._I_lower	38	4	9	3	8	2	2	19	15	**0.5**
	13/7 dist.	23	5	2	3	12	2	2	26	25	**0.1**
	13/1 dist.	33	4	6	3	10	2	3	24	16	**0.2**
	12/6 dist.	35	4	2	4	12	3	2	22	18	**0.1**
River bed	Griesler Ache	32		11			5	5	48		**0.2**
	Kienbach	8		90					2		**37.6**
	Wangauer Ache	57		6				3	33		**0.2**
	Fischbach	19		4			6	7	64		**0.1**
Detrital layers	DL 1986 dist.	18	3	64		2			8	5	**7.7**
	DL 2002 prox.	21	5	2	4	13	3	4	28	20	**0.1**

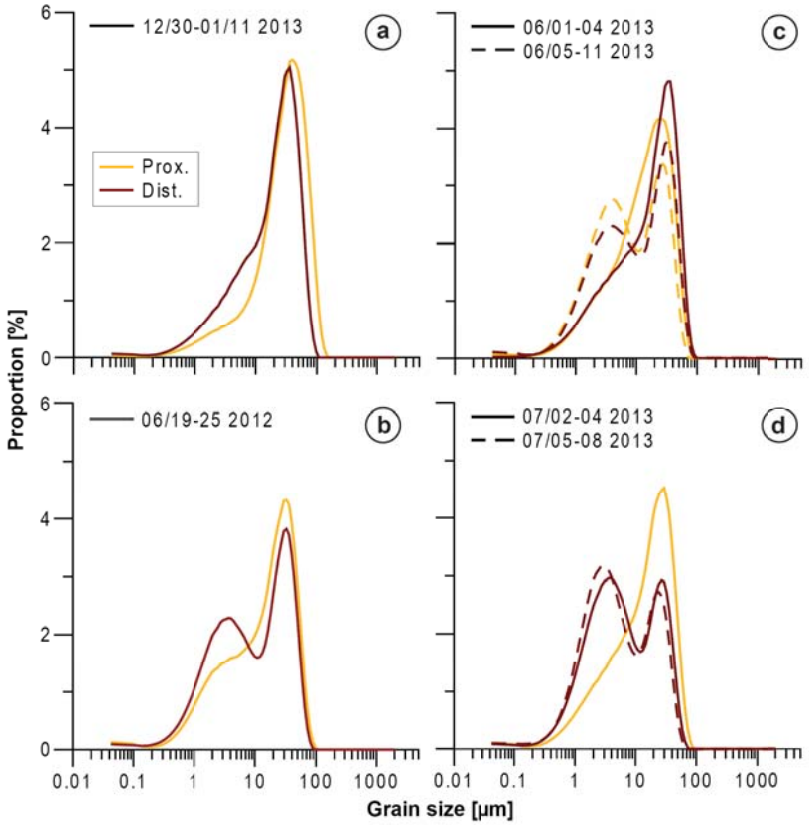

Figure 4.9. Grain size distribution of trapped sediment samples related to flood events (a) 01/13, (b) 06/12, (c) 06/13, (d) 07/13. Straight-lined plots indicate sediment flux peak samples; dashed plots indicate samples after the sediment flux peaks.

Sediment availability

The measured variations in suspended sediment concentration in the streams provide evidence for the sediment availability in the catchment as an important factor (Fig. 4.10). Fine sediments are mainly derived from the channel bank of the streams but sometimes also from patches of local erosion events, e.g. landslides, as revealed by field observations after the 06/13 flood (Supplementary Fig. 4.3). The sediment input to the streams further depends on the season since measured sediment concentrations were much lower during the winter flood (01/13: max. 1 g l^{-1}) compared to summer floods (20-103 g l^{-1}). Although only two strong winter floods are observed, we assume that this seasonal difference is generally valid and can be explained by reduced soil erosion in winter due to snow cover and frozen ground (Dugan *et al.* 2009).

Sediment availability is further changing within the course of a flood as demonstrated by the relation of river SSC and discharge (Fig. 4.10). Clockwise hysteresis functions indicate higher sediment concentrations during the rising limbs of the flood hydrographs proving river transport capacity as the main driver for riverine sediment transport in the initial phase of a flood when fine sediments are sufficiently available. In the later flood stage when sediments have been washed out and less fine material is available the riverine sediment transport is reduced as has been observed in various rivers (e.g. Forbes and Lamoureux 2005; López-Tarazón *et al.* 2010). This effect is also obvious from lower SSC values during the higher second flood peak of the 01/13 event which followed 13 days after a lower first runoff peak, which, in contrast, resulted in higher SSC values. For floods of only short duration, like the 06/12 event that lasted only for 18 hrs, river SSC followed the flood hydrograph during the rising and falling limb for the main flooding interval (> 40 m^3s^{-1}, 5 h) suggesting no limitations in sediment availability during such short floods.

Although the interpretation of the hysteresis plot of the strongest event (06/13) is limited because runoff during peak flow conditions (>100 m^3s^{-1}) was likely underestimated due to river bank overflow, this example demonstrates that extreme high SSC values (>100 g l^{-1}) not necessarily result in the highest suspended sediment transport into the lake. If a certain threshold is reached and the floodplain becomes flooded, the flow velocity decreases and suspended sediment accumulates in the floodplain (Supplementary Fig. 4.3). This process is known as catchment storage (e.g. Orwin *et al.* 2010) and is observed for the very strong 06/13 flood which led to lower amounts of trapped sediments than, for example, the 06/12 flood with much lower SSC values (max. 20 g l^{-1}).

Contrary to factors reducing sediment input to the lake, we also found few cases when sediment deposition can be significantly increased by additional sediment releases from local sources. Evidence for mixing of flood-triggered sediments from different sources is revealed for the distal location which is located ca. 800

m in front of the secondary Kienbach creek inflow (Fig. 4.1). The development of an underflow originating from the Kienbach and its impact on sediment deposition at the distal site can be demonstrated for the June 2013 flood. Besides tracing slumps in the head-catchment and the deposition of an approximately 0.5 m thick sediment fan of sand and gravel in the delta area of the Kienbach creek (Supplementary Fig. 4.3), we measured a 0.2 K temperature increase at the lake bottom at the distal site even one hour before the temperature rise of the deep water at the proximal site (Fig. 4.7). This underflow did not reach the proximal site and thus reflects a local event with short travel time reaching the distal site before the underflow triggered by the main tributary (Griesler Ache). The Kienbach creek as sediment source is confirmed by coarser grain sizes (Fig. 4.9) and predominant dolomitic composition of the trapped sediments (Tab. 2) which reflects the Kienbach catchment geology of the Northern Calcareous Alps. In the depositional record, local sediment flux from the Kienbach sub-catchment to the distal location has been suggested for five flood layers and for one debris flow layer (DL 16 in Fig. 4.11) deposited between 1976 and 2005 (Swierczynski *et al.* 2009; Kämpf *et al.* 2014).

In summary, the occurrence and thickness of detrital layers depends also on timing and preconditions of floods that might led to either an over- or an underestimation of the number of palaeofloods in the depositional record. On the one hand, detrital layers can be disproportionally thin or even miss when a flood followed a previous flood after a short time not sufficient to refill the riverbed with sediment or when catchment erosion is reduced (Czymzik *et al.*, 2010; Kämpf *et al.* 2012b). On the other hand, additional sediment release from local sediment sources can result in the formation of non-flood triggered detrital layers or increase flood layer thickness (Girardclos *et al.* 2007; Dugan *et al.* 2009; Swierczynski *et al.* 2009; Czymzik *et al.* 2010). However, the potential bias by such local layers can be reduced by detailed micro-facies and geochemical analyses of individual detrital layers (Mangili *et al.* 2005; Swierczynski *et al.* 2009) and tracing detrital layers in multiple sediment cores (Lamoureux 1999; Schiefer *et al.* 2006, 2011; Kämpf *et al.* 2012b, 2014).

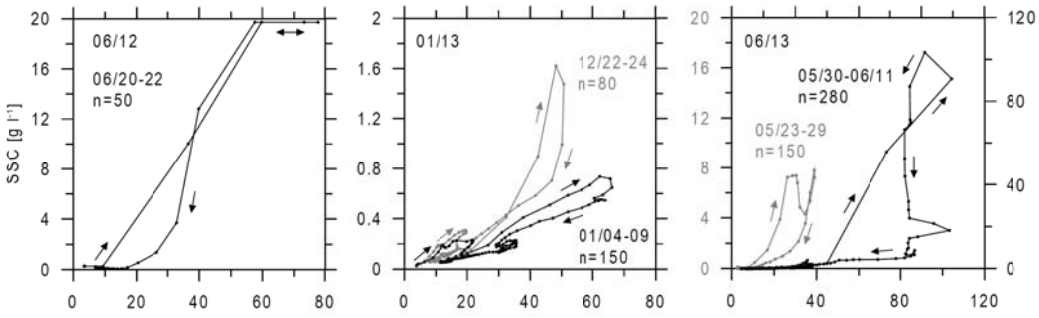

Figure 4.10. River runoff – suspended sediment (SSC) hysteresis plots for the three recorded flood events in the Griesler Ache river (06/12, 01/13, 06/13). Note the different scaling of the y-axes. Dots mark single measurements in 1-hr intervals.

Lake internal sediment distribution

The different spatial sediment distribution in the lake basin of individual events (PDI=2-25) is related to variations in the formation of hyperpycnal underflows and mesopycnal interflows (Sturm and Matter 1978; Chapron *et al.* 2005). Sudden temperature increases of 2-3.5 K recorded in the deep water column during the largest summer floods proved the occurrence of underflows (Fig. 4.7). In winter, temperature fluctuations were less distinct or even negative (-0.4 K to +0.1 K in Fig. 4.8) due to the lower river water temperature. Underflows developed during the four strongest floods, but reached the distal site only during the 06/13 event seven hours after passing the proximal site. From this time lag, a minimum current speed of 9 cm s^{-1} can be calculated which is rather low compared to larger lakes where much stronger underflows were measured like, for example, lakes Walensee (20-50 cm s^{-1}), Geneva (30-90 cm s^{-1}) and Constance (30-130 cm s^{-1}) (Lambert *et al.* 1976; Lambert and Giovanoli 1988). The resulting lower sediment transport capacity of underflows in Lake Mondsee is proven also by the measured vertical differences in sediment flux in the proximal ($L:U_{prox.}$ 2-8) and distal locations ($L:U_{dist.}$1-2) indicating underflows as the predominant transport mechanism in the proximal and interflows in the distal lake basin.

The rather low number of underflows reaching the distal site compared to observations from other lakes (Schiefer *et al.* 2006; Cockburn and Lamoureux 2008; Jenny *et al.* 2014) can be explained by the specific basin morphometry of Lake Mondsee (Fig. 4.1). At the point where the main tributary, the Griesler Ache, enters the lake, the elongated shape of the basin turns from NW-SE to N-S direction and later back to the original NW-SE direction. Due to this pronounced kink, the inflowing waters from the Griesler Ache are not straightaway directed towards the outflow but deflected first to the South and then to the East. Consequently, the flow velocity is expected to decrease, resulting in a lower sediment transport capacity. Lakes with frequent occurrence of underflows commonly have one large tributary stream and a simple elongated basin shape with straight flow direction from the main tributary inflow towards the outflow (Lambert *et al.* 1976; Best *et al.* 2005; Crookshanks and Gilbert 2008; Jenny *et al.* 2014).

The observed processes of detrital sediment distribution within Lake Mondsee provide explanations for the occurrence or absence of detrital layers in the depositional record obtained at the distal location (Swierczynski *et al.* 2013). There, flood layers are mainly transported by interflows and appear as very fine, only microscopically detectable (0.2-0.8 mm), non-graded silt/clay layers, whereas graded layers triggered by underflows only occur at the proximal site in an area within 1.5 km around the river mouths (Fig. 4.11). Importantly, interflows are favoured in the summer season when the water column is stratified and a pycnocline develops along which sediment is transported. In contrast, even high amplitude winter floods supplied only small sediment amounts to the distal lake

basin like the January 2013 flood; the sediment deposition (245 g m^{-2}) most likely was not sufficient to form a discernible detrital layer. This explains why the flood record from the distal site has been regarded as summer time series (Swierczynski *et al.* 2012). In order to obtain a flood record including both summer and winter floods a coring site at the proximal position should be selected. However, the disadvantage of this coring location might be a possible bias through reworked delta sediments (e.g. Schiefer *et al.* 2006) providing additional local sediment flux, which, in turn, can be excluded for the distal site.

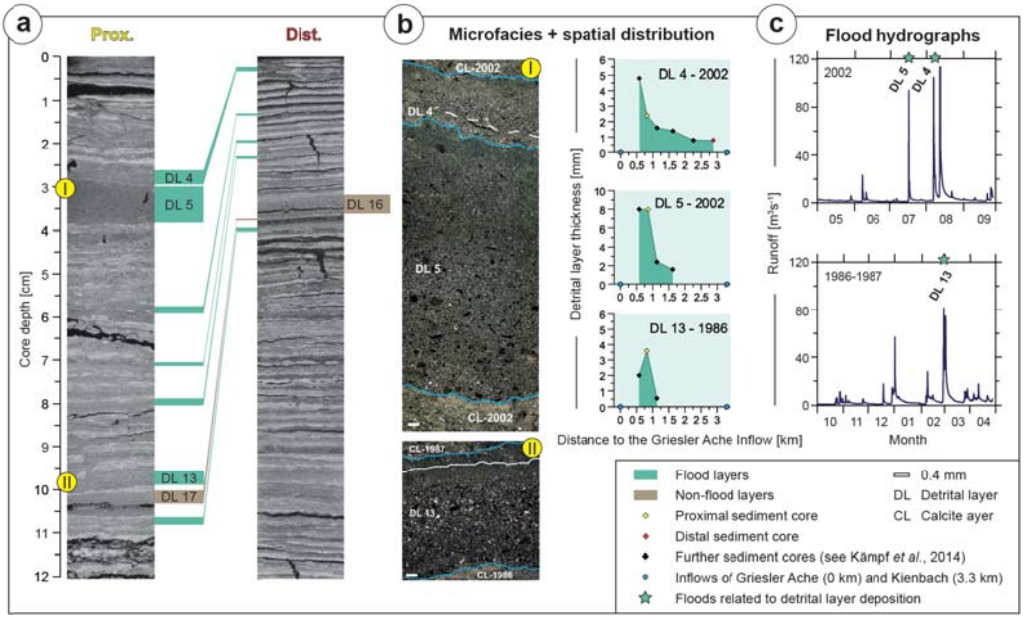

Figure 4.11. Detrital layers in the varved sediment record of Lake Mondsee: (a) Thin section scans (polarized light) of the upper 12 cm of sediment cores close to the proximal and distal trap location (Fig. 4.1) and correlation of detrital layers, (b) microfacies of selected detrital layers (microscopic images under polarized light, 20-100x magnification) showing graded layers in the proximal core and different spatial distribution patterns, (c) seasonal flood hydrographs (hourly values) of the Griesler Ache River coincided to detrital layer deposition according to the seasonal resolution of the varved detrital layer record: summer= May-Sep and winter= Oct-Apr.

Another factor controlling the spatial distribution of detrital sediment within the lake basin is the flood duration. This can be demonstrated for sediment deposition during the short 06/12 event (74 mm rainfall in 4 h, Tab.1) with a focal area at the proximal location since the under- and interflows broke down quickly when river discharge dropped and thus did not reach the distal basin as reflected by low sedimentation rates in the distal trap (Fig. 4.7). In contrast, the 06/13 flood lasted for nine days resulting in strong and long lasting interflows as reflected by elevated sediment deposition at the distal trap over ten days (Fig. 4.7).

Reconstructing palaeoflood time series in particular from distal sediment records, therefore, needs to concern not only about peak discharges but also the duration of floods. Strong but short floods might not reach the distal location but result in

thick detrital layers in proximal cores (e.g. DL 5 in Fig. 4.11; associated peak runoff: 100 m^3s^{-1}, daily mean: 24 m^3s^{-1}). Hence, daily instead of hourly runoff values are more appropriate for defining discharge thresholds for detrital layer formation in the depositional records.

4.5.2 Implications for the use of detrital layers as flood proxies

Our monitoring data provide clues for both, (1) reliable interpretation of detrital layers as flood proxies and (2) selecting suitable coring locations for palaeoflood reconstruction.

The monitoring data reveals that thresholds in discharge exist, above which flood layer formation becomes very likely. Obviously, these thresholds depend on the coring location and most likely vary also for different lakes (Czymzik *et al.* 2010; Kämpf *et al.* 2012b; Corella *et al.* 2014; Jenny *et al.* 2014). However, the monitoring and its comparison with the sediment record demonstrate that these thresholds can be empirically determined and thus provide information about the minimum amplitude of floods recorded in depositional records.

Reconstructing individual flood amplitudes from detrital layer thickness, however, still remains challenging. For Lake Mondsee with a complex lake basin morphometry, a vegetated catchment and sediments predominantly produced in the water column through biological productivity, this approach failed because several other factors including sediment availability, local sediment supply and lake internal sediment distribution significantly bias magnitude estimates of palaeofloods. In contrast, for small proglacial and nival lakes with one main tributary inflow and predominantly clastic-detrital sedimentation a correlation between peak runoff and sediment flux has been demonstrated (Desloges and Gilbert 1994; Chutko and Lamoureux 2008; Schiefer *et al.* 2011). More lakes must be investigated in order to find out if there is a systematic difference between lakes with different settings and sediment types.

Detrital layer successions in depositional records should not per se be considered as complete flood time series. We have demonstrated that there might be additional layers due to local sediment transport but also ‘missing’ layers, i.e. floods that did not result in detrital layer formation. This can be either due to random or systematic processes, like the lack of winter flood layers at the distal location in Lake Mondsee. Both, additional, non-flood triggered, and missing layers represent a potential and assumedly site specific bias in flood reconstruction. However, we have also demonstrated that it is possible to reduce the potential bias through (1) detailed micro-facies and geochemical analyses and (2) a careful choice of coring sites ideally integrating proximal and distal locations (Czymzik *et al.* 2010; Schiefer *et al.* 2011; Kämpf *et al.* 2014; Jenny *et al.* 2014).

Although flood reconstructions are conducted to a wide range of lakes, varved sediment records provide particularly suitable archives for process studies in order to develop quantitative flood proxies in terms of their hydrological characteristics.

4.6 Conclusions

The three-year integrated lake and catchment flood monitoring at Lake Mondsee revealed detailed insights into the complex chain of processes leading to flood layer formation. In particular, reasons for variable sediment flux at the lake floor could be identified including hydrological factors such as runoff magnitude and duration, local geomorphological factors influencing sediment availability in the catchment and factors controlling the spatial distribution of detrital material within the lake. This knowledge has implications for the long flood record established at the distal lake basin of Lake Mondsee:

1. Threshold processes in the runoff - sediment flux relation define flood magnitudes above which suspended matter is transported and detrital layers are formed. The long Lake Mondsee flood layer chronology records all floods exceeding 80 m^3s^{-1} river discharge and lasting for at least two days.
2. The depositional record at the distal site represents mainly summer floods due to the seasonally favoured development of mesopycnal interflows, the main transport agent for lake internal sediment distribution. Winter flood layers, deposited by hyperpycnal underflows, can be only found at core locations close to the river inflow.
3. Reconstruction of flood amplitudes by layer thickness is limited because the sediment yield after floods is not linearly related to runoff but is additionally affected by various other geomorphological and lake internal factors.
4. The potential bias of detrital layers triggered by local erosion events rather than by high magnitude floods can be reduced by detailed micro-facies and high-resolution geochemical analyses.

It has been shown that comparison of sediment monitoring with sub-recent detrital layer records provides valuable information for an advanced interpretation of detrital layers as flood recorders and for systematic selection of the most suitable coring location within a lake basin. Even if our dataset obviously is to a certain degree site specific for Lake Mondsee, we expect the fundamental mechanisms and controlling processes as valid also for many other lake sites.

Acknowledgements. This study contributes to the Potsdam Research Cluster for Georisk Analysis, Environmental Change and Sustainability (PROGRESS) part

A.3 'Extreme events in geoarchives' funded by the German Federal Ministry for Education and Research (BMBF). We are especially grateful to Prof. Rainer Kurmayer and Prof. Thomas Weisse (both University of Innsbruck, Research Institute for Limnology Mondsee) for their support and scientific collaboration as well as to Kurt Mayrhofer (University of Innsbruck, Research Institute for Limnology Mondsee), Richard Niederreiter (UWITEC) and numerous students for technical support and help during field work. We further thank Sebastian Lorenz (University of Greifswald) for his help during grain size measurements, Petra Meyer (GFZ Potsdam) for elemental analyses as well as Georg Schettler and Jens Mingram (both GFZ Potsdam) for useful advices regarding the monitoring set-up and lab analyses. Andreas Hendrich (GFZ) is acknowledged for his help with illustrating the figures.

Supplementary Material

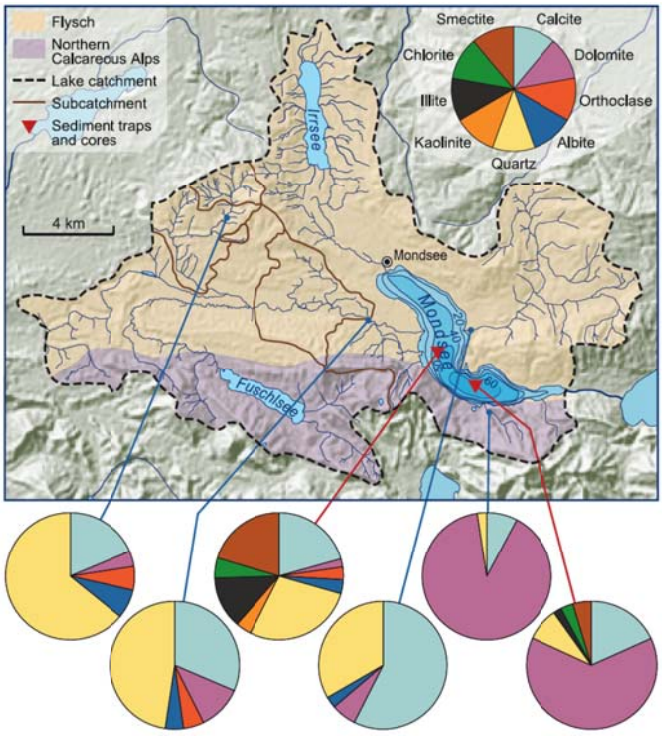

Supplementary Figure 4.1. Mineralogical composition of river bed samples (blue arrow) and detrital layers in sediment cores (red arrow).

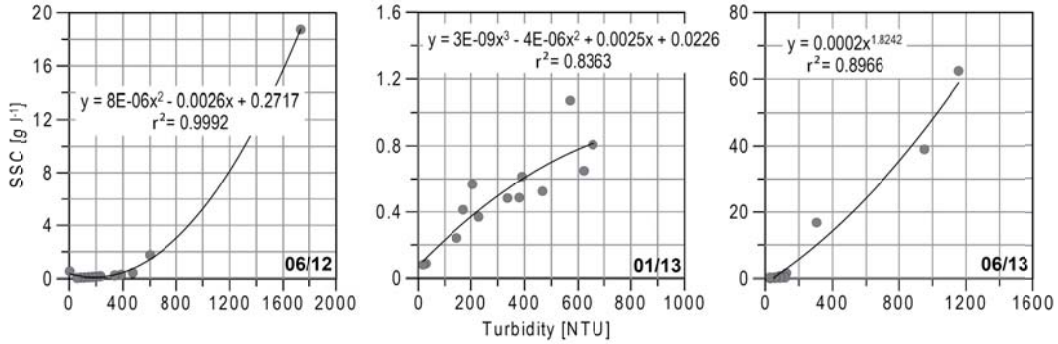

Supplementary Figure 4.2. Calibration of turbidity of the Griesler Ache River at St. Lorenz gauging station against suspended sediment concentration (SSC) derived from automatically taken water samples for the three recorded flood events 06/12, 01/13 and 06/13.

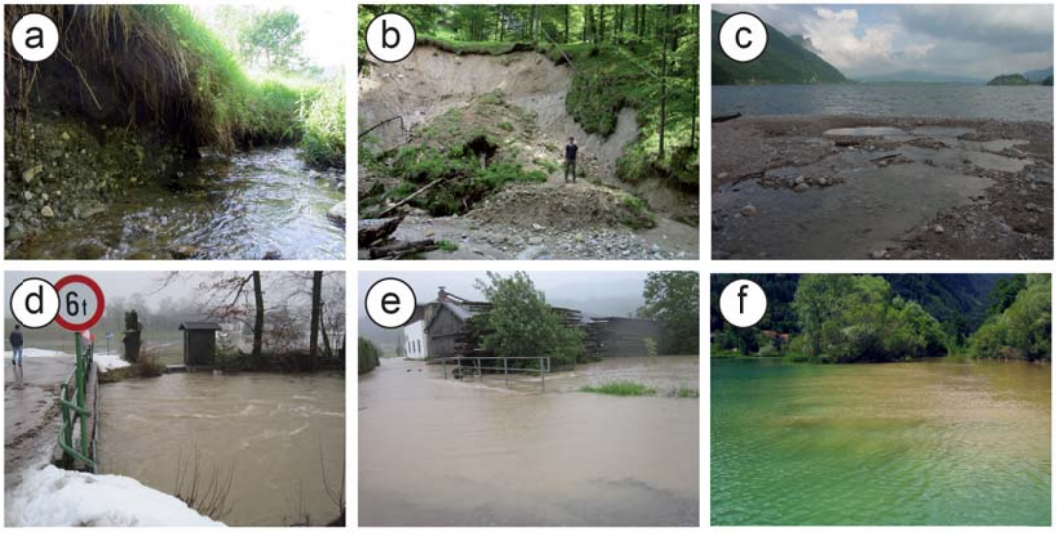

Supplementary Figure 4.3. Photographs documenting fluvial and in-lake sediment transport: (a) 06/13 event: channel bank erosion at Fischbach (SWB station), (b) 06/13 event: slump in the Kienbach valley, (c) 06/13 event: massive sediment deposition at the Kienbach Creek inflow into Lake Mondsee (a-c: 12 June 2013), (d) 01/11 event: Griesler Ache at St. Lorenz gauging station (14 January 2011 09:36 a.m.; Q=48 m^3s^{-1}), (e) 06/13 event: Griesler Ache close to St. Lorenz gauging station (02 June 2013 06:00 p.m.; Q=83 m^3s^{-1}, SSC=7 g l^{-1}), (c) 06/12 event: Griesler Ache inflow into Lake Mondsee; (21 June 2012 12:11 p.m., Q=10 m^3s^{-1}, SSC=0.1 g l^{-1}).

5 Summary and future perspectives

The main objective of this thesis is to improve the interpretation of lake sediments as recorders for past flood events by gaining knowledge about processes of detrital flood layer formation. Therefore, I first compared sub-recent detrital layer records of two different peri-Alpine lakes (Lago Maggiore, Mondsee) with instrumental flood data to test the possibility of linking sediment-based and instrumental flood records. In a second step, I investigated processes of detrital layer formation in Lake Mondsee using a combined hydro-sedimentary monitoring in the lake and its catchment.

5.1 Calibrating lacustrine flood layer records of Lake Mondsee and Lago Maggiore with instrumental data

Establishing detrital layer records for calibration. Detrital layer records from varved sediments of Lake Mondsee (MO) and non-varved sediments of Lago Maggiore (LM) were compared with instrumental flood data for the time period when sedimentological and hydrological datasets are available (MO: 1976-2005, LM: 1965-2006). The sub-mm to 17 mm thick detrital layers (MO, LM: 23) have been detected by using microfacies and µ-XRF scanning techniques. Analyses have been carried out on multiple sediment cores (MO: 13, LM: 5) to track spatial distribution patterns of detrital layers from the inflow of the main tributary rivers to the depocentre of the lakes. The event-based comparison of sedimentological and instrumental data requires a precise dating of the sediment sequences which was achieved for Lake Mondsee by varve counting in each investigated sediment core and for the non-varved sediments of Lago Maggiore by correlating the individual sediment cores to a previously dated core sequence (^{210}Pb, ^{137}Cs, biological markers) using detrital marker layers.

Sedimentological features of detrital layers in two dissimilar lakes. In both lakes, we observed three different types of detrital layer microfacies. (1) *Graded layers* consist of clay to coarse silt and in Lago Maggiore even up to fine sand sized mineral grains. Layers of this type exhibit an upward fining sediment texture or, in few cases, two inversely or normally graded beds. (2) *Silt/clay layers* are exclusively formed by fine silt to clay sized mineral grains without a visible textural organization. (3) *Matrix-supported layers* are composed of up to sand-

sized detrital grains in a fine grained sediment matrix. Typical features for matrix-supported layers are dispersed littoral debris and endogenic sediment components reflected by aggregates of precipitated calcite in Lake Mondsee and scattered grains of authigenic iron sulphide in Lago Maggiore indicating erosion of lacustrine sediments in the shallow lake areas.

The correlation of detrital layers between the individual sediment cores revealed spatial distribution patterns of the three layer types which remarkably differ between both lakes. In Lago Maggiore graded layers are found at each coring site and only very thin layers do not exhibit a clear grading. In Lake Mondsee, graded layers occur only close to the delta area of the inflowing tributary streams whereas in the depocentre silt/clay layers are most abundant. In both lakes, matrix-supported layers occur only close to the lake shores.

Comparing hydrological and detrital layer time series. The event-based comparison with runoff data of the main tributaries revealed for both lakes that all graded and silt/clay layers are triggered by floods (MO: 10, LM: 20). Matrix-supported layers are triggered by local erosion events (MO: 6, LM: 3) and, in Lake Mondsee, additionally by snow melt floods (MO: 7). By their different microfacies and geochemical features detrital layers triggered by local erosion could be reliably distinguish from flood layers and thereby, removed from the flood layer record. In summary, the flood layer record contains 20 layers in Lago Maggiore (1965-2006) and 17 layers in Lake Mondsee (1976-2005).

For both lakes, we found empirical runoff thresholds above which the formation of a detrital layer becomes likely. Whereas this threshold is the same for each coring site in Lago Maggiore (daily discharge: 600 m^3s^{-1}), the flood threshold increases with distance to the river mouth in Lake Mondsee. Close to the river inflow detrital layers correspond to floods with a daily discharge exceeding 40 m^3s^{-1}. In the depocentre of the lake, an hourly peak discharge of 80 m^3s^{-1} and at least 2 days > 40 m^3s^{-1} are necessary to form a detrital layer. Cases of missing flood layers, i.e., floods with an amplitude above the empirical threshold which did not lead to a detrital layer, have been found in both lakes (MO: 1, LM: 5). Inferred reasons for Lago Maggiore are multiple flooding in one year and therewith mixing of sediment, erosion by large turbidity currents, and a disturbed and/or highly clastic background sedimentation inhibiting the detection of fine detrital layers. Moreover, the spatial distribution of detrital material in Lake Mondsee is not, as in Lago Maggiore, the same for each event but depends on the flood season. Whereas winter floods are deposited confined to the delta area, 60% of the summer floods are distributed to the depocentre of the lake likely due to the role of the established thermocline in summer for detrital sediment distribution in Lake Mondsee.

Besides the potential of lacustrine detrital layer records for reconstructing flood frequencies we tested for both lakes the relation of layer thickness and amplitude of the triggering flood events. Therefore, we applied a simple linear correlation model to all investigated sediment sequences. Although the number of sampling points is very small for both lakes (MO: 6-16, LM: 7-14), the obtained results give some indications about factors controlling detrital layer thickness in lake sediments. Close to the river delta, layer thickness weakly correlates to flood amplitude (r^2, MO: 0.3-0.5, LM: 0.3-0.4) since individual exceptional thick layers are not triggered by the strongest floods. The depocentre of the lake basins in a more distal position towards the main inflows are less affected by such individual events and therefore better reflect flood amplitude (MO: 0.8, LM: 0.5). However, for both lakes the amount of detrital sediment deposited at a certain location at the lake floor is obviously controlled by many variables including the amount of material mobilized in the catchment and sediment distribution within the lake. In the most distal area of Lake Mondsee, for example, the signal of the main tributary is overprinted by variable sediment supply from a local sediment source.

Processes of detrital layer formation in two dissimilar lakes. The dual calibration of sub-recent detrital layer records in sediments of lakes Mondsee and Maggiore revealed several differences between both sediment records especially in thickness, microfacies and spatial distribution patterns of detrital layers as well as in the amplitudes of flood thresholds. Hence, we infer that sedimentation processes are not the same for the dissimilar lakes. As described above, the main difference between Lago Maggiore and Mondsee are basin morphometry and size of the inflowing streams (mean discharge MO: 4 m^3s^{-1}, LM: 70 m^3s^{-1}, catchment size MO: 247 km^2, LM: 1551 km^2).

In Lago Maggiore, most of the flood layers are graded over the whole investigated part of the basin and exhibit traces of micro-scale erosion at most proximal sites pointing to sediment deposition by high-energetic hyperpycnal underflows. In Lake Mondsee, most of the flood layers are graded in the proximal lake area and exhibit a non-graded silt/clay microfacies in the depocentre of the lake without any erosional features. This indicates a separation of the flooding river plumes into spatially confined hyperpycnal underflows and low-energetic mesopycnal interflows spreading to the depocentre of Lake Mondsee. Therefore, lake-internal processes play a larger role for flood layer formation in the low-energetic environment of Lake Mondsee than in the high-energetic Lago Maggiore evidenced by the spatially varying flood thresholds for detrital layer formation and correlation of layer thickness and flood amplitude. Most conspicuous is the fact that in the depocentre of Lake Mondsee flood layers are only formed in summer most likely due to the established thermocline as a necessary precondition for basin-wide sediment dispersal by mesopycnal flows.

The applied dual calibration approach has shown to be suitable to distinguish layers triggered by floods from those triggered by local erosion and decipher flood layer formation processes in two dissimilar lakes and, thereby, improve the interpretation of lake sediment based flood time series from different lake settings.

5.2 Monitoring hydro-sedimentary processes during floods in Lake Mondsee

To understand processes of detrital layer formation in more detail, sediment flux was trapped at two locations in Lake Mondsee and compared to local hydro-meteorological data.

Flood-related sediment flux 2011-2013. Within the three-year monitoring period from January 2011 to December 2013 26 river floods of very different magnitude (10-110 m^3s^{-1}) have been recorded resulting into a highly variable sediment response of 4 to 760 g m-2d-1 at the lake floor. Vertical and lateral variations in trapped sediment flux give explanations for spatial changes in detrital microfacies and point to different sediment transport processes within the lake water column: spatially confined sediment transport by underflows in winter and basin wide sediment distribution by interflows in summer. The comparison of hydrological and sedimentological data revealed (i) a rapid sedimentation within three days after the peak runoff in the proximal and within six to ten days in the distal lake basin, (ii) empirical flood thresholds for triggering detrital sediment flux at the lake floor increasing from the proximal (20 m^3s^{-1}) to the distal part of the lake (30 m^3s^{-1}) and (iii) factors controlling the detrital sediment flux at a certain location in the lake basin. The amount of sediment transported to the lake is mainly controlled by runoff magnitude, variable sediment availability due to sediment wash out by previous floods, snow cover and catchment storage by overbank deposition as well as episodic sediment input by local sources like the Kienbach creek. Besides the total input of detrital sediment, the spatial distribution within the lake is also variable and further determines the sediment flux at the lake floor. Since the lake internal sediment transport in Lake Mondsee is mainly driven by interflows, lake stratification is a requirement for basin wide sediment distribution and only summer floods are recorded in the long Lake Mondsee flood layer record in the distal lake basin. Another important role plays the duration of a flood since the sedimentation of interflows lasts over several days and is driven by momentum from the tributary streams.

The monitoring results give mechanistic explanations for detrital layers found in the long sediment record of Lake Mondsee in the distal lake basin (Swierczynski *et al.*, 2013) including the limitation of sediment deposition to the summer season, the occurrence of local layers and reasons for floods which did not result into detrital layer deposition.

5.3 Conclusions

The two applied approaches, (i) calibrating sub-recent detrital layer records with instrumental flood data and (ii) monitoring flood related sediment flux turned out to be suitable to decipher processes controlling flood layer formation in great detail. The impact of hydrological and local geomorphological factors in the catchment and the lake might substantially differ for different lake/catchment settings and thus, the results of this thesis contribute to identifying ideal sites for flood reconstructions based on lake sediments for future investigations. Determining factors are:

Sediment characteristics. Linking sediment based and instrumental flood time series requires an accurate and precise timing of individual detrital layers. With a seasonal resolution, varved sediments provide the most precise and, in combination with independent time markers, the most accurate flood archives. Besides the exact timing of flood layers varved sediments even allow establishing palaeoflood records for different seasons.

Lake and catchment size. Investigating two medium- (Mondsee) to large-scale peri-alpine lakes (Lago Maggiore) showed that detrital layers in larger lakes predominately represent regional-sized floods whereas in smaller lakes local thunderstorms or even local erosion events not related to floods can also lead to detrital layer formation.

Lake morphometry. The differences in flood-related sedimentation in Lake Mondsee and Lago Maggiore were mainly attributed to the different lake morphometry including the size and arrangement of the tributary streams and the shape of the lake basin. Lakes with a simple elongated shape and one large tributary stream, like Lago Maggiore, favour the formation of underflows and a clear sediment imprint of floods over the whole lake basin. In lakes with several smaller tributaries and a more complex basin shape, like Lake Mondsee, interflows are more the dominant sediment transport mechanisms and further factors such as thermal stratification have to be considered.

Coring location. Flood reconstructions are often based on one sediment sequence and finding the ideal coring location within a lake basin determines the significance of a flood layer record. Areas located close to the river inflow record variations in fluvial sediment flux most directly but are also exposed to erosion by large turbidity currents and deposits of local erosion events not related to floods. In contrast, locations in the distal lake basin predominately record the largest flood events, however, with a lower completeness due to the variable spatial extension of river plumes. In large lakes such as Lago Maggiore, distal coring locations are more favourable for flood reconstructions since the generation of strong underflows might cause sediment erosion in proximal areas and variable sediment distribution is less important leading to complete flood records even at distal locations. In contrast, the lake internal sediment distribution is highly variable in smaller lakes with several tributaries, as Lake Mondsee, and thus,

flood reconstructions solely based on distal sediment records includes more uncertainties in such lakes. Ideally, flood reconstructions should integrate multiple sites or at least two sediment sequences, one obtained from the deepest part and one closer to the main sediment source.

The hydro-sedimentary monitoring at Lake Mondsee revealed close links between flood behaviour and detrital sediment deposition at the lake floor. The fact that the largest floods result into the largest sediment deposition prove that detrital layers are indicative for strong flood events since low amplitude floods do not supply sufficient amounts of detrital material to produce a visible detrital layer. This is proven by comparing detrital layer records with instrumental flood time-series at Lake Mondsee and Lago Maggiore revealing empirical flood thresholds for detrital layer deposition in both lakes enabling connecting sediment based and hydrological flood time-series.

However, this in turn does not necessarily mean that the amount of deposited material after a flood, i.e. the thickness of detrital layers, is representative for the intensity of floods since other factors affecting the sediment transport to the lake and the lake internal sediment distribution can have a great impact on sediment deposition at a certain location in a lake basin. Hence, lake sediments provide ideal archives to reconstruct flood frequencies but the applicability for reconstructing flood amplitudes is more complex and presumably limited to individual sites.

5.4 Further data

The combined hydro-sedimentary monitoring was designed as joint interdisciplinary project including a further doctoral thesis of Philip Mueller in the field of Hydrology. Therefore, the comprehensive set of hydrological data from five gauging stations in the catchment and monitoring buoys in the lake (Fig. 1.2) was not presented entirely within this thesis and provides further unpublished information for a more in-depth processes understanding.

(I) The three year monitoring period comprises 20 flood events during which precipitation, water level and suspended sediment concentration were measured at the five gauging stations along the Griesler Ache river. In addition, suspended sediments were sampled in the river by pumping water samplers and in the lake by sediment traps for each individual event (Fig. 1.2). This comprehensive set of hydrological and sedimentological data enables a very detailed investigation of hydro-sedimentary processes from the transformation of precipitation into discharge to sediment mobilization under different pre-conditions (e.g. season, soil moisture) and within different catchment settings (steep-sloped forest and gentle pasture land).

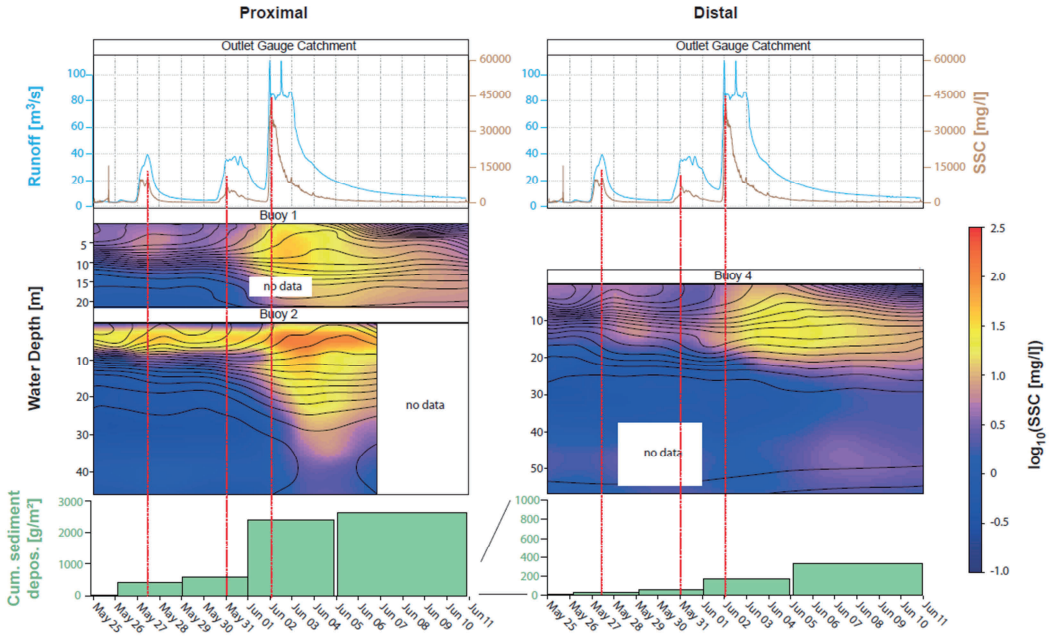

Figure 5.1. Hydro-sedimentary dynamics during the June 2013 flood: Runoff, suspended sediment concentration (SSC) in the Griesler Ache River and in the lake water column, trapped sediment deposition at the lake floor.

(II) A novel buoy system for monitoring limno-physical variables within the lake water column (turbidity, current velocity, temperature) and meteorological boundary conditions was developed within this project (Mueller *et al.*, 2013). Together with the river monitoring stations and the sediment traps, the buoys collected data during the most severe flood event in June 2013 (Fig. 5.1). Suspended sediment concentration could be derived from rating curves based on water samples taken automatically for the river gauging stations and manually for the buoys during the time of maximum turbidity. With a peak runoff of 104 m^3s^{-1}, the flood was within the range of the strongest flood ever recorded at Lake Mondsee in August 2002 (113 m^3s^{-1}). Hence, the monitoring data spanning from precipitation to sediment deposition will provide unique insights into hydro-sedimentary dynamics during a century-scale flood event.

Moreover, the three-year monitoring provided further data which can aid an improved understanding an interpretation of other paleoenvironmental proxies beyond detrital flood layers.

(I) Down to daily data on calcite precipitation and stable carbon, oxygen and nitrogen isotopes provide valuable information on the interpretation of microfacies (Brauer *et al.*, 2008; Neugebauer *et al.*, 2012) and isotopic composition of calcite varves (Leng and Marshal, 2004; Mangili *et al.*, 2010).

(II) The trapped sediment samples have been further investigated for amount, species and stable oxygen isotopic composition of diatom assemblages. Monitoring phytoplankton communities within the water column conducted by the Research Institute for Limnogy at the University of Innsbruck parallel to our

monitoring allow detailed comparisons of water column and sediment trap data. The results can help to decipher factors influencing diatom blooms, species dependent rates of deposition as well as the isotopic fractionation in diatoms providing valuable information for their use as paleothermometer (Leng and Marshall, 2004).

5.5 Outlook

Perspectives of applying lake sediments for flood frequency hydrology. Apart of the growing number of flood reconstructions from lake sediments (e.g. Wirth *et al.*, 2013) the potential of lacustrine flood layers records is still not fully recognized in related research areas like hydrology and climate modelling. However, lake sediments could potentially help to solve a major challenge in the field of flood frequency hydrology: the temporal and spatial expansion of existing instrumental flood time-series (Merz & Blöschl, 2008). Lake sediments are the only geoarchives providing continuous and, especially in the case of varved lake sediments, high-resolution flood data on centennial to millennial time scales. However, the hydrological information of single detrital layers is, in most cases, unknown making these records difficult to use for modelling purposes. However, the results of this thesis reveal some promising hints for linking instrumental data and lake sediment records.

Monitoring and sediment core data both revealed that detrital layers are formed by floods over certain runoff thresholds. The identification of such thresholds in turn gives the basis for linking instrumental flood records, limited in time, and sediment-based flood records with the previous unknown hydrological information and allows establishing flood frequency plots and estimate return periods for floods on a long-term data basis. An application of the monitoring and calibration approaches to selected other lake settings from different regions of the world could help to establish master profiles for flood reconstructions with quantified hydrological information. Such investigations should focus on varved sediment records due to their precise sediment chronology. In a next step, detailed comparisons between the established flood archives would allow deciphering regional differences in flood occurrence, flood prone weather regimes and the impact of climatic boundary conditions on a regional scale.

Future challenges for understanding flood layer formation in lake sediments. The two approaches, (i) calibrating sub-recent detrital layer records in multiple sediment cores and (ii) monitoring flood-related sediment flux from the catchment to the lake revealed detailed insights into processes of flood layer formation. However, during answering some questions within this thesis, further questions became apparent which are yet not answered.

(I) One of the major aims of the study, linking detrital layers in lake sediments to hydrological data is not fully reached since the varves deposited between 2011 and 2013 have yet not been investigated in sediment cores. The acquisition of

undisturbed sediments is challenging due to the high water content and unconsolidated structure of the uppermost millimetres of sediment. Therefore a freeze core has been retrieved from the distal lake basin in October 2014 which likely also contains the summer 2013 flood layer (Fig. 5.3).

(II) The monitoring set up properly worked under a wide range of hydrological conditions and was proven to be able to track suspended sediment dynamics from the catchment to the lake floor. However, the use in practice also revealed some points of improvement that could help to gain more complementary datasets for future studies. For Lake Mondsee, we found strong evidence for considerable sediment input from the ungauged Kienbach creek. However, the catchment and in-lake monitoring were aligned to track sediment flux from the main tributary stream, the Griesler Ache. Gauging all relevant tributary streams would allow quantifying the total sediment supply from the catchment and the contribution of the different source areas. This is especially relevant if sediment supply from local sources, as the Wangauer Ache, cannot be distinguished in the sediment records.

Moreover, tracking river plumes in the lake water column turned out to be challenging especially for underflows. The lowermost turbidity devices and traps were arranged 3 m above the sediment-water interface, and thus, likely too high to completely record underflows with a confined vertical extension. Hence, future studies should consider additional measurement and trapping devices for event specific sediment sampling, which ideally are (i) mounted directly at the lake bottom and (ii) remote-controlled for high-resolution sampling during flood events.

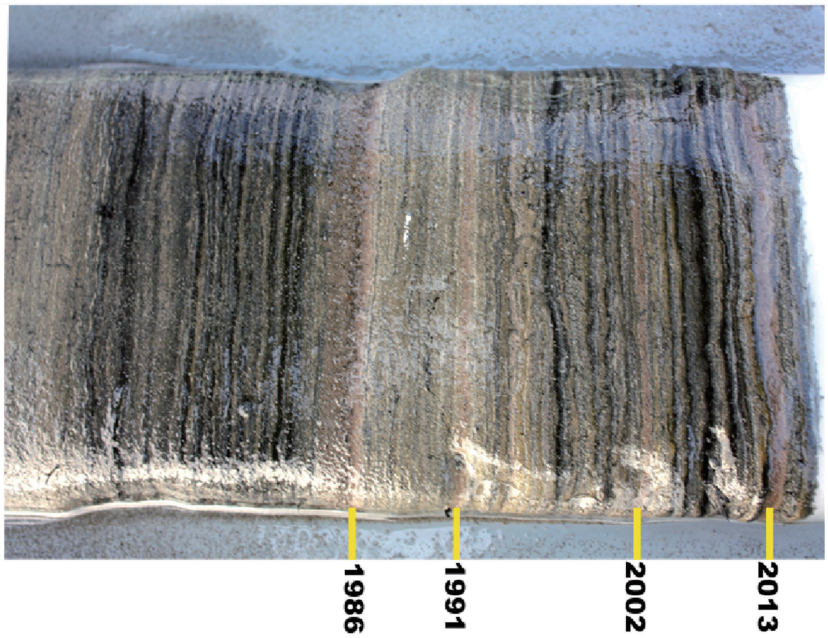

Figure 5.2. Photograph of a freeze core retrieved from the distal lake basin in October 2014. Indicated are the thickest detrital flood layers of the calibration period and the uppermost flood layer likely deposited by the flood event in summer 2013.

6 References

Agren A, Berggren M, Laudon H, Jansson, M (2008) Terrestrial export of highly bioavailable carbon from small boreal catchments in spring floods, *Freshwater Biology*, **53**, 964-972.

Ambrosetti W, Barbanti L, de Bernardi R, Libera V (1980) Alcune risposte limnologiche ad un evento meteorologico eccezionale: il nubifragio del 7 Agosto 1978 nel bacino del Lago Maggiore, *Atti del 3° Congresso della Società Italiana di Oceanologia e Limnologia, Sorrento 18-20 December, 1978*, 389-406.

Ambrosetti W, Barbanti L (1999) Deep water warming in lakes: an indicator of climatic change, *Journal of Limnology*, **58**, 1-9.

Ambrosetti W, Barbanti L, Rolla A (2006) The climate of Lago Maggiore area during the last fifty years, *Journal of Limnology*, **65** (Supplement 1), 1-62.

Anselmetti FS, Buhler R, Finger D, Girardclos S, Lancini A, Rellstab C, Sturm M (2007) Effects of Alpine hydropower dams on particle transport and lacustrine sedimentation, *Aquatic Sciences,* **69**, 179-198.

Arnaud F, Revel M, Chapron E, Desmet M, Tribovillard N (2005) 7200 years of Rhone river flooding activity in Lake Le Bourget, France: a high-resolution sediment record of NW Alps hydrology, *Holocene,* **15**, 420-428

Arnaud F, Révillon S, Debret M, Revel M, Chapron E, Jacob J, Giguet-Covex C, Poulenard J, Magny M (2012) Lake Bourget regional erosion patterns reconstruction reveals Holocene NW European Alps soil evolution and paleohydrology, *Quaternary Science Reviews,* **51**, 81-92.

Bacchi B, Ranzi R (2003) Hydrological and meteorological aspects of floods in the Alps: an overview, *Hydrology and Earth System Sciences*, **7**, 785-798.

Barbanti L, Ambrosetti W (1989) Geological and geographical features of the Lago Maggiore drainage basin, *Memorie dell'Istituto Italiano di Idrobiologia*, **46**, 1-20.

Battarbee RW, Jones VJ, Flower RJ, Cameron NG, Bennion H, Carvalho L, Juggins S (2001) Diatoms, In: *Tracking Environmental Change Using Lake Sediments Volume 3: Terrestrial, Algal, and Siliceous Indicators,* Smol JP, Birks HJB, Last WM (Eds), Kluwer Academic Publishers: Dordrecht.

Baudo R, Cenci RM, Sena F, Darbergami D, Leva F, Trincherini PR, Beltrami M, Barbero P, Corace C, Murray CN (2002) Chemical composition of the Lago Maggiore sediments, *Fresenius Environmental Bulletin*, **11**, 675-680.

Best JL, Kostaschuk RA, Peakall J, Villard PV, Franklin M (2005) Whole flow field dynamics and velocity pulsing within natural sediment-laden underflows, *Geology*, **33**, 765.

Blass A, Grosjean M, Troxler A, Sturm M (2007) How stable are twentieth-century calibration models? A high-resolution summer temperature reconstruction for the eastern Swiss Alps back to AD 1580 derived from proglacial varved sediments, *The Holocene*, **17**, 51–63.

Bloesch J, Sturm M (1986) Settling flux and sinking velocities of particulate phosphorus (PP) and particulate organic carbon (POC) in Lake Zug, Switzerland, In: *Sediments and Water Interactions* (Ed Sly PG), pp 481–490 Springer Press, New York.

Blöschl G, Nester T, Komma J, Parajka J, Perdigão RAP (2013) The June (2013) flood in the Upper Danube basin, and comparisons with the 2002, 1954 and 1899 floods, *Hydrology and Earth System Sciences*, **17**, 5197–5212

BMLFUW (2011) Hydrographisches Jahrbuch von Österreich 2011, BMLFUW, Vienna, 967 pp.

Brauer A, Casanova J (2001) Chronology and depositional processes of the laminated sediment record from Lac d'Annecy, French Alps, *Journal of Paleolimnology,* **25**, 163-177.

Brauer A, Haug GH, Dulski P, Sigman DM, Negendank JFW (2008) An abrupt wind shift in western Europe at the onset of the Younger Dryas cold period, *Nature Geoscience,* **1**, 520-523.

Brauer A, Dulski P, Mangili C, Mingram J, Liu J (2009) The potential of varves in high-resolution paleolimnological studies, *PAGES news,* **17**, 96-98.

Brown SL, Bierman PR, Lini A, Southon J (2000) 10 000 yr record of extreme hydrologic events, *Geology,* **28**, 335-338.

Carollo A, Libera V, Contardi F (1989) Hydroclimatic features of Lago Maggiore drainage basin, *Memorie dell'Istituto Italiano di Idrobiologia*, **46**, 21-40.

Chapron E, Arnaud F, Noël H, Revel M, Desmet M, Perdereau L (2005) Rhone River flood deposits in Lake Le Bourget: a proxy for Holocene environmental changes in the NW Alps, France, *Boreas* **34**, 404-416.

Chutko KJ, Lamoureux SF (2008) Identification of coherent links between interannual sedimentary structures and daily meteorological observations in Arctic proglacial lacustrine varves: potentials and limitations, *Canadian Journal of Earth Sciences,* **45**, 1-13.

CIPAIS (2007) Monitoraggio della presenza del DDT e di altri contaminanti nell'ecosistema Lago Maggiore Rapporto annuale aprile 2006 – marzo 2007 e Rapporto Finale 2001-2007 Ed Commissione Internazionale per la protezione delle acque italo-svizzere, 102 pp.

Cockburn J, Lamoureux S (2008) Inflow and lake controls on short-term mass accumulation and sedimentary particle size in a High Arctic lake: implications for interpreting varved lacustrine sedimentary records, *Journal of Paleolimnology,* **40**, 923-942.

Corella JP, Benito G, Rodriguez-Lloveras X, Brauer A, Valero-Garcés BL (2014) Annually-resolved lake record of extreme hydro-meteorological events since AD 1347 in NE Iberian Peninsula, *Quaternary Science Reviews*, **93**, 77–90.

Crookshanks S, Gilbert R (2008) Continuous, diurnally fluctuating turbidity currents in Kluane Lake, Yukon Territory, *Canadian Journal of Earth Sciences,* **45**, 1123-1138.

Czymzik M, Brauer A, Dulski P, Plessen B, Naumann R, von Grafenstein U, Scheffler R (2013) Orbital and solar forcing of shifts in Mid- to Late Holocene flood intensity from varved sediments of pre-alpine Lake Ammersee (southern Germany), *Quaternary Science Reviews,* **61**, 96-110.

Czymzik M, Dulski P, Plessen B, Grafenstein v, Naumann R, Brauer A (2010) A 450-year record of spring/summer flood layers in annually laminated sediments from Lake Ammersee (Southern Germany) *Water Resources Research,* **46**, W11528.

Debret M, Chapron E, Desmet M, Rolland-Revel M, Magand O, Trentesaux A, Bout-Roumazeille V, Nomade J, Arnaud, F (2010) North western Alps Holocene paleohydrology recorded by flooding activity in Lake Le Bourget, France, *Quaternary Science Reviews*, **29**, 2185-2200.

Desloges JR, Gilbert R 1994 Sediment source and hydroclimatic inferences from glacial lake sediments: the postglacial sedimentary record of Lillooet Lake, British Columbia, *Journal of Hydrology,* **159**, 375-393.

Dokulil M, Skolaut C 1986 Succession of phytoplankton in a deep stratifying lake: Mondsee, Austria, *Hydrobiologica,* **138**, 9-24.

Dugan HA, Lamoureux SF, Lafreniere MJ, Lewis T (2009) Hydrological and sediment yield response to summer rainfall in a small high Arctic watershed, *Hydrological Processes,* **23**, 1514-1526.

Effler SW, Matthews DA, Kaser JW, Prestgiacomo AR, Smith DG (2006): Runoff impacts on a water supply reservoir, suspended sediment loading, turbid plume behavior, and sediment deposition, *Journal of the American Water Resources Association*, **42**, 1697-1710.

Eybl J, Godina R, Lalk P, Lorenz P, Müller G, Pavlik H, Weilguni V, Heilig M (2013) Hochwasser im Juni 2013 - Die hydrographische Analyse, BMLFUW, Vienna, 53 pp.

Francus P, Bradley RS, Abbott MB, Patridge W, Keimig F (2002) Paleoclimate studies of minerogenic sediments using annually resolved textural parameters *Geophysical Research Letters*, **29**, 1998.

Francus P, Lamb H, Marshall M, Brown E (2009) The potential of high-resolution X-ray fluorescence core scanning: Applications in paleolimnology, *PAGES News*, **17**, 93-95.

Gerstengarbe F, Werner P, (2005) Katalog der Großwetterlagen Europas (1881–2004) nach Paul Hess und Helmut Brezowsky Potsdam Institute For Climate Impact Research, Potsdam.

Giguet-Covex C, Arnaud F, Poulenard J, Disnar JR, Delhon C, Francus P, David F, Enters D, Rey PJ, Delannoy JJ (2011) Changes in erosion patterns during the Holocene in a currently treeless subalpine catchment inferred from lake sediment geochemistry (Lake Anterne, 2063 m asl, NW French Alps): The role of climate and human activities, *Holocene,* **21**, 651-665.

Gilbert R (1973) Observations of sedimentation at Lilloet lake, British Columbia, Doctoral thesis, 193 pp.

Gilbert R, Crookshanks S, Hodder KR, Spagnol J, Stull RB (2006) The record of an extreme flood in the sediments of montane Lillooet Lake, British Columbia: Implications for paleoenvironmental assessment, *Journal of Paleolimnology,* **35**, 737-745.

Gilli A, Anselmetti F, Glur L, Wirth S (2013) Lake sediments as archives of recurrence rates and intensities of past flood events, In: *Dating torrential processes on fans and cones*, Schneuwly-Bollschweiler M, Stoffel M, Rudolf-Miklau F (Eds), Springer: Netherlands, 225-242.

Gilli A, Anselmetti FS, Ariztegui D, McKenzie JA (2003) A 600-year sedimentary record of flood events from two sub-alpine lakes (Schwendiseen, Northeastern Switzerland), *Eclogae Geologicae Helvetiae,* **96**, 49-58.

Giovanoli F, Lambert A (1985) Die Einschichtung der Rhone im Genfersee: Ergebnisse von Strömungsmessungen im August 1983, *Schweizerische Zeitschrift für Hydrologie,* **47**, 159-178.

Girardclos S, Schmidt OT, Sturm M, Ariztegui D, Pugin A, Anselmetti, FS (2007) The 1996 AD delta collapse and large turbidite in Lake Brienz, *Marine Geology*, **241**, 137-154.

Glur L, Wirth SB, Büntgen U, Gilli A, Haug GH, Schär C, Beer J, Anselmetti FS (2013) Frequent floods in the European Alps coincide with cooler periods of the past 2500 years, *Scientific Reports,* **3**, 1-5.

Grams C M, Binder H, Pfahl S, Piaget N, Wernli H (2014) Atmospheric processes triggering the central European floods in June 2013, *Natural Hazards and Earth System Science*, **14**, 1691-1702.

Guilizzoni P, Calderoni A (2007) Monitoraggio della presenza del DDT e di altri contaminanti nell'ecosistema del Lago Maggiore Commissione Internazionale per la protezione delle acque Italo-Svizzere, Rapporto quinquennale 2001-2007, *CIPAIS*, 102 pp.

Guilizzoni P, Marchetto A, Lami A, Gerli S, Musazzi S (2010) Use of sedimentary pigments to infer past phosphorus concentration in lakes, *Journal of Paleolimnology*, **45**, 433-445.

Guilizzoni P, Levine SN, Manca M, *et al* (2012) Ecological effects of multiple stressors on a deep lake (L Maggiore, Italy) integrating neo and palaeolimnological approaches, *International Journal of Limnology*, **71**, 1-20.

Hardy DR, Bradley RS, Zolitschka B (1996) The climatic signal in varved sediments from Lake C2, northern Ellesmere Island, Canada, *Journal of Paleolimnology,* **16**, 227-238.

Hodder K, Gilbert R, Desloges J (2007) Glaciolacustrine varved sediment as an alpine hydroclimatic proxy, *Journal of Paleolimnology,* **38**, 365-394.

Hodder K (2009) Flocculation: a key process in the sediment flux of a large, glacier-fed lake, *Earth Surface Processes and Landforms*, **34**, 1151–1163

Hsü KJ, Kelts K (1985) Swiss lakes as a geological laboratory, *Naturwissenschaften,* **72**, 315–321.

Irmler R, Daut G, Mäusbacher R (2006) A debris flow calendar derived from sediments of lake Lago di Braies (N. Italy), *Geomorphology*, **77**, 69-88.

Jenny JP, Wilhelm B, Arnaud F, Sabatier P, Giguet Covex C, Mélo A, Fanget B, Malet E, Ployon E, Perga ME (2014) A 4D sedimentological approach to reconstructing the flood frequency and intensity of the Rhône River (Lake Bourget, NW European Alps) *Journal of Paleolimnology*, **51**, 469–483.

Kämpf L, Brauer A, Dulski P, Feger K-H, Jacob F, Klemt E (2012a) Sediment imprint of the severe 2002 summer flood in the Lehnmühle reservoir, eastern Erzgebirge (Germany), *E&G - Quaternary Science Journal,* **61**, 3-15.

Kämpf L, Brauer A, Dulski P, Lami A, Marchetto A, Gerli S, Ambrosetti W, Guilizzoni P (2012b) Detrital layers marking flood events in recent sediments of Lago Maggiore (N Italy) and their comparison with instrumental data, *Freshwater Biology* **57**, 2076–2090.

Kämpf L, Brauer A, Swierczynski T, Czymzik M, Mueller P and Dulski P (2014) Processes of flood-triggered detrital layer deposition in the varved Lake Mondsee sediment record revealed by a dual calibration approach, *Journal of Quaternary Science*, **29**, 475–486.

Kelts K, Briegel U, Ghilardi K, Hsü KJ (1986) The limnogeology-ETH coring system, *Schweizerische Zeitschrift für Hydrologie*, **48**, 104–115.

Klee R, Schmidt R (1987) Eutrophication of Mondsee (Upper Austria) as indicated by the diatom stratigraphy of a sediment core, *Diatom Research,* **2**, 55-76.

Knox JC (2000) Sensitivity of modern and Holocene floods to climate change, *Quaternary Science Reviews,* **19**, 439-457.

Koschel R, Brenndorf J, Proft G, Recknagel R (1983) Calcite precipitation as a natural mechanism of eutrophication, *Archiv für Hydrobiologie*, **98**, 380–408.

Kulbe T, Livingstone DM, Guilizzoni P, Sturm M (2008) The use of long-term, high-frequency, automatic sampling data in a comparative study of the hypolimnia of two dissimilar Alpine lakes, *Verhandlungen der Internationalen Vereinigung für theoretische und angewandte Limnologie*, **30**, 371-376.

Lamb MP, McElroy B, Kopriva B, Shaw J, Mohrig D (2010) Linking river-flood dynamics to hyperpycnal-plume deposits: Experiments, theory, and geological implications, *Geological Society of America Bulletin*, **122**, 1389-1400.

Lambert A, Giovanoli F (1988) Records of riverbome turbidity currents and indications of slope failures in the Rhone delta of Lake Geneva, *Limnology and Oceanography*, **33**, 458–468.

Lambert A, Kelts K, Marshall NF (1976) Measurements of density underflows from Walensee, Switzerland, *Sedimentology*, **23**, 87- 105.

Lamoureux S (1999(Spatial and interannual variations in sedimentation patterns recorded in nonglacial varved sediments from the Canadian High Arctic, *Journal of Paleolimnology,* **21**, 73-84.

Lamoureux S (2000) Five centuries of interannual sediment yield and rainfall-induced erosion in the Canadian High Arctic recorded in lacustrine varves, *Water Resources Research,* **36**, 309-318.

Lamoureux SF, Stewart KA, Forbes AC, Fortin D (2006) Multidecadal variations and decline in spring discharge in the Canadian middle Arctic since 1550 AD, *Geophysical Research Letters*, **33**, L02403.

Lapointe F, Francus P, Lamoureux S, Saïd M, Cuven S (2012) 1750 years of large rainfall events inferred from particle size at East Lake, Cape Bounty, Melville Island, Canada, *Journal of Paleolimnology,* **48**, 159-173.

Lauterbach S, Brauer A, Andersen N, Danielopol DL, Dulski P, Huls M, Milecka K, Namiotko T, Obremska M, Von Grafenstein U, Declakes Participants (2011) Environmental responses to Lateglacial climatic fluctuations recorded in the sediments of pre-Alpine Lake Mondsee (northeastern Alps), *Journal of Quaternary Science,* **26**, 253-267.

Lauterbach S, Chapron E, Brauer A, Hüls M, Gilli A, Arnaud F, Piccin A, Nomade J, Desmet M, von Grafenstein U, Declakes Participants (2012) A sedimentary record of Holocene surface runoff events and earthquake activity from Lake Iseo (Southern Alps, Italy), *The Holocene*, **22**, 749-760.

Leemann A, Niessen F (1994) Varve formation and the climatic record in an Alpine proglacial lake: calibrating annually- laminated sediments against hydrological and meteorological data, *The Holocene*, **4**, 1-8.

Leng MJ, Marshall JD (2004) Palaeoclimate interpretation of stable isotope data from lake sediment archives, *Quaternary Science Reviews,* **23**, 811-831.

Lewis J (1996) Turbidity-controlled suspended sediment sampling for runoff-event load estimation, *Water Resources Research*, **32**, 2299–2310.

Lewis J, Eads R (2009) Implementation guide for turbidity threshold sampling: principles, procedures, and analysis, USDA, Albany, 87 pp.

López-Tarazón JA, Batalla RJ, Vericat D, Balasch JC (2010) Rainfall, runoff and sediment transport relations in a mesoscale mountainous catchment: The River Isábena (Ebro basin), *Catena,* **82**, 23-34.

Ludlam SD (1974) Fayetteville Green Lake, New York 6 The role of turbidity currents in lake sedimentation, *Limnology and Oceanography*, **19**, 656-664.

Manca M, Calderoni A, Mosello R, (1992) Limnological research in Lago Maggiore: studies on hydrochemistry and plankton, *Memorie dell'Istituto Italiano di Idrobiologia*, **50**, 171-200.

Manca M, Torretta B, Comoli P, Amsinck S, Jeppesen E (2007) Major changes in trophic dynamics in large, deep sub-alpine Lago Maggiore from 1940s to 2002: a high resolution comparative palaeo-neolimnological study, *Freshwater Biology*, **52**, 2256-2269.

Mangili C, Brauer A, Moscariello A, Naumann R (2005) Microfacies of detrital event layers deposited in quaternary varved lake sediments of the Pianico-Sellere Basin (northern Italy), *Sedimentology,* **52**, 927-943.

Mangili C, Plessen B, Wolff C, Brauer A (2010) Climatic implications of annual to decadal resolution stable isotope data from calcite varves of the Piànico interglacial lake record, Southern Alps, *Global and Planetary Change,* **71**, 168-174.

Marchetto A, Lami A, Musazzi S, Massaferro J, Langone L, Guilizzoni P (2004) Lago Maggiore (N Italy) trophic history, fossil diatoms, plant pigments, chironomids and comparison with long-term limnological data, *Quaternary International*, **113**, 97-110.

Menounos B, Clague, JJ (2008) Reconstructin g hydro-climatic events and glacier fluctuations over the p ast millennium from annually lam inated sediments of Cheakamus Lake, southern Coast Mountains , British Colum bia, Canada, *Quaternary Science Reviews*, **27**, 701-713.

Merz R, Blöschl G (2008) Flood frequency hydrology: 1. Temporal, spatial, and causal expansion of information, *Water Resources Research*, **44**, W08432.

Merz R, Blöschl G (2009) A regional analysis of event runoff coefficients with respect to climate and catchment characteristics in Austria, *Water Resources Research,* **45**, W01405.

Merz B, Aerts J, Arnbjerg-Nielsen K, Baldi M, Becker A, Bichet A, Blöschl G, Bouwer LM, Brauer A, Cioffi F, Delgado JM, Gocht M, Guzzetti F, Harrigan S, Hirschboeck K, Kilsby C, Kron W, Kwon H-H, Lall U, Merz R, Nissen K, Salvati P, Swierczynski T, Ulbrich U, Viglione A, Ward PJ, Weiler M, Wilhelm B, Nied M (2014) Floods and climate: emerging perspectives for flood risk assessment and management, *Natural Hazards and Earth System Sciences*, **14**, 1921–1942.

Meyers PA, Teranes JL (2001) Sediment organic matter In: *Tracking Environmental Change Using Lake Sediments Volume 2: Physical and Geochemical Methods*, Last,WM and Smol JP (Eds), p 239–269, Kluwer Academic Publishers, Dordrecht.

Milly PCD, Wetherald RT, Dunne, KA, Delworth, TL (2002) Increasing risk of great floods in a changing climate, *Nature*, **415**, 514-517.

Min S-K, Zhang X, Zwiers FW, Hegerl GC (2011) Human contribution to more-intense precipitation extremes, *Nature*, **470**, 378-381.

Montaldo N, Ravazzani G, Mancini M (2007) On the prediction of the Toce alpine basin f oods with distributed hydrologic models, *Hydrological Processes*, **21**, 608-621.

Mosello R, Calderoni A, de Bernardi R (1997) Le indagini sulla evoluzione dei laghi sudalpini svolte dal CNR Istituto Italiano di Idrobiologia, *Documenta dell'Istituto Italiano di Idrobiologia*, **61**, 19-32.

Mudelsee M, Borngen M, Tetzlaff G, Grunewald U (2003) No upward trends in the occurrence of extreme floods in central Europe, *Nature*, **425**, 166-169.

Mudelsee M, Borngen M, Tetzlaff G, Grunewald U (2004) Extreme floods in central Europe over the past 500 years: Role of cyclone pathway "Zugstrasse Vb", *J Geophys Res* **109**, D23101.

Mueller P, Thoss H, Kaempf L, Güntner A (2013) A buoy for continuous monitoring of suspended sediment dynamics, *Sensors* **13**, 13779-13801.

Mulder T, Alexander J (2001) The physical character of subaqueous sedimentary density flows and their deposits, *Sedimentology*, **48**, 269-299.

Neugebauer I, Brauer A, Dräger N, Dulski P, Wulf S, Plessen B, Mingram J, Herzschuh U, Brande A (2012) A Younger Dryas varve chronology from the Rehwiese palaeolake record in NE-Germany, *Quaternary Science Reviews,* **36**, 91-102.

Nied M, Pardowitz T, Nissen K, Ulbrich U, Hundecha Y, Merz B (2014) On the relationship between hydro-meteorological patterns and flood types, *Journal of Hydrology*, (accepted).

Parajka J, Kohnová S, Bálint G, Barbuc M, Borga M, Claps P, Cheval S, Dumitrescu A, Gaume E, Hlavcová K, Merz R, Pfaundler M, Stancalie G, Szolgay J, Blöschl G (2010) Seasonal characteristics of flood regimes across the Alpine–Carpathian range, *Journal of Hydrology,* **394**, 78-89.

Perkins MG, Effler SW, Peng, F, Pierson, D, Smith, DG, Agrawal YC (2007) Particle characterization and settling velocities for a water supply rervoir during a turbidity event, *Journal of Environmental Engineering*, **133**, 800-808.

Petrow T, Merz B (2009) Trends in flood magnitude, frequency and seasonality in Germany in the period 1951–2002, *Journal of Hydrology*, **371**, 129–141.

Petrow T, Zimmer J, Merz B (2009) Changes in the flood hazard in Germany through changing frequency and persistence of circulation patterns, *Natural Hazards and Earth System Sciences,* **9**, 1409-1423.

Pinto JG, Klawa M, Ulbrich U, Rudari R, Speth P (2001) Extreme precipitation events over north-west Italy and their relationship with tropical–extratropical interactions over the Atlantic, In: *Proceedings of the third EGS Plinius Conference on Mediterranean Storms*: Baja Sardinia, Italy, GNDCI Publication no 2560, *Editorial Bios*, 321–332.

Putyrskaya V, Klemt E, Röllin S (2009) Migration of ^{137}Cs in tributaries, lake water and sediment of Lago Maggiore – analysis and comparison to Lago di Lugano and other lakes, *Journal of Environmental Radioactivity*, **100**, 35-48.

Rotunno R, Ferretti R (2003) Orographic effects on rainfall in MAP cases IOP 2b and IOP 8, *Quarterly Journal of the Royal Meteorological Society*, **129**, 373-390.

Rudari R, Entekhabi D, Roth G (2005) Large-scale atmospheric patterns associated with mesoscale features leading to extreme precipitation events in Northwestern Italy, *Advances in Water Resources*, **28**, 601–614.

Salmaso N, Morabito G, Garibaldi L, Mosello R (2007) Trophic development of the deep lakes south of the Alps: a comparative analysis, *Fundamental and Applied Limnology*, **170**, 177-196.

Schiefer E (2006) Depositional regimes and areal continuity of sedimentation in a montane lake basin, British Columbia, Canada, *Journal of Paleolimnology* **35**, 617-628.

Schiefer E, Menounos B, Slaymaker O (2006) Extreme sediment delivery events recorded in the contemporary sediment record of a montane lake, southern Coast Mountains, British Columbia, *Canadian Journal of Earth Sciences,* **43**, 1777-1790.

Schiefer E, Gilbert R, Hassan MA (2011) A lake sediment-based proxy of floods in the Rocky Mountain Front Ranges, Canada, *Journal of Paleolimnology,* **45**, 137-149.

Schmidt R (1991) Recent re-oligotrophictaion in Mondsee (Austria) as indicated by sediment diatom and chemical stratigraphy, *Verhandlungen der Internatationalen Vereinigung Limnologie,* **24**, 963-967.

Schmocker-Fackel P, Naef F (2010) More frequent flooding? Changes in flood frequency in Switzerland since 1850, *Journal of Hydrology*, **381**, 1-8.

Schröter K, Kunz M, Elmer F, Mühr B, Merz B (2014) What made the June 2013 flood in Germany an exceptional event? A hydro-meteorological evaluation, *Hydrology and Earth System Sciences*, (accepted).

Siegenthaler C, Sturm M (1991) Die Häufigkeit von Ablagerungen extremer Reuss-Hochwasser: Die Sedimentationsgeschichte im Urnersee seit dem Mittelalter, *Mitteilungen Bundesamt für Wasserwirtschaft*, **4**, 127-139.

Simonneau A, Chapron E, Vannière B, Wirth SB, Gilli A, Di Giovanni C, Anselmetti FS, Desmet M, Magny M (2013) Mass-movement and flood-induced deposits in Lake Ledro, southern Alps, Italy: implications for Holocene palaeohydrology and natural hazards, *Climate of the Past,* **9**, 825-840.

Sodemann H, Zubler E (2005) Seasonal and inter-annual variability of the moisture sources for Alpine precipitation during 1995–2002, *International Journal of Climatology*, **30**, 947–961.

Støren EN, Dahl SO, Nesje A, Paasche Ø (2010) Identifying the sedimentary imprint of high-frequency Holocene river floods in lake sediments: development and application of a new method, *Quaternary Science Reviews*, **29**, 3021-3033.

Sturm M, Matter A (1978) Turbidites and varves in Lake Brienz (Switzerland): deposition of clastic detritus by density currents, *International Association of Sedimentologists, Special Publication*, **2**, 147–168.

Swierczynski T, Lauterbach S, Dulski P, Brauer A (2009) Die Sedimentablagerungen des Mondsees (Oberösterreich) als ein Archiv extremer Abflussereignisse der letzten 100 Jahre, In: *Klimawandel in Österreich - Die letzten 20000 Jahreund ein Blick voraus*, Schmidt R, Matulla C, Psenner R (Eds) Innsbruck University Press, Innsbruck, 115-126.

Swierczynski T, Brauer A, Lauterbach S, Martín-Puertas C, Dulski P, von Grafenstein U, Rohr C (2012) A 1600 yr seasonally resolved record of decadal-scale flood variability from the Austrian Pre-Alps, *Geology,* **40**, 1047-1050.

Swierczynski T, Lauterbach S, Dulski P, Delgado J, Merz B, Brauer A (2013) Mid- to late Holocene flood frequency changes in the northeastern Alps as recorded in varved sediments of Lake Mondsee (Upper Austria), *Quaternary Science Reviews,* **80**, 78-90.

Thorndycraft V, Hu Y, Oldfield F,Crooks PRJ, Appleby PG (1998) Individual flood events detected in the recent sediments of the Petit Lac d'Annecy, eastern France, *The Holocene*, **8**, 741-746.

Thorndycraft VR, Benito G (2006) The Holocene fluvial chronology of Spain: Evidence from a newly compiled radiocarbon database, *Quaternary Science Reviews*, **25**, 223–234.

Trachsel M, Eggenberger U, Grosjean M Blass A Sturm M (2008) Mineralogy-based quantitative precipitation and temperature reconstructions from annually laminated lake sediments (Swiss Alps) since AD 1580, *Geophysical Research Letters*, **35**, L13707.

van Husen D, 1989 Blatt 65–Mondsee, Geologische Karte der Republik Österreich 1:50 000, Geologische Bundesanstalt, Wien.

Vollenweider R (1956) L'influenza della torbidità provocata dalle acque di piena nel bacino di Pallanza (Lago Maggiore), *Memorie dell'Istituto Italiano di Idrobiologia*, **9,** 85-111.

Weirich F (1986) The record of density-induced underflows in a glacial lake, *Sedimentology*, **33**, 261-277.

Wilhelm B, Arnaud F, Sabatier P, Crouzet C, Brisset E, Chaumillon E, Disnar JR, Guiter F, Malet E, Reyss JL, Tachikawa K, Bard E, Delannoy JJ (2012) 1400 yr of extreme precipitation patterns over the Mediterranean French Alps and possible forcing mechanisms, *Quaternary Research*, **78**,1-12.

Wilhelm B, Arnaud F, Sabatier P, Magand O, Chapron E, Courp T, Tachikawa K, Fanget B, Malet E, Pignol C, Bard E, Delannoy JJ (2013) Palaeoflood activity and climate change over the last 1400 years recorded by lake sediments in the north-west European Alps, *Journal of Quaternary Science,* **28**, 189-199.

Wirth SB, Gilli A, Simonneau A, Ariztegui D, Vannière B, Glur L, Chapron E, Magny M, Anselmetti FS (2013a), A (2000) year long seasonal record of floods in the southern European Alps, *Geophysical Research Letters,* **40**, 4025-4029.

Wirth SB, Glur L, Gilli A, Anselmetti FS (2013b) Holocene flood frequency across the Central Alps e solar forcing and evidence for variations in North Atlantic atmospheric circulation, *Quaternary Science Reviews,* **80**, 112-128.